Moisture Transport and Convection in Building Envelopes

Ventilation in Light Weight Outer Walls

Charlotte Gudum

PhD thesis
R-047
ISBN 87-7877-107-2
Final Edition
February 2003

Moisture Transport and Convection in Building Envelopes
Ventilation in Light Weight Outer Walls

Charlotte Gudum

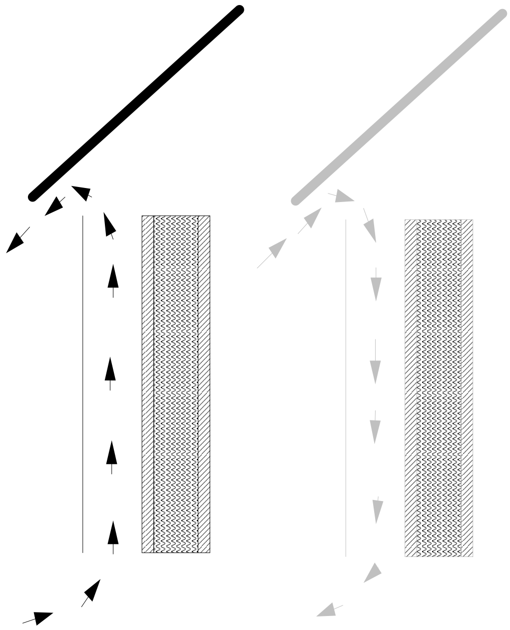

PhD thesis
R-047
ISBN 87-7877-107-2
Final Edition
February 2003

Preface

The present dissertation concludes the PhD work entitled ‘Moisture Transport and Convection in Building Envelopes’. The Technical University of Denmark have financed this project with support from ‘Martha and Paul Kerrn-Jespersens Fond’. Also Birch & Krogboe A/S and the Centre for Indoor Climate and Energy at DTU have most kindly offered valuable loan of equipments.

The work was carried out at the former Department of Building and Energy, now Department of Civil Engineering under supervision of Associated Professor PhD Carsten Rode, who managed to find the time for discussion, when it was needed. And who positively supported me in balancing the project with raising a family.

I would like to thank for the interest people has shown in the project. A special thanks to people from the Danish Building and Urban Research, who have most kindly shared their measuring data with me. I warmly thank Arsen Melikov from the Indoor Climate Centre, who has been most inspiring and an example to follow in both human relations and scientific work. And thanks to associated professor Carl Erik Hyldgård from Aalborg University, who supported the idea of measuring air velocity by tracer gas. I’m grateful to Bas Knoll, TNO, for valuable discussions on wind pressure measurements and not at least for his estimated wind pressure coefficients, using his computer code ‘Cp-Generator’.

I extend my sincere gratitude to the many people from the department, who have inspired me and taken part in the work during the project. Especially I would like to thank my colleague PhD student Ruut Peuhkuri for collaboration in Simulink programming, and for her valuable comments to the thesis. I also feel in deep debt to the rest of the ‘Simulink-group’ PhD student Toke Rammer Nielsen and PhD student Peter Weitzmann. Thank also to Jørgen Schultz for assistance with data recording, to Gitte Nørholt for making the drawings in the report, to Mogens Jørgensen and Poul Dedenroth from the laboratory staff, whos assistance I could always count on.

The tourough reading and discussion by the committee of censors Professor Carl-Eric Hagentoft, Senior Researcher Karl Terpager Andersen and Professor Svend Aage Svendsen is also gratefully acknowledged.

Finally, I wish to express my heartfelt gratitude to my dear husband Anders Broe Bendtsen for his admirable patience and support, and long hours of discussions. And to my dearest children Elise and Valdemar, who didn’t see much of their mother in the final period of this work.

Lyngby, January 2003

Charlotte Gudum

Summary

When occurring, convection is known to be the dominant type of moisture transport. The different parts of the building envelope are protected against convection by ensuring that connections are airtight. In ventilated building components the outdoor air passes through a ventilated cavity on the outside part of the insulation, in order to keep the design dry by exploiting the potential of convection to transport moisture coming from inside the building.

Previously light weight facades have been ventilated and used only in one or two storeys. The Danish building regulation were however in 1995 adjusted to permit wooden facades in up to four storeys, provided that the façade was designed without cavity. Another change in façade designs has been a continuing increase in insulation thickness as a function of demands for decreased heat loss. For these reasons the present PhD project has focussed on designing and validating a model for analysis of the effect of ventilation and insulation thickness upon the moisture load of the wall.

On a ventilated 25 mm cavity (height 1650 mm, width 559 mm) placed on a north facing wall of an outdoor test house the cavity air velocity and the wind pressure at the top and bottom of the cavity were measured together with the wind velocity and wind direction 4.8 m above ground.

The cavity air velocity was determined from the air change, using a gas analyser and the constant dose method. Tracer gas was dosed constantly across the cavity and samples were taken upstream and downstream from the dosing tube. The highest tracer gas concentration was used for determination of the flow direction and air velocity. Using the tracer gas the cavity air velocity was measured from –1 to +1 m/s for wind velocities in the interval 0.5-10 m/s 4.8 mabove ground level. A shortcoming of the method was, that erroneous results were observed when changes in the cavity air direction were faster than the methods time constant of 4-5 minutes. The use of a gas analyser also facilitated the measurement of convective moisture transport.

A comparison between the tracer gas method and thermo anemometers showed a satisfactory correspondence between the average velocities over a 9 minute period. The velocities measured with the thermo anemometers in the centre of the cavity were adjusted by multiplication of the factor 2/3 to match the velocities measured with tracer gas. The factor of 2/3 matches the expected value for laminar flow. A similar velocity profile was also observed in parallel with the wall, but this velocity profile was dependent on the wind direction.

The roughness of the surroundings was measured to a high value of 6.1.m, which was attributed to turbulence in the vicinity of one measuring position. The wind pressure coefficients outside the cavity vents were determined with a high standard deviation from pressure measurements as a function of the wind direction. A set of wind pressure coefficients was estimated for the façade (Knoll, 2000). They showed that the pressure difference between top and bottom were highest for side wind and lowest when the façade was in leeside.
A model for simulation of coupled moisture and heat transport in a ventilated façade was designed using Simulink under Matlab. The model simulated one-dimensional coupled moisture and heat transport by conduction and diffusion in the material layers, and cross-flowing one-dimensional air stream in the cavity. The model was validated with satisfactory results: By comparison of a non-ventilated case with MATCH and by comparison with a one-year outdoors measurement on four examples of composite ventilated façade designs and a non-ventilated design.

A simulation model, of the coupled heat and moisture transfer in a ventilated wall, was made using Simulink in Matlab.

9 different yearly simulations using the Danish reference year (DRY) as outdoors boundary condition and an in-door climate varying from 21-23ºC and 40-66% RH was used too study the effect of insulation thickness (100 mm, 200 mm and 300 mm); presence or absence of vapour

barrier and the degree of ventilation (none, low or high). A critical condition level was defined as simultaneous RH above 80% and temperature above 5ºC. The simulated RH and temperature behind the wind barrier were compared. Simulations showed that the time of critical moisture load was increased with increasing insulation for a ventilated façade with vapour barrier, but not to a critical length of time. For designs with vapour barrier ventilation increased the period of critical moisture load, but again not to a critical length of time. For a design without vapour retarder the period with critical moisture load was longer in the absence of ventilation than in the presence of ventilation, but in either case the period length was critical.

Based on the simulations it was concluded that a non-ventilated wooden façade may be considered a durable design, provided that the vapour barrier is both vapour and airtight. Furthermore a ventilated façade may compensate for a non-perfect vapour retarder.

Resumé

Konvektion er kendt som værende den dominerende transportform for fugt når den forekommer. Klimaskærmens dele beskyttes mod konvektion ved at sørge for at samlinger er lufttætte. I ventilerede bygningsdele passerer udeluften igennem et ventileret hulrum på den udvendige side af isoleringen, herved udnyttes konvektionens potentiale for at transportere indefra kommende fugt væk og dermed holde konstruktionen tør.

Tidligere har lette facader med træbeklædning været ventilerede og kun benyttet i 1-2 etager. Et Tillæg 1 til Bygningsreglement 1995 gav som noget nyt mulighed for at benytte træ facader i op til 4 etagers højde, under forudsætning af at væggen var uden bagvedliggende hulrum. En anden ændring i konstruktionen af facader er at isoleringstykkelsen øges i takt med skærpede varmetabskrav. I dette projekt blev der derfor fokuseret på at lave og validere en model der kunne analysere hvad effekten af ventilation og isoleringstykkelse havde på væggens fugtbelastning og dens holdbarhed.

På en ventileret spalte, højde 1650 mm og bredde 559 mm, placeret på en nordvendt facade af et udendørs forsøgshus blev der målt lufthastighed i en 25 mm spalte, vindtryk ved top og bund af spalten, samt vindhastighed og vindretning 4.8 m over terræn.

Lufthastigheden i en ventileret spalte blev målt med gasanalysator og konstant doseringsmetoden. Gas blev doseret jævnt over tværsnittet midt i spalten, og prøver til analysatoren blev taget et stykke opstrøms og nedstrøms fra doseringsslangen. Hastighed og retning blev bestemt udfra den største koncentration. Med sporgassen blev der målt opadrettet lufthastighed i intervallet –1 til 1 m/s for vindhastigheder imellem 0.5 og 10 m/s i 4.8 m's højde. Metoden viste sig dog også at måle forkert når luftretningen skiftende hurtigere end metodens tidskonstant på 4-5 minutter. Metoden blev desuden fundet anvendelig til måling den konvektive fugttransport igennem spalten.

Sammenlignende målinger med sporgas og termo anemometre viste en tilfredsstillende overensstemmelse mellem middelhastigheden over en 9 minutters måleperiode. De viste også at målinger midt i spalten (vinkelret på væg) måler en maksimums hastighed der skal ganges med en faktor 2/3 for at få middelhastighed i overensstemmelse med sporgasmålingerne, svarende til et laminart hastighedsprofil. Desuden viste målinger med 6 anemometre på tværs (parrallel med væg) af spalten at hastighedsprofilet også her var parabelformet. Ved forskellige vindretninger viste profilet at ændre form.

Ruheden for omgivelserne blev målt meget højt til 6.1 m, hvilket menes at skyldes turbulens omkring den ene af målerne. Vindtrykskoefficienter udfor spaltens åbninger blev beregnet med stor spredning udfra trykmålinger som funktion af vindretningen. Et sæt af vindtrykskoefficienter blev beregnet for facaden (Knoll, 2000). De viste at trykforskellen mellem top og bund var størst for sidevind, og mindst når facaden var i læ.

En model til simulering af koblet fugt og varmetransport i en ventileret facade blev lavet med Simulink i Matlab. Modellen simulerede endimensional koblet fugt og varmetransport ved ledning og diffusion i materialelagene, og tværgående endimensional luftstrømning i spalten. Modellen blev valideret med tilfredsstillende resultater, dels for et ikke ventileret eksempel mod *MATCH*, og dels mod 1 års udendørs målinger på 4 eksempler på sammensatte ventilerede konstruktioner og en ikke ventileret konstruktion.

Årssimuleringer med det danske referenceår DRY som udvendig randbetingelse og varierende indeklima mellem 21-23ºC og 40-66% relativ fugtighed blev lave for 9 facader med isoleringstykkelse 100, 200 og 300 mm mineraluld, med og uden dampspærre, samt med ingen, lidt og megen ventilation. Et kritisk fugtkriterium blev sat til samtidig relativ fugtighed over 80% og en temperatur på mere end 5ºC. Den simulerede relative fugtighed og temperatur bag vindspærren blev sammenlignet. Simuleringer viste at tiden med kritisk fugtbelastning steg med øget isolering for en ventileret facade med dampspærre, dog var perioden ikke kritisk lang. For konstruktion med dampspærre, øgede ventilation periodelængden med kritisk fugtindhold. Var konstuktionen uden dampspærre, var perioden med kritisk fugtindhold længere uden ventilation end med. Dog var forholdene uacceptable i begge tilfælde.

På baggrund af simuleringerne blev det konkluderet at en uventileret træfacade er holdbar såfremt dampspærren er både damp og lufttæt. Samt at en ventileret facade kan kompensere for en ikke perfekt dampspærre.

Contents

Definitions

Air velocity is the velocity inside the cavity

Wind velocity is the velocity outside the cavity

Air barrier is a material layer, which prevents air-movements between the indoor and outdoor climate. The air barrier can be a water vapour permeable material placed on the outside of the insulation, and is also called a wind barrier. In the presented work the air barrier is always placed on the outside of the insulation. The vapour retarder or other continuous material layer on the inside of the insulation can also serve as air barrier.

1 Introduction

1.1 Background

Wood based building structures such as light weight walls, attics and crawl spaces are designed with ventilation openings to dry out moisture coming from the indoor climate or surroundings. Both stack effect and wind force influences the air change rate. An understanding of the airborne moisture transfer (convection) in the ventilated parts of the building envelopes is the task here, in order to estimate the risk of condensation in ventilated structures and for better understanding of what is influencing the balance of appropriate ventilation.

In the literature the advantage and disadvantage of ventilation on the moisture load in a building envelope is discussed. Ventilation of building envelopes for residential houses with outdoor air is the accepted method for controlling moisture accumulation at an acceptable level (Walker and Forest, 1995). Traditionally it is assumed that ventilation is the way to prevent moisture content to rise to a critical level in wood based building envelopes. Recommendations of e.g. opening area for ventilation can be found in the Danish building codes (Andersen et al. 1993).

The ventilation air will for some periods of the year or day increase moisture content, and for other periods decrease the moisture content. For some structures and in some climates the increase of moisture content due to ventilation can result in an unacceptable moisture load for a longer period. The ventilation of the structure is therefore recommended in some cases and deprecated in others. Ventilation is e.g. controlling the moisture content from increasing critically in attic and wood based walls in a cold climate, while the ventilation is deprecated in e.g. flat roofs in cold climate and for walls in hot humid climate.

Today we have only little knowledge of the mechanisms of ventilation flow, i.e. how the airflow is influenced by the temperature difference and wind exposure, and how changes in the flow rate influence the moisture load in the building envelope. To provide more knowledge, the topic of the airflow, and with that the moisture load when e.g. the insulation thickness or the flow rate is changed, is investigated in this work by measurements and simulation with a numerical model that was developed.

Recently, in October 1999, an amendment to the Danish building regulation from 1995, has accepted wood based facades up to 4 storeys high, provided that there is no cavity behind the cladding. Before wood based facades were only accepted for residential houses until 2 storeys high. The required absence of ventilation is due to fire safety reason, but little attention has been given to the moisture conditions in such building envelopes without ventilation. Also a requirement concerning energy savings has increased the insulation thickness, compared to earlier. This will influence the stack effect and the temperatures, in a way that might lead to new considerations about the needed ventilation opening area.

It is generally recognised that convective moisture transport from the indoor climate, has a significant impact on the moisture load in a structure, when it takes place (Ojanen and Kumaran, 1996)(Hagentoft and Harderup, 1996)(TenWolde and Rose, 1996)(Condren, 1982). They find that the convective moisture transport from the indoor climate must be prevented, and suggest the moisture transport to be controlled to some extent, with airtight layer between the indoor climate and the warm side of the insulation, so air transport from the indoor climate into the building envelopes does not occur. Also the Danish building code requires that air tightness between the indoor climate and the warm side of the insulation has the highest priority.

In practice moisture transport from the indoor climate to the building envelope still takes place, by diffusion and through unintended leakage such as electrical joints and missing sealing of the vapour retarder etc. This moisture is removed from the envelope by airflow of outdoor air that carries moisture from the building envelope to the outdoor. The focus here is, however, restricted to the airflow and convective moisture transport through the vents in the screen.

1.2 Scope

This thesis concludes a Ph.D.-project, carried out at the Department of Civil Engineering at the Technical University of Denmark. The purpose has been to obtain an understanding of the nature of convective moisture transport under realistic weather conditions. With a better understanding comes the opportunity of better predictions on how the moisture load on new construction of building parts is influenced by ventilation, and how it should be ventilated to minimise the risk of moisture degradation.

The convective moisture transport is studied with focus on investigation of:

-How will an increased insulation thickness influence on the moisture load of light weight ventilated facades, and does that lead to new considerations for the ventilation?

- Will the wood based facade without ventilation have an acceptable durability?

- Does wind-fluctuation recycle or change the cavity air flow?

The scope of the study extended originally to all parts of the building envelope, although light weight walls were chosen as the object for measurements and simulations of a ventilated building envelope. It was practically suitable for measurements and modelling, and by choosing a north facing façade, the direct sun was eliminated from the measurements.

Analysis by measurements and simulations of a crawl space was included as a part of the Ph.D. project, (Gudum, 1998) (Found in Appendix A). The crawl space case was a specific problem with an interest at that time, where there was an opportunity of access to perform measurements on an existing domestic house placed in an area where the majority of the houses suffered from moisture problems related to the crawl space. The actual crawl space turned out to work perfect, and didn’t explain why these houses in general were so heavy loaded with moisture problems.

1.3 Philosophy of science

Taking one step back, looking at the scientific world it is clear, that it is separated from the surrounding society, or the ‘real world’. The scientific world tries to describe the outside world in general. The approach can be a mathematical model (computer simulation) that is compared to the real object or another model of the real object. The simple model is modified until the difference to the reference object is at an acceptable level. Another approach is to study the real world (case study) and make general assumption and conclusions of the object, (Jakobsen and Pedersen, 1996). Both approaches are seen, but they are not mutually exclusive and are often both used in the same work. Here the crawl space measurements clearly showed how difficult it is to get a general knowledge from a single case study. A more general approach was performed for the ventilated wall, where the model was a physical but theoretical object, which represented some characteristics of a ventilated wall, but also with some simplifications.

To describe it more theoretically, there is a positivistic and a falsification approach. The first try to verify that a hypothesis is true, the latter that a hypothesis is false (Kragh and Pedersen, 1991). If the scientist uses the falsification approach to his work, the case study can prove his hypothesis was false. He will find what is false, but will not be able to know what is then true. I.e. ‘The hypothesis is that crawl spaces always have moisture problems’. Finding one well functioning crawl space without moisture problems shows that this is not true, but it does not explain why so many of the crawl spaces have moisture related problems. Trying to falsify the same hypothesis with computer simulation, one can always claim that the model is not accurate enough.

The ‘positivistic researcher’ can describe the real world with a simplified model, compare the model to a more complex model or existing object (validation of the model). And then extrapolate the results to other objects or for longer periods. E.g. a computer model of the airflow in a ventilated cavity is validated against short time measurements of the airflow in a real scale model of a ventilated façade. Furthermore the computer model is simulating the airflow for a year, using representative yearly weather data. Using this method the limits of the model should be very clear to the user, who should be critical to the results. What are the assumptions that have been made and how do they affect the results? What has not been considered? E.g. fluctuation in the wind speed and direction, the wind pressure coefficient as a function of the wind speed etc.

Both the falsifying approach by the crawl space example and the positivistic approach by the computer modelling of a ventilated façade were used during the PhD project.

1.4 Approach

The approach in the PhD project has been a combination of measurements and simulations, where the measurement results served as validation of the used computer model.

In a crawl space, relative humidity and temperature were measured for a one-year period, and supplemented by short-term air change measurements. Another object studied was a ventilated façade. Measurements on the physical model of a ventilated facade, were performed for short periods (hours), where also a tracer gas method for measuring the air change in the ventilated wall cavity was developed.

Simulations, with the developed mathematical model, analysed the influence of ventilation rate on the moisture content in a lightweight facade, to find moisture content in the wooden parts. Simulations were performed with normal ventilation and without ventilation and with normal and high-insulated walls. The results were used for discussion of future constructions, with increased insulation thickness and without ventilation.

Detailed knowledge about the wind pressure coefficients for the mathematical model was needed, in order to improve the mathematically model for realistic simulations of the wind pressure outside the openings of the cavity. Measurements of the wind pressure coefficients and the area roughness were performed and compared with theoretical values.

1.5 Outline of the thesis

First is a general description of different ventilated building components, and the moisture load benefit together with the problems related to the ventilation with outdoor air.

After some basic theory on the building physics, is a description of the experimental set up and instrumentation on a ventilated façade exposed to outdoor climate. Here a new way of measuring air velocity in the wall cavity, using tracer gas, is described. The tracer gas method is validated against thermo anemometer measurements.

The results of air velocity, by tracer gas, are analysed and afterward used for validation of a simulation model. The chapter ‘Simulation model’ is a description of the equations and assumptions behind a computer model, programmed in Simulink in the Matlab environment.

The model is used for yearly simulations with parameter variations, with conclusions and discussions of the moisture behaviour of a light weight façade wall.

In the ‘Discussion and Conclusions’ general remarks on ventilated envelopes are outlined.

2 Ventilation strategies for building envelopes

This chapter gives an introduction to the parts of the building envelopes, which are typically ventilated. The reason for ventilation is the assumption that outdoor air passing through a building envelope in average over time will dry the structure, even though wetting will occur in some periods.

The influence of ventilation on the moisture contents for different building envelopes and the dominant driving forces will be discussed for each construction, to clarify the similarity and the differences between the moisture behaviour of different ventilated building envelopes.

The question on whether ventilation has a positive or negative effect, on the moisture load of a building envelope, has no clear answer. It depends on many factors such as climate, conditions of the indoor air, the pressure difference between the outside and inside etc. Even in cases where the outdoor conditions together with the indoor seem to be of benefit for drying with ventilation, other factors such as dominating suction and failure in the air tightness can cause the opposite result, when ventilating the building envelope.

Here it is chosen to look at typical residential houses situated in cold climates like the Danish, with a normal indoor climate, and providing that the structures have no clear damages, i.e. the roofs and walls are rain tight and the drainage is functioning well.

2.1 Crawl space

Crawl spaces have a long history. When the first floors of wood were installed in the ancient houses, this was done with an air layer between the soil and floor. From the houses we know of today, this works fine without rot problems or mould damage. What should be noted is first that the floors lay high, so people walk up the house, and the ground floor of the crawl space is in the same level as the surroundings. Second that there is no insulation between the indoor of the house and the crawl space, so the temperature of the crawl space is close to that of the indoor climate.

The ground construction by a modern crawl space foundation became a commonly used construction in Denmark in the nineteen-sixties and -seventies. This modern type of crawl space lies below the surrounding ground terrain. The crawl space was designed as a cold or warm crawl space; referring to the temperature in the crawl space, see Figure 2.1.

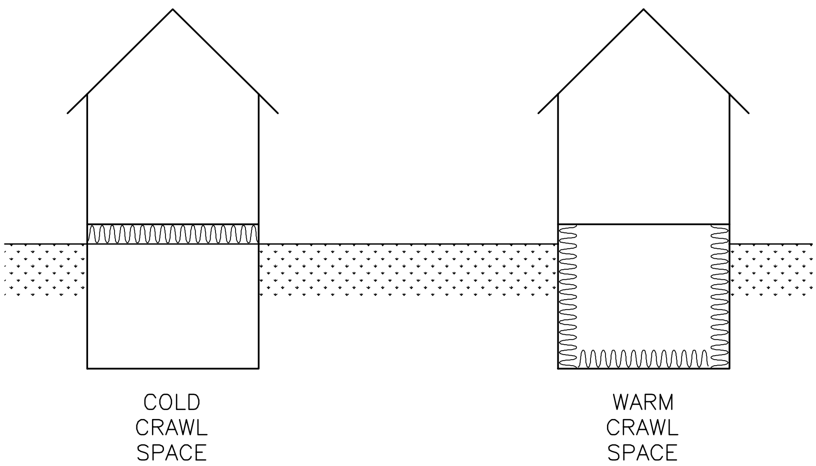

Figure 2.1The difference between cold and warm crawl space where the floor between crawl space and dwelling is insulated for the cold crawl space, and the crawl space walls and floor are insulated for the warm crawl space.

Over the last years, indoor air problems related to mould growth and moisture problems in the crawl space have been considered typically for both warm and cold crawl spaces. As a result of this, the crawl space construction is rare in new buildings today. The benefit of crawl spaces was not only cost effectiveness and easy access to water and heat installations, but also the preferable solutions for special wet ground, like boggy land. With the crawl space, the floor is effectively secured from capillary suction from the ground as there is no direct contact between the floor and ground, and the evaporated water can be removed by ventilation.

To understand the moisture problems of the modern ventilated crawl spaces the heat and moisture transfer processes must be understood. The heat transfer balance for the crawl space consists of heat transfer through the walls, ground and floor, the energy carried by the airflow and the radiation between the ground and the floor, Figure 2.2. The moisture balance for the crawl space consists of moisture flows carried by air change and ground moisture evaporation. The ground moisture evaporation depends on the mass transfer over the ground surface and the moisture transfer in the ground (Kurnitski, 2000). The air change rate is driven by wind, and sometimes by buoyancy force by installing a stack from the crawl space. The dominating force depends on the design and position of the ventilation openings.

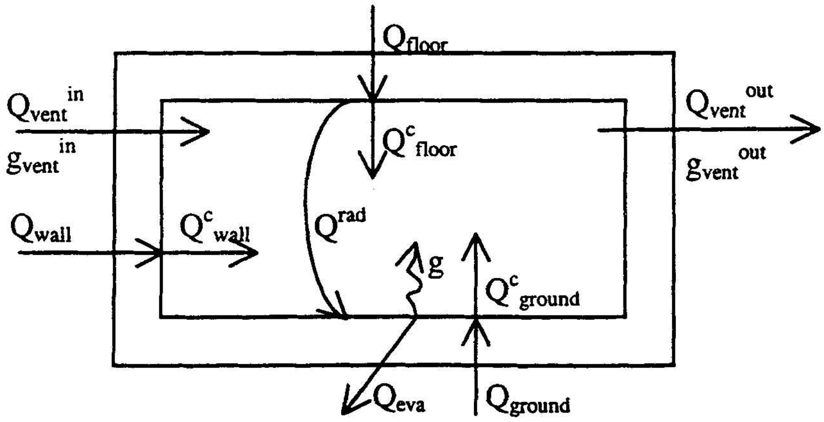

Figure 2.2 Dominating heat (Q) and moisture (g) flows in crawl space. Superscript 'c' marks convection. (From Kurnitski, 2000)

Most of the year, moisture is evaporated from the ground surface, but in the summer when the outdoor air temperature is higher than the temperature of the crawl space air or ground surface, the moisture transport may be reversed. The ventilation air wets the crawl space air and construction, when the warm and humid outdoor air enters the crawl space, and in some cases condensation occurs when the surface temperature of the crawl space is below the dew point temperature of the outdoor air.

Many explanations for crawl space moisture problems in modern buildings have been given, and many explanations are justified since moisture problems occur under different conditions, but are all related to high relative humidity. Kurnitski (2001) states that the main reason for the moist or wet ground surface is uncontrolled ground moisture evaporation and a lack of air change. He points out that modern buildings have the floor level in the crawl space lower than the outside ground level, which was not known in the traditional buildings. With the crawl space floor level lower than the outside ground level rainwater, surface water, and ground water drainage becomes moisture sources, and is one of the explanations for moisture problems in modern crawl spaces.

In a modern crawl space measurements and simulations by Gudum (1998, Appendix A) found the same moisture problems as described by Kurnitski (2001). Investigation of the modern warm crawl spaces by Gudum (1998, Appendix A) showed that identical crawl spaces might have very different moisture loads. Measurements of the relative humidity, temperatures together with air change rate combined with computer simulations using Cics (Åberg, 1997) were made on a warm ventilated crawl space, with reference measurements in two neighbour crawl spaces. The results showed no risk of high relative humidity in the investigated crawl space; however visual inspection in nearby identical crawl spaces showed heavy moisture problems. As the ventilation must be assumed approximately the same in all crawl spaces, the rain-, surface, and ground water drainage was concluded to be the source of moisture problems. In the investigated case of a warm crawl space it was therefore concluded that not the ventilation air of a warm crawl space, but the lack of drainage was the main risk of moisture problems in the crawl spaces.

For cold crawl spaces it is known that drying by ventilation is problematic, because the effect of ventilation can be both drying and wetting depending on the temperature and moisture content in the outdoor air compared to the crawl space air. During a warm summer period the outdoor air often has higher water vapour pressure than the crawl space air. This means that the ventilation air transports moisture into the crawl space in this period. This problem could be avoided with an unventilated crawl space, for a perfectly moisture sealed construction. In practice perfect sealing is very difficult to obtain, and any leakage can cause moisture problem when the diffusive and convective moisture transport takes place. Kurnitski (2001) shows that a higher air change rate increases moisture evaporation from the crawl space ground, but still is preferable because if any evaporation occurs, ventilation will always be needed to remove this moisture and to avoid almost saturated conditions in the crawl space.

Kurnitski (2001) concludes from his studies, that the key issue is to prevent water from entering the crawl space, but also that ventilation is always necessary if any moisture evaporation occurs. He finds that the second most important issue is the effective insulation of the cold ground, and recommends lightweight expanded clay as capillary breaking layer, and expanded polystyrene, which has both relatively high vapour and thermal resistance.

2.2 Light weight facade

Ventilation of light weight facades based on a wood frame is recommended in cold temperate climates i.e. in the Scandinavian Countries and Canada. Different traditions and rules of thumb provide different sizes of ventilation area or ventilation rate, in order to move the diffusive moisture from the indoor climate.

The heat balance for a facade, see Figure 2.3, is conductive heat transfer from the inside to the outside due to temperature difference over the wall, radiation heat loss from the outer surface together with the convective heat transfer, when outdoor air is passing through a ventilated cavity between the outside of the insulation and the rain screen. The moisture balance is diffusive moisture transfer from the warm towards the colder side, where water evaporates from the surface to the ventilation air passing through the structure.

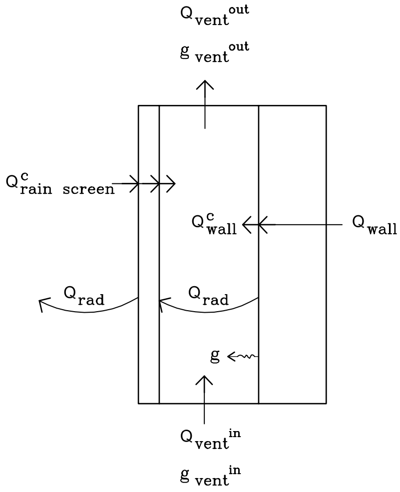

Figure 2.3 Dominating heat transfer (Q) and moisture transfer (g) for a ventilated wall. Superscript 'c' marks convection and 'rad' marks radiation.

For a facade wall, evaporation takes place from the outside of the rain screen. Driving rain gives periods with saturation of the rain screen, but the wetted rain screen also dries rather fast. This assumption of fast drying of rainwater is only valid, when drainage of rain is treated properly, so no rainwater remains in the structure after rain. Proper treatment means drainage behind the rain screen and it is here the pressure equalized rain screen (PER) shows its justification (Rousseau, 1999-b).

The PER stops the rain at the outside, but is open to the wind pressure. Which means that the pressure load is absorbed in the structure behind the rain screen. This prevents water to be pressed into the structure, and furthermore it prevents capillary suction between the rain-wetted surface to the inner layers.

For a facade with an air and vapour tight inner surface the vapour transport from the warm humid indoor climate to the cold and dry outdoor climate will be small. The vapour transport is dominated by convection between the air and the wall materials, when the outdoor air is passing through the cavity. When the moisture transfer from the inside is limited, the materials stay dry and the out-door air wets instead of dries the structure for some periods. Especially at cloudless nights, the temperature of the rain screen may fall below the dew point temperature of the air, due to heat loss by radiation, which also increases the heat loss of the wall behind the rain screen, so when outdoor air passes through the cavity, water condenses on the wall instead of evaporating from the wall. However, this wetting by outdoor ventilation air does not raise the moisture level to critical conditions, and the design is considered rather efficient to separate the wall from direct rain. The wall will, like the crawl space, be wetted and not dried from the ventilation in some periods. The opinion has until now been, that a wood based wall needs ventilation to be durable. However if wood siding is used in a four-storey building, the Danish building regulation (By- og Boligministeriet, 1995) requires compact walls without ventilation.

The ventilation air is driven by combined buoyancy effect and wind pressure difference between the vents. The wind pressure changes with the wind direction and wind speed. The wind pressure increases with the height and near the corners, and will be both positive (pressure) and negative (suction) as the wind direction changes. As the wind direction is mainly coming from few main directions, so will the pressure difference over a pair of vents be dominated by either suction or pressure. The ventilation rate in a wall cavity is driven by combined buoyancy force and wind force. The flow can be both upward and downward, depending on the dominating force. Also the fluctuating nature of the wind has some but unknown influence on the effective ventilation rate (Kronvall, 1980)(Burnett and Straube, 1995). The heat and moisture processes of the cavity air are coupled heat and moisture balances for: a)the air barrier, b)the outdoor ventilation air, and c) the rain screen. Heat transfer through the wall and rain screen is transferred to the air by convection and energy carried by the airflow form the heat balance. The moisture balance includes the moisture carried by the airflow and the evaporation from the wall.

In cold climates the diffusive moisture transport is most of the year from the inside to the outside, due to a higher water vapour pressure on the inside than on the outside. On a warm summer day with direct sun on a facade the temperature increases and the direction of water diffusion is opposite, from the outside to the inside. When the wall is made with a vapour tight layer on the inside, the vapour driven into the wall will condensate on the vapour tight layer (summer condensation).

If exfiltration (outward air movement) with indoor air occurs, the convective moisture transport can be increased significantly, to an amount that cannot be removed by ventilation. The importance of airtight structures are therefore emphasised many places in the literature (Burch and TenWolde, 1993)(Ojanen and Kumaran, 1996) (Hagentoft and Harderup, 1996). Also a vapour resistance on the warm side of the insulation has been shown to be important in order to limit the diffusive moisture transfer to a level, where the ventilation can keep up with the moisture load,(Andersen et al., 2001) (Burch and TenWolde, 1993). Likewise have Simonson and Ojanen (2000) , advised vapour retarder, and they have found that the indoor vapour diffusion resistance should be greater than the outdoor vapour diffusion resistance by a factor of only 3:1, meaning that the vapour retarder can be made of other materials than plastic.

The strategy for facades has been that the building envelope should be prepared for drying, since it is impossible totally to prevent water to enter the structure both from the inside and the outside. By inserting an air layer, ventilated by outdoor air, the envelope is expected to dry. However, as for the crawl space the ventilation air may also wet the structure in periods. If the wall is rather dry due to a perfectly functioning vapour retarder, the ventilation with outdoor air wets the wall, but never to a critical long period with a critical high level. On the other hand if the vapour retarder is imperfect, the ventilation with outdoor air can have a positive effect on the moisture load of the wall according to computer analysis by Burch and TenWolde (1993). Salonvaara et al. (1998) finds similar results from laboratory experiments and advanced computer simulations. They show that a wall with high moisture load from either indoor exfiltration, or vapour retarder replaced by wallpaper dries with ventilated cavity and stays wet without ventilation. Further they conclude that higher vapour diffusion resistance of the inside sheathing layer (vapour retarder) resulted in lower moisture loads from the inner wall into the cavity and lower requirements for cavity ventilation.

Measurements on light weight facades with and without ventilation and with and without vapour retarder by Andersen et al. (2001) show that a ventilated facade wets faster but dries with the same rate as an unventilated facade. This indicates that an airtight wall with vapour retarder will function without ventilation. They also find that mold growth only occurred behind a steel beam for the unventilated facade, and therefore conclude that the unventilated facade is more sensitive towards other effects like cold bridges. In facades without vapour retarder the moisture load was unacceptable high both with and without ventilation, and the highest moisture content was observed in the unventilated facade.

2.3 Flat roof

Flat roofs were popular in the nineteen-sixties and –seventies, and besides from the look they had lower cost of materials and installation than traditionally sloped roof. Problems with the rain tightness were solved with better materials, construction details and a minor slope to drain rainwater. However, dripping water indoor was still seen from rain tight flat roofs.

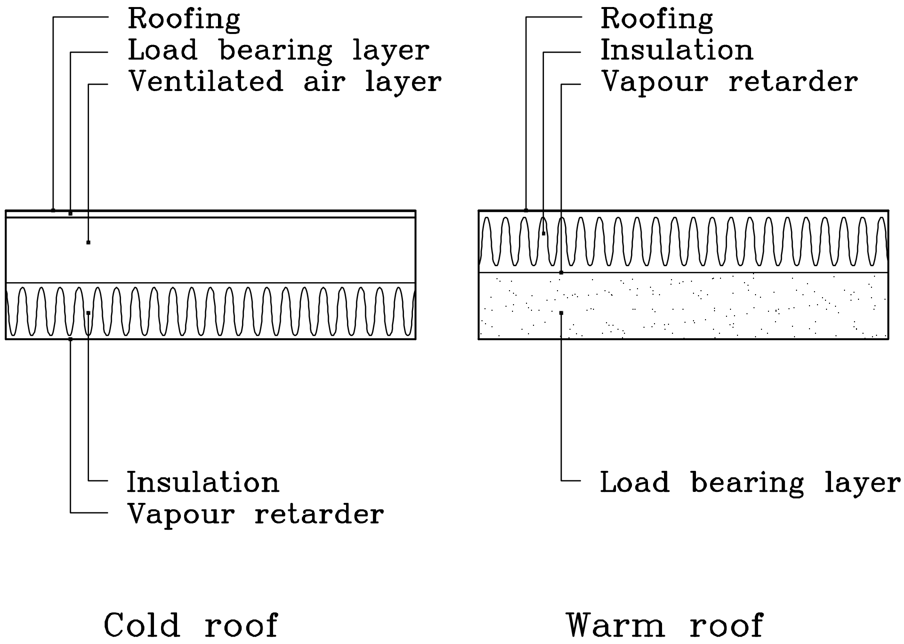

Figure 2.4 The difference between cold and warm roof where the cold roof is ventilated with outdoor air and the warm is not ventilated.

The flat roof can be made with a ventilated layer above the insulation (cold roof) or without ventilation where the insulation is typically placed directly on the top of a load-bearing concrete deck (warm roof), see Figure 2.4. For both the warm and cold roof a vapour retarder and an air-tight layer is imperative (Andersen et al., 1993)(Rasmussen, 1992).

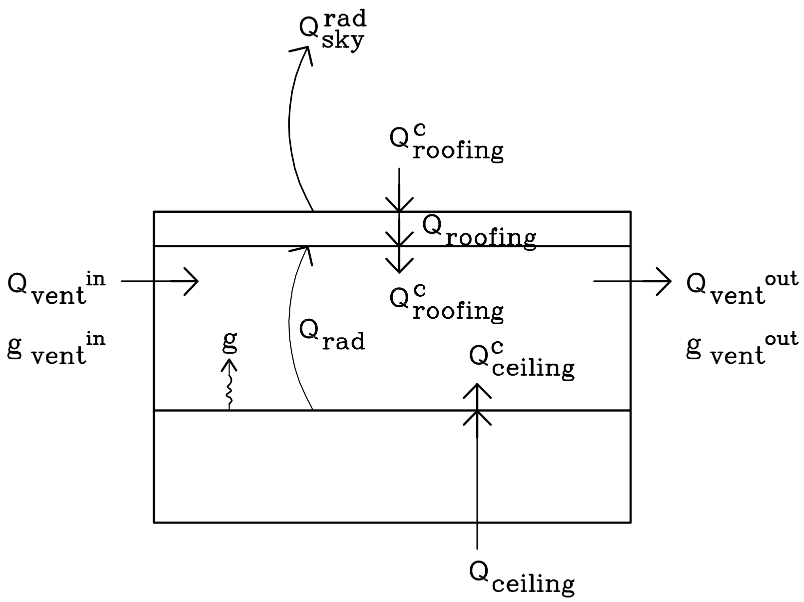

Figure 2.5 Dominating heat transfer (Q) and moisture transfer (g) for a ventilated flat roof. Superscript ‘c’ marks convection and ‘rad marks radiation.

The heat balance of a flat roof, Figure 2.5, is similar to that of the facade, with conductive heat transfer between inside and outside due to temperature difference, radiation heat loss from the outer surface together with the convective heat transfer, when outdoor air is passing through a ventilated cavity between the outside of the insulation and the roofing. The moisture balance is diffusive moisture transfer from the warm towards the colder side; where water evaporates from the surface to the ventilation air passing through the structure.

For a ventilated flat roof a considerable amount of indoor moisture will move into the roof structure by convection, if the vapour barrier of the ceiling is not airtight. Here the ventilated roof will actually have a higher moisture load compared to a non-ventilated flat roof. The explanation is that the wind pressure above a flat roof and at the leeward eave typically cause the air pressure to be less than inside the building. To increase the ventilation for drying of the flat roofs, vents from the cavity to the outer surface of the roof were required in a period. The vents gave good pressure release between the roof cavity and the outside air. However, together with the stack effect during winter, this resulted in lower air pressure in the roof cavity than in the building interior. Thus, moisture was transported by convection into the roof from the dwelling below, through cracks and unintended penetrations of the interior lining of the roof (Vesterløkke et al. 1992). The humid indoor air, which was dragged into the roof construction through any imperfections of the airtight layer or unsealed joints, condenses and causes mould and rot. Vesterløkke et al. (1992) conclude from measurements that the problem with introducing an unvented roof in climates where a vapour retarder is necessary is that construction moisture or moisture from leaks has no way to escape. It should be noted, however, that for roofs with distances less than 10 m between the eaves, ventilation from eave to eave is still regarded as a functional precaution, as long as the roof surface has no vents.

During sunny days the flat roof is heated, and the water is pressed towards the indoor where the vapour can either condensate on the vapour retarder causing damage on the wood parts, or dripping water from the ceiling can be observed, (Andersen et al., 1993).

The heat loss by radiation is rather significant for a flat roof. This causes the temperature of the roof to decrease below the dew point temperature of the outdoor air, and risk of condensation of water from the air, which is ventilated through the roof, is high.

In contrast to other parts of the building, where changing wind direction forms pressure and suction, there is constantly suction over a flat roof due to wind pattern and indoor air pressure. The flat roof is therefore more sensitive towards air-leakages, when only exfiltration and no infiltration occur.

Ventilation for drying the cold part of the roof is normally recommended from eave to eave in combination with an airtight ceiling. Due to the indoor overpressure, this has shown to be quite risky as it can increase the convection from the indoor to the construction considerably. On the other hand moisture from the indoor transferred by diffusion and construction moisture must be removed from the roof to avoid critical moisture load.

2.4 Sloped roof and attic

The ceiling can either be horizontal with an attic above or sloped, parallel to the outer roof surface. The attic is often used for storage, whereas the space under the sloped roof serves as habitation. For sloped roofing like tile, it is common to use an underroof to drain melted drifting snow and driving rain. The underroof can be vapour permeable or vapour tight. If the more closed material is chosen, ventilation is performed between the insulation and the underroof. If instead the vapour permeable material is used, the underroof can be placed directly on the top of the insulation material, with ventilation above the underroof, see Figure 2.6.

A problem known from the sloped roof is, that it might be problematic to keep a free passage for the air between the insulation and the under-roofing. The under-roofing tends to stretch with time, and ends on the insulation stopping the ventilation air to pass. This problem can be avoided by using a board material as under-roofing.

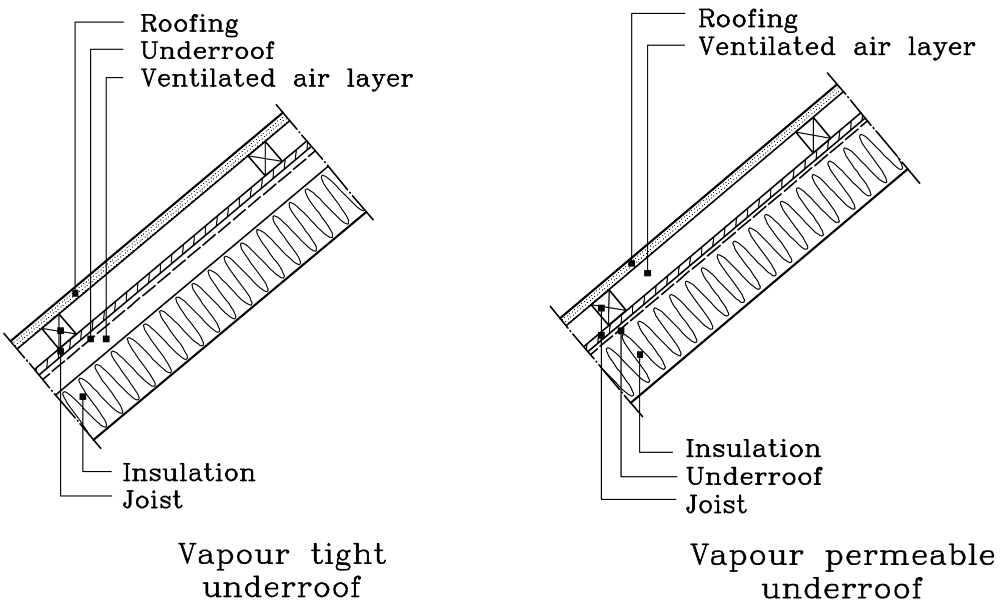

Figure 2.6 Sloped roof construction with a vapour tight underroof is ventilated below the underroof., where a permeable underroof is ventilated above the underroof

The dominating heat and moisture effects are seen in Figure 2.7. The heat balance for the ventilated cavity of a sloped roof or an attic, is heat loss by conduction between the cavity or attic and the dwelling, convective heat loss when outdoor air passing through the structure, and radiation between the surfaces, where the roofing can be rather cold due to sky radiation. As for the ventilated facade and ventilated flat roof, unintended moisture coming into the roof or attic is moved by ventilation with outdoor air. Again the risk of condensation of the moist in the ventilation air occurs, when the heat loss by sky radiation cools the roofing. The ventilation is driven by a combination of stack effect and wind pressure, like for the facade, the change in wind direction changes the wind load and the air flow change direction.

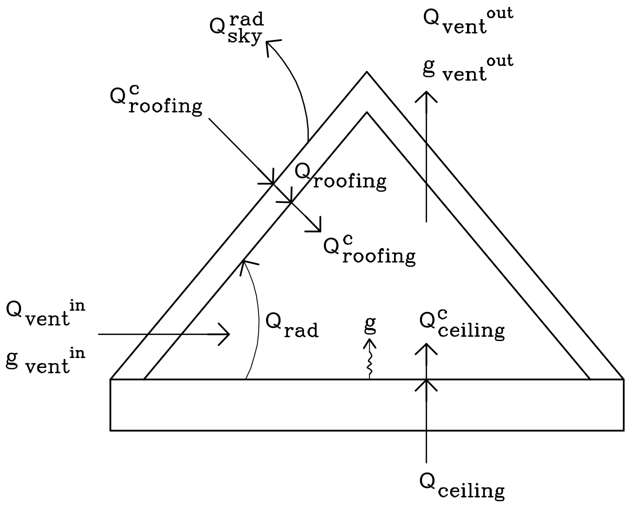

Figure 2.7 The dominating heat transfer (Q) and moisture transfer (g) for a ventilated attic. Superscript 'c' marks convection and 'rad' marks radiation

Exfiltration of humid indoor air will take place to the roof or attic through cracks and unsealed joints, and further moisture will be transferred to the roof by diffusion. The ventilated cavity, of either the sloped roof or attic, moves the moisture and keeps the relative humidity below critical moisture conditions. As for the flat roof, the wind has a significant impact on the ventilation. However, when sloped roof and attic are exposed to the outdoor climate, changing suction and pressure due to the wind load will affect the air change of the roof cavities, meaning that the ventilation will not have the same dragging effect of indoor air into the roof (exfiltration) as was the case for the flat roof, because infiltration (outwards air movement) may also occur. Even though the airflow moves both in and out of the construction, the importance of airtight and also vapour tight lining on the warm side of the insulation is also significant here for balancing the moisture content of the materials in the structure.

For both the sloped and horizontal ceiling, with permeable or closed underroof the ventilation should be rather high, Nevander (1994). He points out that the air change and leakages to the inside are normally unknown. However, it is considered to be approximately 2 ach (air change per hour), with the normal used vents, although the ventilation will vary with the wind speed.

The effect of sun heating of the roof increases the ventilation by stack effect, and increases the drying by rise of temperature. Furthermore, with the sun the risk of summer condensation increases, which means that moisture condenses on the outside of the vapour retarder. The heat loss due to sky radiation is another important factor, for understanding the heat and moisture transfer processes in roofs. Due to radiation the roof temperature can decrease below the dew point temperature of the outdoor air, causing outdoor ventilation air to wet the roof structure.

Larsson(2001) studied the heat and moisture balance, together with the critical moisture conditions in an attic with high-insulated ceiling construction. He found that a better (increased) ventilation during winter induced a higher amount of moisture in the roof sheathing, quite the reverse of what might be expected. From Larssons results it was evident, that a more intensive ventilation of the attic, when a thick insulation of the top of the ceiling was used, did not ensure the expected drying out of the attic during the winter. Therefore it was concluded that ‘the risk for fungus growth appears to have increased when we have begun to insulate the attic ceilings more heavily in order to save energy’. Larsson suggested that a way to design the attic is to put all the heat insulation on the roof.

Samuelson (1996) finds, through measurements on ventilated attics, that the higher the amount of outdoor-air ventilation, the greater the variations in relative humidity and temperature. He also finds that the climate in the attic becomes drier the less it is ventilated. He emphasis, that the measurements have been performed on an experimental house, where the moisture from inside the building has been eliminated by totally airtight ceiling and by negative pressure in the structure beneath the attic.

Janssens and Hens (1996) find for sloped roof, that perfect air tightness is not needed to prevent problems if either an underroof with high vapour permeance or a board with high moisture capacity is used. Janssens (1998) supplement this with measurements and computer simulations, where he concludes that the effectiveness of vented cavity is uncertain for sloped roof. He suggests that if the insulation thickness is increased a minimum portion of the roof thermal resistance is located outboard of the structural cavity, like Larsson suggested it.

Janssens' conclusions for reliable roof design is that layers located at the inside of the roofing system have a minor influence on the condensation risk but the risk for condensation due to a lack of continuity of air-tightness in a cavity insulated roof essentially depends on the properties and design of the roofing system, which contains all the layers outside of the structural cavity. This was what also Larsson suggested, although he emphasized the importance of an airtight and vapour tight layer on the inside.

2.5 Summary

The general conclusions for ventilated building envelopes are, that a both airtight and vapour tight layer is required on the warm side of the insulation, and that some ventilation keeps the structure dry, but too much ventilation increases the moisture load.

For the perfectly sealed structure, ventilation with outdoor air on the cold side of the insulation increases the moisture load. However, in cases of imperfections, the ventilation with outdoor air seems to help the structure to stay on an acceptable moisture level.

Increased insulation thickness seem to be problematic, because it reduces the temperature of the ventilated cavity, while the relative humidity is raised to an unacceptable level for a longer period compared to a situation with thinner insulation.

If parts of or all the insulation is placed on the outer surface, then condensation on cold surfaces due to radiation could be avoided, even with increasing the insulation thickness, and keeping the ventilation on a minimum.

3. Basic theory

The chapter describes the transport mechanisms and the overall equations for the heat, air, and moisture transport (HAM), which are considered in the present work. The more detailed choices between models and equations are described in the chapters where they were used, especially in the Chapter 7 ‘Simulation model’.

The theory for convective heat and moisture transfer is essential to the topic of the thesis and was described first followed by the theory for volume airflow through vents and ducts. The volume airflow is driven by a pressure difference, which is described separately for wind force and for buoyancy force. As the reader is expected unfamiliar with wind-induced pressure, this part has been given high priority. The chapter ends with theory for moisture equilibrium in air and materials.

To help the understanding of the following section a few definitions are needed. Heat is energy transferred due to a temperature difference by convection, conduction and radiation. Thermal convection is energy transferred by fluid movement and molecular conduction. Thermal conduction is kinetic energy transferred between particles at atomic level. Thermal radiation is transfer of electromagnetic energy between surfaces.
Where conduction and convection heat transfer takes place through matter, thermal radiation is between surfaces, (ASHRAE, 1997).

In general when mass in the form of liquid or gas is transferred due to a mass concentration gradient, it is called diffusion. If there is a fluid movement, the mass is also transported by movement of the fluid itself, called convection (Kays and Crawford, 1993).

Specific for mass transfer in building physics, it is common to analyse the moisture transfer in the form of either water vapour or liquid water, Nevander (1994). Moisture transfer is a product of a transfer coefficient and a gradient of the driving potential Eq 3.1

Eq 3.1 $g_x = -k \cdot \frac{d\psi}{dx}$

where

g_x	is the moisture transfer in the x-direction
ψ	is the potential, e.g. vapour pressure, water pressure, temperature, suction pressure, air pressure, wind pressure, gravity etc.
x	is the place coordinate
k	is the transfer coefficient

The mechanisms that are considered the most important, and the ones that are included here are listed in the Table 3.1.

Table 3.1 The HAM mechanisms included here in the analysis of a ventilated building envelope.

Mechanism:	**Material layer**	**Cavity**	**Surface**
Heat transfer	Conduction	Convection Radiation	Convection Radiation
Moisture transfer	Diffusion	Convection	Convection

However, some important potentials are not considered. Both heat and moisture transfer by convection is neglected in the material layers for simplifications, even though Dyrbøl (1998) has shown that significant heat convection occurs even in ‘perfectly’ installed materials with low permeability, impermeable boundaries and at small temperature differences. The moisture transport through the rain screen is considered insignificant, which is a rough assumption for hygroscopic surfaces exposed to direct rain.

In air-ventilated cavities the heat and moisture transfer is dominated by convection. Here the conduction and diffusion are neglected. For the heat transfer also the radiation between surfaces of the ventilated cavity is considered. For HAM transport for the outside surface of a structure to the surroundings, the convection and radiation are considered as the most important transfer mechanisms as well.

3.1. Convective heat and moisture transfer

Convective heat transfer and convective mass transfer are heat transfer and mass transfer processes by fluid flow. This transport mechanism has been investigated in detail in many fields when there is a fluid motion. One example is a heat exchanger, where the fluid motion is used for increasing the transport of thermal energy.

When air is streaming along a surface, heat and vapour exchange will take place if there is a difference in temperature or water vapour pressure. The rate of transport is described by a transfer coefficient, which changes with temperature, velocity, and moisture concentration.

The convective moisture transport in a ventilated cavity takes place when the passing air changes its moisture content, resulting in either drying or wetting the structure. A moisture balance for the cavity air, Eq 3.2, describes the moisture flow rate, *g*, of the cavity air. The vapour that evaporates from or condensates on the cavity surfaces, Eq 3.3, is equal to the convective moisture transport, *g*, where the moisture transfer coefficient will depend on the air velocity over the surfaces.

The vapour mass flow, *g*, carried by ventilation air is described as:

Eq 3.2 $g = (c_{out} - c_{in}) \cdot Q$

where

g	is the mass flow rate [kg/s]
c_{out}	is the water vapour concentration of the air leaving the building envelope [kg/m^3]
c_{in}	is the water vapour concentration of the air entering the building envelope, i.e. water concentration of the outdoor air [kg/m^3]
Q	is the air change by volume [m^3/s]

Since the moisture transport through the rain screen is considered insignificant here, the vapour mass flow carried by ventilation air is equal to the moisture that evaporates from or condensates on the inner surface. The mass flow can also be found as:

Eq 3.3 $g = \beta \cdot \left(p_{surface} - p_{air}\right) \cdot A$

where

β	is the moisture transfer coefficient [kg/(Pa m^{2}s)]
p	is the water vapour pressure for the *surface* and cavity *air* respectively [Pa]
A	is the area [m^2]

3.1.1. Convective heat transfer coefficient

Thermal convection is the energy transport due to fluid movement (liquid or gas) over a surface. Three regimes of convection may be defined; natural, mixed and forced convection. Natural convection involves motion in a fluid due to difference in density and the action of gravity. Forced convection, when an outside force influences the fluid flow, such as wind pressure or fans. In between the natural and the forced regime is the mixed convection regime. For mixed convection the natural convection can affect the heat transfer coefficient in the presence of weak forced convection (ASHRAE, 1997), i.e. the theory for natural convection can be used for mixed convection too. For normal building structures the airflow will typically be affected by both buoyancy effect (natural convection) and wind pressure (forced convection) and therefore, the convection is considered as mixed. The flow in each regime may be characterised as laminar, transitional or turbulent, described by the size of the dimensionless Reynolds number (Re). Where (ASHRAE, 1989) states for ducts:

Laminar region	is for Re<2000
Transition region	is for 2000<Re<10,000
Turbulent region	is for Re>10,000

Where Reynolds number $\mathrm{Re} = \frac{u \cdot d}{v}$

u	is the mean velocity [m/s]
d	is the hydraulic diameter [m]
v	is the kinematic viscosity [m^2/s]

The convective heat transfer coefficient is described for many different geometries and cases in the literature, based on empirical constants. It is common to divide the different cases after the ventilation force and further distinguish between the types of flow (laminar, transitional or turbulent) (Kays and Crawford (1993) and ASHRAE (1997)).

For natural convection, the heat transfer coefficient, h [W/m^2K], can be described by the general relationship (ASHRAE, 1997):

Eq 3.4 $h = \frac{Nu \cdot \lambda}{D_h}$

where

Nu	is the Nusselt number [-]
D_h	is the hydraulic diameter [m]
λ	is the thermal conductivity for the fluid [W/mK]

The dimensionless Nusselt number is defined as the ratio between heat transfer with convection and heat transfer without convection (Dyrbøll, 1998). Empirical equations for the Nusselt number can be found in the literature for the different regions in each regimes (Bird et al.,1960)(Kays and Crawford, 1993)(ASHRAE, 1997).

3.1.2. Convective moisture transfer coefficient

To determine the moisture transfer coefficient between surfaces and the air, it is common to use the Lewis correlation for building applications, [Kurnitski, 2000] [Burnett & Straube, 1995]. The moisture transfer coefficient in terms of water vapour pressure as driving potential, β [kg/(s Pa m^2)], can be determined in terms of the convective heat transfer coefficient.

Eq 3.5 $$\beta = \frac{h}{R_v \cdot T \cdot \rho \cdot c_p}$$

where

h	is the convective heat transfer coefficient [W/m^{2}K]
R_v	is the gas constant for water vapour, 461.5 J/kg K
T	is the absolute temperature [K]
ρ	is the air density, 1.25 kg/m^3
c_p	is the specific heat capacity of air, 1003 J/kg K

It should be noted that the Lewis correlation is valid with the assumption of a laminar boundary layer, and theoretically it cannot be transformed into turbulent flow ((Kurnitski, 2000), who refers Lampinin (1996)). Kurnitski (2000) also states that in practice, Lewis correlation is widely used for turbulent flow as well , and what was also done here.

3.2. Heat transfer by radiation

The energy exchange by radiation between bodies depends on the absolute temperature, emissivities, the areas, and the view factors.

In order to retain the simplicity of linear equations, a radiation heat transfer coefficient, h_r, is defined. The heat transfer by radiation in between two surfaces 1 and 2 gets the form:

Eq 3.6 $$q_r = h_r \cdot (T_2 - T_1)$$

where

Eq 3.7 $$h_r = \frac{\sigma_s \cdot (T_2^2 + T_1^2) \cdot (T_2 + T_1)}{\frac{1-\varepsilon_1}{\varepsilon_1} + \frac{1}{F_{12}} + \frac{(1-\varepsilon_2)A_1}{\varepsilon_2 A_2}}$$

where

σ_s	is the Stefan Boltzmann's constant
F_{12}	is the view factor between surface 1 and surface 2
A	is the area of the surface [m^2]
T	is the temperature of the surface [K]
ε	is the emmisivity of the surface

The cavity radiation between two parallel plates with a small distance, compared to the surface area of the plates, has a view factor F_{12}≈1 (Hadvig, 1986) and A_1=A_2. The radiation heat transfer coefficient can be simplified to:

Eq 3.8 $h_r = \dfrac{\sigma_s \cdot \left(T_2^2 + T_1^2\right) \cdot \left(T_2 + T_1\right)}{\dfrac{1}{\varepsilon_2} + \dfrac{1}{\varepsilon_1} - 1}$

Duffie & Beckmann (1991) states in accordance with Hagentoft (2001-b) and Andersen (1989) that when T_1 and T_2 are close together:

Eq 3.9 $\sigma_s \cdot \left(T_2^2 + T_1^2\right) \cdot \left(T_2 + T_1\right) \cong 4 \cdot \sigma_s \cdot \left(\dfrac{T_2 + T_1}{2}\right)^3$

Andersen (1989) shows using Eq 3.9 causes less than 1% error, for a temperature difference up to 50°C. By introducing the mean temperature T_m and an overall emissivity ε_{12}, the radiation heat transfer coefficient, Eq 3.8 becomes:

Eq 3.10 $h_r = 4 \cdot \varepsilon_{12} \cdot \sigma_s \cdot T_m^3$

where

Eq 3.11 $T_m = \dfrac{T_2 + T_1}{2}$ and

Eq 3.12 $\dfrac{1}{\varepsilon_{12}} = \dfrac{1}{\varepsilon_1} + \dfrac{1}{\varepsilon_2} - 1$

3.3. Volume air flow by power law

The volume airflow in a duct, *Q* [m^3/s], depends on the pressure difference (driving potential) and the total pressure resistance along the flow path. The pressure difference depends on both the wind pressure difference between the openings and the buoyancy force. The effective pressure difference is found by addition of the wind and buoyancy force.

The power law is commonly used for calculations of the volume airflow rate, *Q*, across a cavity for buildings, like i.e. a ventilated facade cavity (Straube and Burnett, 1995). The power law is expressed as:

Eq 3.13 $Q = C_D \cdot A \cdot \left(\dfrac{2 \cdot \Delta P}{\rho}\right)^n$

where

C_D	is the discharge coefficient
A	is the area of the orifice
ρ	is the density of air [kg/m^3]
ΔP	is the pressure difference between the vents, including both wind pressure and buoyancy effect [Pa]
n	is the flow exponent, 0.5<n<1 with n=0.5 for turbulent flow and n=1 for laminar flow

The discharge coefficient, C_D, is the reduction of airflow across openings due to contraction of the flow and friction and turbulence losses. The discharge coefficients, or the friction factor for different vents and orifices, used for ventilation systems can be found in the literature for high velocity flow (typically >2 m/s) (Sørensen, 1996). The flow rate through building envelope assemblies and components is found in the literature, where airflow in ventilated facades is described by Straube and Burnett (1995), Kronvall (1980), and Andersen (2000).

The Darcy-Weisbach equation is commonly used to give the pressure drop due to friction in airflow through pipes:

Eq 3.14 $\Delta P_{pipe} = f \cdot \frac{L}{D_H} \cdot P_V$

where

f	is the friction factor [-]
L	is length of flow path [m]
D_H	is the hydraulic diameter [m]
P_V	is the dynamic pressure due to kinetic energy [Pa], $P_V = \frac{1}{2} \cdot \rho \cdot V^2$
V	is the mean air velocity [m/s]

For laminar flow in a channel the friction factor can be estimated from

Eq 3.15 $f = \frac{96}{\mathrm{Re} \cdot \gamma}$

where

γ	is a blockage factor, accounting for rough surfaces and obstructed cavities
Re	is Reynolds number

The Darcy-Weisbach equation can also be written in terms of resistance factor, ξ:

Eq 3.16 $\Delta P_{pipe} = \xi \cdot \left(\frac{1}{2} \cdot \rho \cdot V^2\right)$

In order to compare different estimates for the volume air flow, based in either the power law or the Darcy-Weisbach formula, the correlation between discharge coefficient and the contraction loss factor is derived.

The pressure loss across two vents and cavity, will equal the pressure drop due to external driving forces (Burnett and Straube, 1995)

Eq 3.17 $\Delta P_{drive} = \Delta P_{vent,entrance} + \Delta P_{pipe} + \Delta P_{vent,exit}$

Eq 3.18 $\Delta P_{drive} = \left(\xi_{entrance} + \xi_{pipe} + \xi_{exit}\right) \cdot \left(\frac{1}{2} \cdot \rho \cdot V^2\right)$

It is seen that the power law, Eq 3.13, can be derived from the equation above, using

Eq 3.19 $V = \frac{Q}{A_C}$

where

A_C	is the cross sectional area

We now find:

$$\Delta P_{drive} = (\Sigma\xi)\cdot \tfrac{1}{2}\cdot \rho \cdot \left(\frac{Q}{A_C}\right)^2$$

$$\Updownarrow$$

$$\left(\frac{\Delta P_{drive}}{\Sigma\xi \cdot \frac{1}{2}\cdot \rho}\right)^{\frac{1}{2}} = \frac{Q}{A_C}$$

$$\Updownarrow$$

$$Q = \left(\frac{1}{\Sigma\xi}\right)^{\frac{1}{2}} \cdot A_C \cdot \left(\frac{\Delta P_{drive}\cdot 2}{\rho}\right)^{\frac{1}{2}}$$

$$\Downarrow$$

Eq 3.20 $C_D = C_C \cdot \sqrt{\frac{1}{\Sigma\xi}}$

where C_C is the contraction factor (≈ 0.7)

Using Darcy-Weisbach, the resistance factor varies with the flow rate and is different for laminar and turbulent flow. It is noted that the exponent *n*=0.5, which is used for turbulent flow in the power law. In the Darcy-Weisbach the distinguishing is in the resistance factors, where they are different for laminar and turbulent flow.

For laminar channel flow

Eq 3.21 $\xi = \frac{96}{\mathrm{Re}\cdot \gamma} \cdot \frac{L}{D_h}$

where

ξ	is the resistance factor
γ	is a blockage factor used for very rough or partially obstructed cavities. (Straube and Burnett, 1995)(Kays and Crawford,1993).
Re	is Reynolds number
L	is the length of the channel in the flow direction
D_h	is the hydraulic diameter of the duct

For turbulent flow, where *f*>0.018, Eq 3.15 (Straube and Burnett, 1995)

Eq 3.22 $\xi = 0.11 \cdot \left(\frac{\varepsilon}{D_h} + \frac{68}{\mathrm{Re}}\right)^{0.25} \cdot \frac{L}{D_h}$

where

ξ	is the resistance factor
ε	is the absolute roughness
D_h	is the hydraulic diameter of the duct
Re	is Reynolds number
L	is the length of the channel in the flow direction

3.3.1. Flow exponent

For practical building calculations, Nevander (1994) suggests power law, Eq 3.13, with a constant value for the exponent, n=0.70. Burnett and Straube (1995) finds from test of steady-state flow through different sizes of orifices, that an exponent of n=0.5 fit fairly well. Only the very small orifices seem to have a larger exponent than 0.5. Andersen (2000) operates for flow in ventilated facades with an exponent of 0.5.

As Burnett & Straube (1995) and Andersen (2001) agree about an exponent of 0.5, and they are working with ventilation of wall cavities, where Nevander (1994) considers buildings in general, n=0.5 is chosen as exponent for later calculations of the flow rate with power law, for a ventilated facade.

3.4. Pressure difference between vents

The total pressure difference is found from addition of the wind and buoyancy force (Hagentoft, 2001).

$$P_{total} = P_{wind} + P_{buoyancy}$$

3.4.1. Pressure difference due to buoyancy force

Natural convection, buoyancy, or stack effect is the air movements due to difference in density. The density of the air decreases with the temperature, while warm air tend to rise over cold air. The buoyancy effect, $P_{buoyancy}$ [Pa], can be expressed as:

Eq 3.23 $P_{buoyancy} = \rho \cdot g \cdot h \cdot \Delta T$

where

ρ	is the density of air [kg/m^3]
g	is the gravity [m/s^2]
h	is the vertical height between two vents [m]
ΔT	is the air temperature difference between the vents [K]

3.4.2. Wind induced pressure

The wind is fluctuating both in velocity and direction, which influence the resulting air pressure and therefore the resulting airflow inside ventilated building envelopes.

Airflow around buildings are traditionally studied by means of scaled model tests in wind tunnel facilities, in order to estimate the wind load on the building site, and to find the static strength required for the building. The wind tunnel experiments are expensive, and less costly alternatives using computer modelling is under development.

The pressure induced by the wind, which acts on a surface, varies over the surface and with the wind angle. The wind pressure has been investigated for building purposes (Jensen, 1959), in order to find the structural load. Wind pressure coefficients over a building surface can be found for different building heights, width to length ratio and surface orientation in (Jensen, 1959) and (Orme et al., 1994).

Recently the wind load has been given some interest from the ventilation perspective (Orme et al., 1994) (Roussau, 1999-b), where especially the pressure distribution over the surface has been given interest in order to improve the estimation of the wind driven ventilation.

The commonly accepted and used model, being proposed to quantify the correlation between wind velocity and wall pressure, is a quasi-steady theory assuming that the flow is proportional to the squares of the instantaneous velocity components (Swami and Chandra, 1994). Others have shown that a better description is found by using wavelet analysis (Jordan et al.,1997), which is not fully validated or approached, and will not be used here.

The quasi-steady theory involves the wind pressure coefficient, *Cp*, which gives the ratio between energy transformed to static pressure at a location on a given façade and the kinetic wind energy (dynamic pressure) in the free wind field.

The pressure difference between a specific location and a reference point is related to the mean horizontal wind speed at a reference height, the correlation is described by the wind pressure coefficient (*Cp*). The *Cp* is defined (Swami and Chandra, 1994) as

Eq 3.24 $$Cp = \frac{P - P_{ref}}{0.5 \cdot \rho \cdot u_{ref}^2}$$

where

P	is the local static wind pressure measured on a surface [Pa]
P_{ref}	is the static wind pressure measured in the free steam at the reference height [Pa]
ρ	is the density of the air [kg/m^3]
u_{ref}	is the wind velocity in the reference height [m/s]

The wind pressure coefficient depends on the wind direction, but is independent of the wind velocity. Both the geometry of the building, the roughness of the surroundings and obstacles near the building will influence the Cp-value. A numerical model for estimation of the wind pressure coefficients has been developed by Knoll et al. (1996). Here the calculated coefficients were called ‘theoretical value’ to distinguish them from experimental ‘measured values’.

The wind pressure coefficients changes over the surface, i.e. a pressure difference between two vents, due to wind acting on the building, will occur. When knowing the wind pressure coefficients at position of the vents A and B, the pressure difference is estimated as

Eq 3.25 $$\Delta P = (Cp_A - Cp_B) \cdot \tfrac{1}{2} \cdot \rho \cdot u_{ref}^2$$

3.5. Wind direction

Wind velocity and wind direction are common values found in weather reference years. The Danish Design reference year (DRY) has, as other reference years, hourly mean values of the wind direction and the wind velocity, with a time-constant for the measurements at 10 minutes.

As the wind velocity changes with the height over the ground, the wind velocity is given for a reference height of 10 m above the ground in an open terrain without obstacles.

Calculation of the average wind direction from measurements should be carried out with special care. The wind direction is measured in the interval [0-360°], when calculating the mean value of the wind direction for direction around 0° (north) the mean value is 180° (south). If the mean value is calculated together with the standard deviation of the wind direction, it will be clear, that if the standard deviation is high i.e. >90° the mean value cannot be considered as the average wind direction. A solution could be changing the interval to [–180°-180°], but now the same problem will occur when the wind direction is south. Instead of the arithmetic mean value the dominant direction could be used.

An alternative solution could be defining the wind direction as a vector, with direction as the wind and length 1. The vectors should then be added, and the direction of the resulting vector would then be the average direction of the wind.

3.6. Wind velocity

The atmospheric boundary layer (ABL) is the layer where the flow is directly influenced by the surface of the earth, and where the flow is retarded by surface friction (Bottoma, 1993). In the ABL the air is mixed by turbulence, so terrain roughness becomes the dominant parameter for the flow and the thermal stratification becomes insignificant. The depth of ABL is not constant, but depends upon the strength of surface generated mixing. The depth is smallest by clear nights, where the earth's surface is relatively cold, and might be as small as 100 m. At daytime the ABL depth can be 1000 m or more. (Bottoma, 1993)

In this study, we concentrate on the surface layer, meaning the lowest 10-20% of the ABL. Eq 3.26 models the mean wind speed as a function of height in the ABL, using the logarithmic wind profile (Kragh, 1998):

Eq 3.26 $$u(z) = \frac{u_*}{\kappa} \ln\left(\frac{z}{z_0}\right) \qquad \text{for } z > 20 \cdot z_0 + z_d$$

where

$u(z)$	is the wind speed at height z	[m/s]
u_*	is the friction velocity $= \sqrt{\dfrac{surface \quad drag \quad per \quad unit \quad area}{density}}$	[m/s]
κ	is the Von Karman constant	[0.4]
z	is the height	[m]
z_0	is the aerodynamic roughness length	[m]
z_d	is the displacement height	[m]

Values of z_o range from about 0.0002 m for the open sea and 0.25 m for rural land with few large obstacles to greater than 2 m in city centres.

Bottoma (1993) states that the Eq 3.26 is valid for $z > 20z_0+z_d$. z_d is the zero plane displacement, which is about half of the obstacles height. In contrast to Bottoma (1993), Simiu & Scanlan (1996) claim that the displacement, $z_{d,}$ is normally assumed equal to zero. This means that a reference velocity cannot be deduced for a reference height of e.g. 10 m in too rough a terrain such as a village with z_0 =0.5, using Eq 3.26.

Orme et al. (1994) suggest Eq 3.27 instead of Eq 3.26. In Eq 3.27 the displacement height, z_d, is employed to introduce a reference (datum) ground level at 0.5-0.75 of height of the obstacles. The logarithmic profile then becomes:

Eq 3.27 $$u(z) = \begin{cases} \dfrac{u_*}{\kappa}\ln\left(\dfrac{10}{z_0}\right) & z \le z_d + 10 \\ \dfrac{u_*}{\kappa}\ln\left(\dfrac{z - z_d}{z_0}\right) & z \ge z_d + 10 \end{cases}$$

It is noted that the wind profile is constant in the lowest part of ABL for $z \le z_d + 10$.

Other (Dyrbye and Hansen, 1989) suggest Eq 3.27 for $z > z_0$. Here the static load on a structure is in focus, while the change in load between two heights near the ground (as is of interest for ventilation) has been less important.

Table 3.2 Classification for visual determination of roughness length. H is the height of obstacles.

No.	z_0 (m)		Landscape description
1.	0.0002	Sea	Open sea or lake, desert all with a free fetch of several kilometres.
2.	0.005	Smooth	Featureless land surface without any noticeable obstacles.
3.	0.03	Open	Level country with low vegetation and isolated obstacles with separations of at least 50 obstacle heights (50H).
4.	0.10	Roughly open	Cultivated area with regular cover of low crops, or moderately open country with occasional obstacles at relative horizontal distances of at least 20H.
5.	0.25	Rough	Recently developed with high crops and scattered obstacles at relative distances of about 15H.
6.	0.5	Very rough	Old cultivated landscape with many rather large obstacles groups separated by open spaces of about 10H. Dense low buildings
7.	1.0	Closed	Landscape totally and quite regularly covered with similar size large obstacles with open spaces comparable to the obstacle heights.
8.	≥2.0	Chaotic	Centres of large towns with mixture of low-rise and high rise buildings, or irregular forests with many clearings.

The variation of mean wind speed with height is determined by two parameters, the roughness length z_0 and the zero plane displacement z_d. The aerodynamic roughness length z_0 is not a real obstacle height, but a measure of the size of eddies at the surface. A roughness classification is described for visual determination of roughness length, Table 3.2 (Bottoma, 1993). The values of z_0 can be used in conjunction with the assumption z_d=0 (Simiu and Scanlan, 1996).

EXAMPLE: Reference wind speed u(20 m)= 10 m/s
Roughness length z_0= 2.0 m (centre of large town), obstacles of 4 m. The friction velocity is found using Eq 3.27 for z>10 and Orme et al.'s suggestion of z_d equal the 0.5-0.75 of height of the obstacles.

z_d =0.6·4=2.4 m

$$u(z) = \frac{u_*}{\kappa}\ln\left(\frac{z}{z_0}\right) \Rightarrow 10 = \frac{u_*}{0.4}\ln\left(\frac{20-2.4}{2}\right) \Rightarrow u_* = 1.8$$

An estimate of the wind speed at 4.8 meters height, using Eq 3.27 for z<10 would thus be

$$u(4.8m) = \frac{1.8}{0.4}\ln\left(\frac{10}{2}\right) \approx 7.4\,\tfrac{m}{s}$$

Swami and Chandra (1994) suggest a correlation between the velocities in two different heights, when the reference velocity is measured in one class of terrain and one height, and calculated according to another class of terrain in another height. Swami and Chandra (1994) classify the different types of landscape in 5 categories, Table 3.3.

Eq 3.28 $$V_{ref} = V_{vH} = \left(\frac{33}{h}\right)^{b_r} \cdot \left(\frac{H}{33}\right)^{b_b} \cdot \frac{a_b}{a_r} \cdot v_{rh}$$

where

V_{ref}	is the reference velocity [m/s]
V_{vH}	is the reference velocity at height H [m/s]
v_{rh}	is the wind speed in the reference terrain at height h [m/s]
H	is the height in building terrain where V_{ref} is required [m]
h	is the mast height in the reference terrain
a_r and b_r	are terrain constants of the reference terrain
a_b and b_b	are terrain constants of the building terrain

Table 3.3 Terrain parameters for different terrain classes

Class	b	a	Description
1	0.10	1.30	Ocean or other body of water with at least 5 km of unrestricted expanse
2	0.15	1.0	Flat terrain with some isolated obstacles
3	0.20	0.85	Rural areas with low buildings
4	0.25	0.67	Urban, industrial or forest areas
5	0.35	0.47	Centre of large city

3.7. Wind velocity fluctuation

The wind effect on buildings is highly unstable, which can be important in natural ventilation (Etheridge, 1999). However until now the collections of weather data has normally only included an hourly mean wind velocity and wind direction, which have been measured with an interval of 10 minutes. Air infiltration (airflow from outside to inside) due to wind-induced pressure is highly influenced by the turbulent nature of wind especially when the fluctuations are large compared to the average wind pressures. In steady-state models the mean values are used, and the fluctuations of wind speed and direction are not considered.

Kronvall (1980), Burnett & Straube (1995), and Etheridge (1999) mention the impact of the fluctuation on the resulting volume airflow. Kronvall finds that rapid fluctuations influence the flow rate only little. If the fluctuations are slow it is possible to calculate the flow rate as if the system is in a steady state, using time averaged values. They conclude differently whether the fluctuating effect should be included or excluded in calculations of the airflow.

Burnett and Straube (1995) find from laboratory experiments on vents, based on the power law theory Eq 3.13, that with an imposed mean flow, no single discharge coefficient, C_D, would fit some of the results, even approximately. They have discovered no strong theoretical reasons for the observed behaviour of the vent flow under dynamic pressures. They also conclude that in service, the dynamic pressure differences are small and should therefore play a relatively smaller role on the flow rate. Etheridge (2000) introduces a method to determine whether unsteady flow effects can be ignored. His work indicates that for the ventilated facade the unsteady flow should be considered.

Etheridge (2000) bases his work on natural ventilation in buildings, where Kronvall (1980) and Burnette & Straube (1995) have been studying ventilated cavities with size and shape as they are normally seen in building envelopes like roofs and facades. It was therefore decided to follow the assumption that wind influence is important on the airflow, but rapid fluctuations in the wind pressure only influence the airflow little.

3.8. Water concentration and vapour pressure in the air

The humidity of the air is changing with a daily and yearly cycle. In winter the relative humidity is high, but the moisture content is low due to low temperatures. The moisture content is higher in the summer and fall, and both temperature and relative humidity are high.

The gas law for ideal gasses gives the correlation between pressure and concentration:

Eq 3.29 $p = c \cdot R_v \cdot T$

where

p	is the partial pressure of the water vapour [Pa]
c	is the water vapour concentration [kg/m3]
R_v	is the gas constant for water vapour [461.5 J/kgK]
T	is the absolute temperature [K]

The relative humidity depends on the water vapour pressure compared to the saturation water vapour pressure. Kjerulf-Jensen (1986) suggests the empirical equation Eq 3.30 for calculation of the saturation water vapour pressure as a function of temperature. When knowing the temperature and relative humidity, the vapour pressure can be calculated from equations Eq 3.30 and Eq 3.31.

Eq 3.30 $p_s(T) = \exp\left(23.5771 - \frac{4042.90}{T - 37.58}\right)$

where

T is the absolute temperature [K]

and where

Eq 3.31 $p = p_s \cdot \varphi$

where

φ is the relative humidity [-]
p_s is the saturation water vapour pressure [Pa]

The Eq 3.30 is valid in the temperature range 0-80°C with uncertainty of –0.07 to 0.14%.

3.9. Moisture and materials

Porous materials in contact with air, at constant temperature and relative humidity, will reach equilibrium of moisture content after some time. The equilibrium moisture content varies highly for different materials, and is described by sorption isotherms. It depends mainly on the relative humidity and the pore size and the pore distribution of the material, but also whether the material is wetted (absorption) or dried (desorption). The equilibrium moisture content is also a function of the temperature, giving smaller equilibrium moisture content for increasing temperature, but this effect is minor compared to the other mechanisms mentioned above. (Nevander, 1994). The relation between the moisture content in a material, u [kg water/kg dry material], and the relative humidity is given with the sorption isotherm.

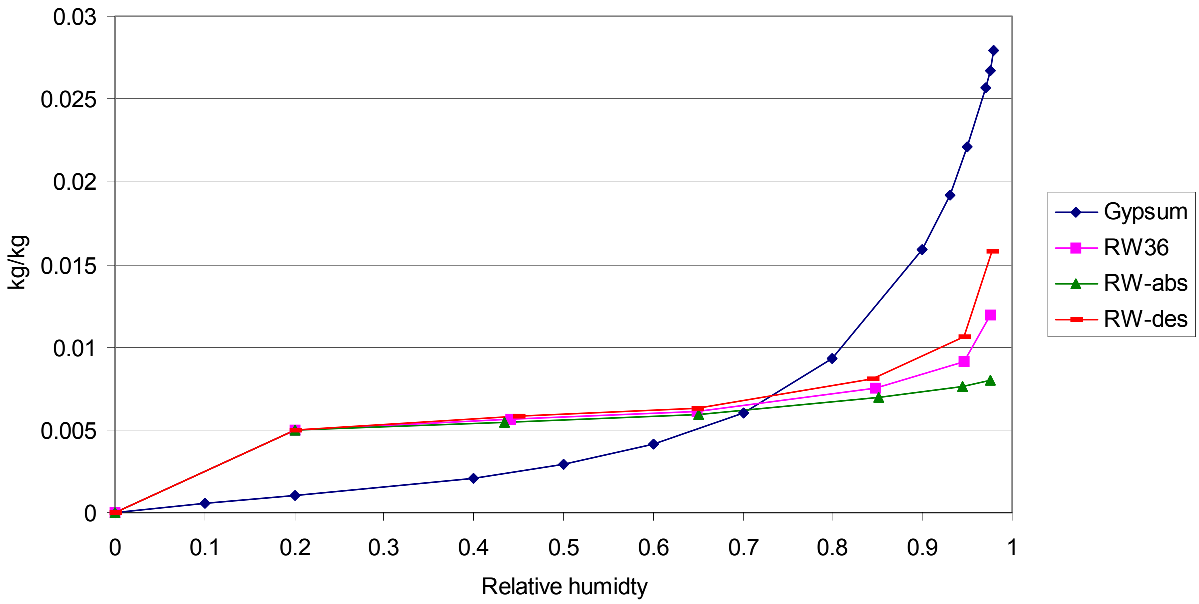

Figure 3.1 Sorption isotherm for gypsum and Rockwool, together with the absorption (RW-abs) and desorption (RW-des) isotherms for Rockwool. Data from (Rode, 1996).

The equilibrium moisture content increases with increasing relative humidity. Hysteresis produces a difference in moisture content, for a given relative humidity, depending on weather the material is drying (desorption) or wetting (absorption), Figure 3.1. The temperature also influences the moisture content. For increasing temperature the moisture content decreases (Nevander, 1994). However, the thermal influence on the sorption isotherm is rarely included in calculations, due to lack of data and a minor influence compared to the relative humidity dependence.

The heat transfer, q [W/m^2], by conduction, and the moisture transfer, g [kg/ m^{2}s] by diffusion within materials are described using the well-known equations from Fourier, Eq 3.32 and Fick, Eq 3.33.

Eq 3.32 $q = -\lambda \cdot \frac{\partial T}{\partial x}$

where

λ	is the thermal conductivity [W/mK]
T	is the temperature [K]
x	is the place [m]

Eq 3.33 $g = -\delta_p \cdot \frac{\partial p}{\partial x}$

where

δ_p	is the vapour permeability [kg/s m Pa]
p	is the water vapour pressure [Pa]
x	is the place [m]

In the literature the vapour permeability, δ, will be listed for either water vapour pressure or water content as driven potential. The correlation between them is:

Eq 3.34 $\delta_p = \frac{\delta_c}{R_v \cdot T}$

where

δ_p	is the vapour permeability [kg/m s Pa]
δ_c	is the vapour permeability [m^2/s]
R_v	is the gas constant for water vapour [461.5 J/kg K]
T	is the absolute temperature [K]

4. Experimental set up, ventilated wall.

A test-wall on an existing test-house was modified to investigate the airflow in a ventilated cavity on a façade wall exposed to real climate. The test-house was placed on the outdoor test facilities of the Technical University of Denmark. The test-house had different wall sections with variations of insulation materials, to investigate the hygro thermal performance of alternative insulation materials together with traditionally materials. The modification was to change the rain screen of fibreboard to Plexiglas, for a section with traditional stone wool insulation material.

Measurements of air velocity, pressure differences, temperatures and moisture transport were carried out on the test-wall.

The wind pressures on the outside of the façade were measured using pressure transducers. The pressure differences between a reference point above the roof and a point just outside each vents were measured. Temperatures were measured with thermo couples, close to the pressure measurement points.

Tracer gas equipment was used to measure the directional air velocity by measuring air change in the cavity, and reveal pumping effect that reduces the air change (see Chapter 5 'Air velocity measurements' for details). Due to high frequency fluctuations in wind velocity and wind direction, measurements with a fast response were found important. The gas equipment had a long response time and the measurements were therefore validated against high frequency air velocity measurements with thermo anemometers. Both the pressure measurements and the velocity measurements were hold against measurements of the wind velocity and wind direction. An ultra sonic anemometer placed above the roof of the test house measured the wind direction and the wind velocity.

4.1. Description of test house and wall model

The test house was placed at the Technical University of Denmark in Lyngby, 20 km north of Copenhagen. The surrounding landscape can be described as 'closed' with a roughness length z_0 estimated to approximately 1.0 m in accordance with the roughness classification of terrain types proposed by Bottoma (1993).

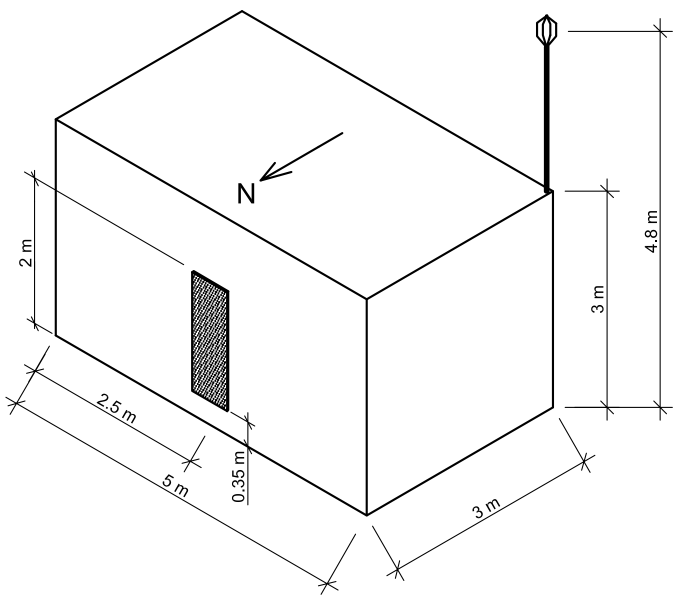

Figure 4.1Test house with a full-scale model of a ventilated facade cavity. A ultra sonic anemometer and a reference point for pressure measurements are placed 4.8 m above the ground level.

The test house was a low-rise building with a flat roof. The length was 5 m, the height about 3 m, and the width 3 m, where the long sides were facing north and south respectively, see Figure 4.1. The wall of the test house was from the inside made of 13 mm gypsum board, vapour retarder, 100 mm mineral wool, 13 mm gypsum board, 25 mm ventilated air cavity, and 10 mm Plexiglas, see Figure 4.2.

The cavity model was situated at the centre of the north side, with the bottom 0.35 m above ground. To protect the cavity against rain an overhang of 0.25 m with a slope of 15° was placed 0.2 m above the top of the cavity. The north facade was chosen for the experiments in order to eliminate influence from the sun radiation.

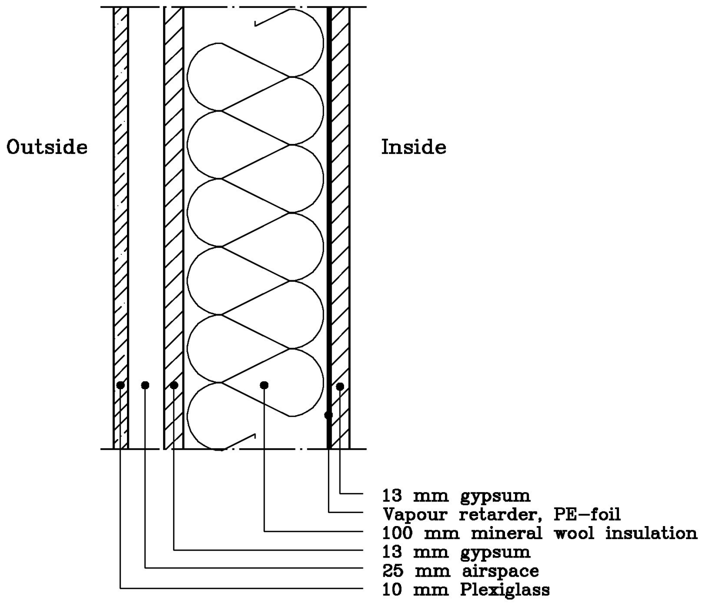

Figure 4.2 Material layers in the experimental wall of the test house

The cavity was formed by a 10 mm Plexiglas sheet mounted in a distance of 25 mm from the wall. Holes of Ø 9 mm were drilled in the Plexiglas sheet, for inserting tracer gas tubes. The Plexiglas sheet was separated from a gypsum air barrier by a vertical wood stud in each side. The wood studs had Ø 15 mm holes to insert thermo anemometers; which were plugged when the thermo anemometers were not used. The dimensions of the cavity are shown in Figure 4.3. The ventilation openings were the horizontal slits with the width and depth of the cavity.

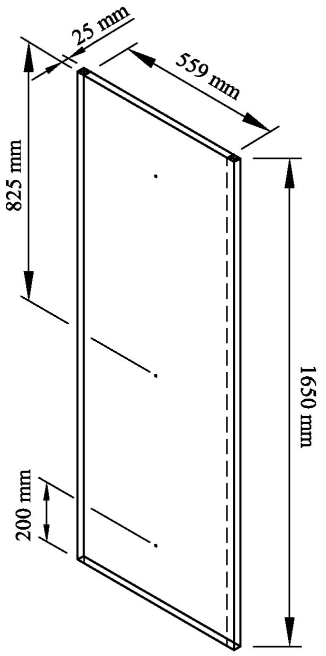

Figure 4.3 Model of a ventilated wall cavity with drilled holes for tracer gas equipment

4.2. Wind pressure coefficients measured by pressure transducer

The wind pressure difference between a reference point and a specific point together with the wind velocity were measured to obtain data for calculating the wind pressure coefficient. The pressure difference between a specific point and the reference point is the dynamic pressure needed to estimate the pressure coefficient Cp, assuming the dynamic pressure to be zero at the reference point.

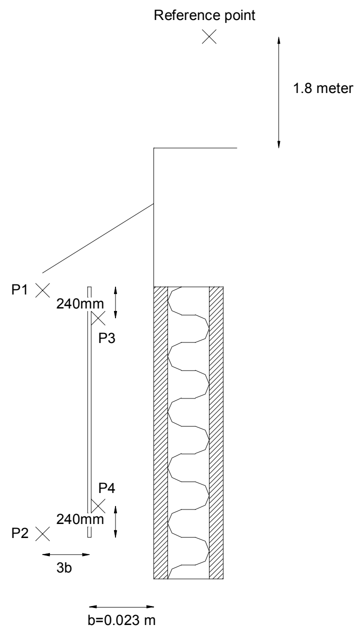

Figure 4.4 Pressure differences measured between P1and P2, between P3 and P4 and between the reference point and the points P1and P2.

The static pressure differences were measured using 4 pressure transducers.
The transducers were: Difference Pressure Transducers FKA-P1 from Staefa Control.

Table 4.1 Manufacturers specifications for the pressure transducer.

FKA-P1	
Range	0...1mbar (0...100Pa)
Linearity	<± 1.5% of full scale
Operating temperature	0...40°C

Transducer:

No 1 measures the outside pressure difference, between P1 and P2.
No 2 measures the inside pressure difference between P3 and P4.
No 3 measures the pressure difference between the reference point and P1.
No 4 measures the pressure difference between the reference point and P2.

For determination of Cp_1-Cp_2 the pressure difference P_1-P_2 was measured directly (No 1) to obtain higher accuracy.

The pressure at the reference point was connected to a manifold, which leads to the negative side of the two pressure transducers 3 and 4. The outside points (P1 and P2) were placed at the height of the openings in a horizontal distance of three times the width of the cavity (3 x b). The two points inside the cavity (P3 and P4) were placed in the plane of the rain screen, in a distance of 240 mm from the openings. See Figure 4.4.

The reference point was placed 1.8 m above the roof surface, where also the wind velocity and direction were measured. According to Bas Knoll (2000), the airflow can be considered undisturbed in a position 1/3 of the building height above the roof surface. The reference point was chosen from where the wind could be considered undisturbed.

The reference point was placed just below the ultra sonic anemometer at the same mast. The pressure tubes were led through two holes at the same level to the inside of the house. Inside the cavity the measuring tubes were placed so the opening was parallel to the airflow.

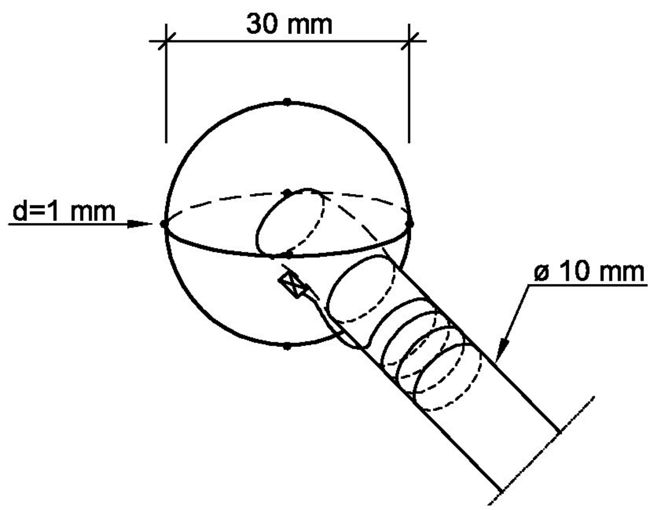

Figure 4.5 Ball with 6 holes protect the static pressure measurements from dynamic pressure.

To eliminate the dynamic pressure in the open flow field, table tennis balls of approximate 4 cm in diameter were used for measurements. The balls had 6 holes of diameter 1 mm, which were distributed uniformly over the body. A plastic tube of outer diameter Ø 10 mm was fastened airtight to the ball through a hole. Further a thermo couple was wrapped around the plastic tube with the open end centred inside the ball, see Figure 4.5. These special devices were used 3 places outside, for the reference point, P1 and P2. Bas Knoll, TNO, who used small cubes, inspired this construction. The small cubes of Bas Knoll, have holes in all six sides and were connected to a larger centre tube that leads to the pressure measurement device.

4.3. Measurement of air velocity in cavity by thermo anemometer

Multi channel low velocity thermal anemometer was used to measure the airflow velocity. The system consisted of eight identical velocity probes, eight transducer units and a multi channel power supplier. The velocity probe had a spherical (omni directional) velocity mass sensor of 2 mm in diameter made of enamelled copper wire moulded into a sphere. The overheating temperature of the sensor is 25°C. The velocity probe has also an unheated sensor, which measures the air temperature. The specifications for the sensors are listed in Table 4.2.

Table 4.2 Manufacturers specifications for the thermal anemometer

Thermal anemometer HT-412 from Sensor, Poland.	
Type of velocity sensor	Omnidirectional, spherical
Velocity range	0.05- 5 m/s
Repeatability	0.02 m/s ±2%
Temperature range	0 to 50°C
Accuracy of temperature measurement	0.3°C

The sensors were individually calibrated by the manufacturer. On a computer, an analogue signal of instantaneous velocity and temperature measured by the sensors with a frequency of 5 Hz.

Six of the probes were used to measure the airflow in the cavity. They were placed symmetrically in the cavity, three in each side of the centre line, see Figure 4.6. The probes were inserted through holes and were positioned by a specially designed device. In order to avoid disturbances between the probes, due to the natural convection flow generated by the heated velocity sensor, the probes were positioned 100 mm from each other in vertical direction. Further, two more probes were used to measure the air velocity near the ventilation openings, one at each opening.

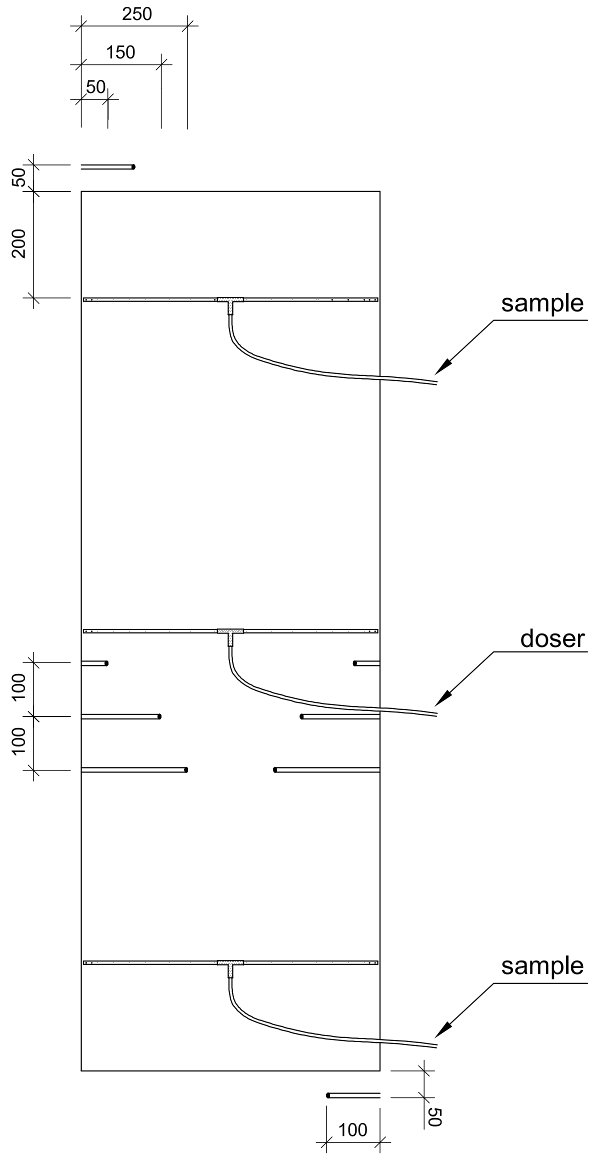

Figure 4.6 Thermo anemometer probes inserted from the sides into the cavity and tubes for tracer gas dosing and sampling. A close up in Figure 4.7 shows decreasing distance between the drilled holes in the tracer gas tubes.

The average velocity through the ventilation cavity was calculated assuming that the thermo anemometer probes did not influence the airflow. The cross sectional area of the cavity and the cross section of measurement were constant and equal to the area of the ventilation opening.

4.4. Air velocity and moisture content measured with tracer gas equipment.

Tracer gas measurements were performed with a gas analyser, based on the photo-acoustic infrared detection method. The instrument quantifies the concentration of any gas that absorbs infrared radiation. In a given air sample it makes individual measurements of the concentration of a maximum of five gases, and water vapour, with optical filters. Dinitrogenoxide (N_2O) was used as a tracer gas during the present measurements. The choice of N_2O instead of the normally used sulphurhexaflouride (SF_6), was due to a density close to density of atmospheric air.

The gas analyser can measure N_2O in the range 0.03 to 30,000 ppm with a repeatability of 1% of the measured value, of a 140 ml sample (Brüel & Kjær, 1990). Cross compensation between the measured gas and water was included in the calculation of the measured N_2O concentration. The gas analyser was used in conjunction with a multi point doser and sampler, which enables measurements in up to six points.

Table 4.3 Manufactures specification for multi-gas monitor.

Multi-gas Monitor Type 1302 from Brüel&Kjær	
Response time	~30 sec per gas
Measurement range (N_2O)	0.3 ppm to $3{\cdot}10^5$ ppm
Repeatability	1% of measured value
Operating temperature	5-40°C
Relative humidity	-90% at 30°C
Volume of air required	140 ml/sample

A constant dose of tracer gas, was added to the flow in the cavity. The dosing valve delivers approximately 0.5 ml/s depending on the chosen nozzle. The dosage is calculated with ±2% accuracy (Brüel & Kjær 1989).

Table 4.4 Manufactures specifications for the multipoint sampler.

Multipoint Sampler and Doser Type 1303 from Brüel&Kjær	
Dosage	0.5 ml/s, 3.0 ml/s or 15 ml/s
Accuracy of calculated dosage	±2%
Sampler volume flow rate	15 ml/s

In order to distribute the tracer gas uniformly in the flow, a horizontal tube with nine drilled holes was used, as shown in Figure 4.7. The seven holes nearest the middle had diameter of 1 mm and the two at the end had diameter of 2 mm. The uniformity of the tracer gas distribution, through a tube with drilled holes in the width of the cavity, was tested, by observing that smoke exits all nine holes in each side, (Gudum 2000-a) (Found in Appendix B). The tracer gas was supplied in the middle of the tube through the outer wall of the cavity. The analysed result from the air sample downstream to the dosing tube was used for calculation of the air velocity. The flow direction in the cavity was determined by sampling both upwards and downwards to the dosing tube. The two sampling tubes placed in the cavity, at a distance of 200 mm from the openings (see Figure 4.6) were identical to the dosing tube.

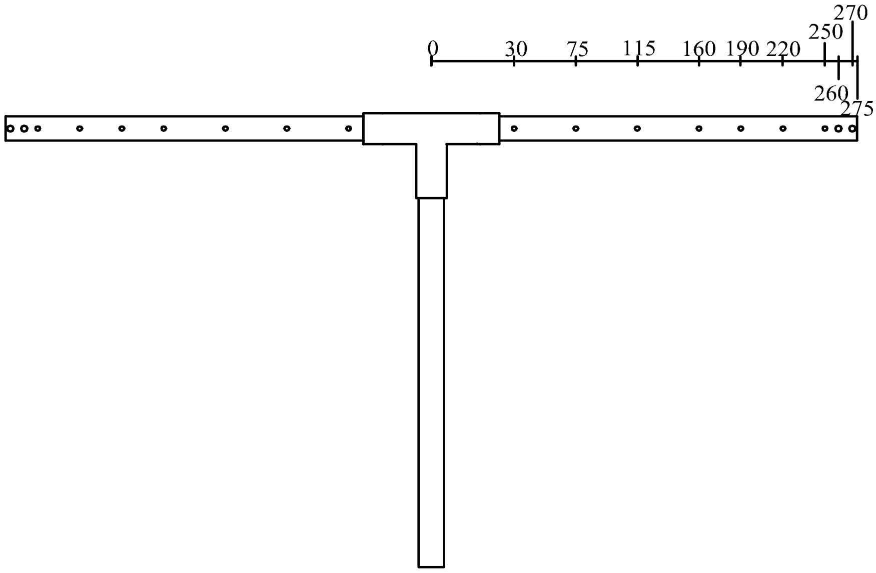

Figure 4.7 Uniform distribution of tracer gas and air sampling to analyser was ensured through tube with drilled holes.

Further, a sample of the outdoor air collected to the west of the test house model, was analysed to compensate for background N_2O concentration, and one sample inside the test house was analysed for safety reasons during operation of the instruments. The sampling and analysis of the four air-samples (one from each tube in the cavity, outdoor air, and indoor air) were performed one by one in a loop of about eight minutes, as the time for sampling and analysis was about 1-2 minute for each sample.

The uncertainty of the average air velocity determined with the tracer gas method, depends on accuracy of determination of the cross sectional area, the accuracy of the concentration measurements, and the accuracy calculation of tracer gas dosing. In the velocity range of 0.02-1.4 m/s the uncertainty was estimated to be 0.003-0.17 m/s (Gudum 2000-b) (Found in Appendix C), providing uniform distribution and complete mixing of tracer gas.

4.5. Wind data measured by Ultra Sonic Anemometer

To register the wind velocity and direction above the expected turbulent layer (Knoll 2000), an ultra-sonic anemometer was placed at 1.8 m above the roof equal to 4.8 m above ground level. The standard height for meteorological wind measurement is 10 m. However, in this experiment 4.8 m was chosen due to available mast height.

The ultra sonic anemometer was of the type WindMaster from Gill Instruments LTD. The specifications for the instrument are listed in Table 4.5.

Table 4.5 Manufacturers specifications for the ultra sonic anemometer

Gill SOLENT WindMaster, 3-Axis Ultrasonic Meteorological Anemometer		
Wind speed range		0-60 m/s
Accuracy	0-20 m/s	1.5%
	20-35 m/s	1.5%-3%
	35-60 m/s	3 %
Wind direction		0-360°
Accuracy	<25 m/s	±2°
	>25 m/s	±4°
Operating temperature		-40°-60°C
Operating relative humidity		5-100%

An identical ultra sonic anemometer was installed as a part of the weather station of the Department of Civil Engineering. The weather station, including the ultra sonic anemometer, was mounted 4 meter above a 3-storeyed office building with flat roof. The office building was placed where the terrain change rapidly with 4 meters, while the wind data was measured at a height of 20 m compared to the ground level of the test house. The weather station was placed approximately 200 m west to the test house. At the weather station, data was logged and stored every 10th second, where it on the test house was measured at its maximum of 1 Hz.

4.6. Data collection

Collecting of the measured data from the pressure equipment and the ultra sonic anemometer was performed simultaneously through a multi channel data card S135951C IMP from Schlumberger connected to a stationary computer. For programming the data card and collecting data the software 359574A-IMPVIEW version V_DA from Solartron was used. Data was logged with 0.3 Hz.

5. Air velocity measurements

To measure the airflow in the cavity two methods were used in this study: the air change based tracer gas technique and the thermo anemometer. The tracer gas technique (TG) enables determination of the directional average air velocity over the cross section of the cavity. However, TG has a long response time.

A thermo anemometer (TA) typically has a high sampling rate i.e. short response time. Therefore it is appropriate for point measurements in the flow and thus determination of average air velocity as well as more detailed investigation of the airflow.

The detailed measurements can be used for investigation in regard to uniformity of the airflow distribution in the cavity and its characteristics (mean velocity, standard deviation of velocity, turbulence intensity, frequency of velocity fluctuations, etc.).

Alternative methods for air velocity measurement are particle image velocimetry (PIV) or pressure measurement with a Pitot tube. The PIV is only for laboratory experiments, and the Pitot tube measures in one direction only. While none of the techniques were considered appropriate for the measurements of the air velocity in the cavity placed outdoor.

In the following the '*horizontal average velocity*' is defined as the average of several positions across the cross section of the ventilated cavity at one time, while the '*time average velocity*' is defined as the mean of several times in a single physical position. When more than one measurement result per time defines the velocity, the expression '*average*' or '*mean*' is used.

In this chapter the air velocity measured by tracer gas method and thermo anemometers were compared, in order to validate the tracer gas method under realistic weather conditions with fluctuations in wind direction and wind velocity. The influence of wind velocity and wind direction on the airflow will be analysed in the next chapter.

5.1. Tracer gas

The tracer gas method was calibrated under laboratory conditions using a separate experimental model, with dimensions similar to the outdoor model. In the laboratory the measurements with tracer gas of vertical air velocity inside a cavity, were compared to measurements of the volume flow rate (Gudum 2000-b) (Found in Appendix C). Here it was found that the mean air velocity, *u* [m/s], over the cross sectional area of the ventilation opening area, including an empirical found constant A_{eff}, is:

Eq 5.1 $$u = \frac{F}{A \cdot b_{corr} \cdot (c_c - c_b)}$$

where

A_{eff}	is the cross sectional area [m^2]
b_{corr}	is a experimental found correlation factor
c_c, c_b	is the gas concentration in the cavity and background (surroundings) respectively [mg/m3]
F	is the dose of tracer gas [mg/s]

The air flow by volume, Q [m^3/s], through the vents was assumed to be equal for in-, outlet, and over the cross sectional area:

Eq 5.2 $Q = u \cdot A$

where

A	is the cross sectional area [m^2]
u	is the average air velocity over the cross sectional area [m/s]

5.2. Thermal anemometers

The horizontal average velocity through the ventilated cavity was calculated from the 6 points measurements, assuming that the thermal anemometer probes did not influence the airflow. The cross sectional area of the cavity were constant and equal to the area of the ventilation openings.

A number of experiments were run. Data were logged in a five minutes interval, except in experiment # 16 where the logging interval was three minutes, see Table 5.1.

According to Andersen (2000) the mean velocity across the cavity depth is equal to 2/3 of the maximum velocity for laminar flow. The present measurements identified a non-laminar airflow in the cavity with large velocity fluctuations and moderate variation across the cavity width. Nevertheless the 2/3 criteria was applied to estimate the average velocity in the cavity, from the time average velocity in the middle of the ventilated cavity, where the velocity probes were placed:

Eq 5.3 $u_{average} = \frac{2}{3} \cdot \frac{\sum_{1}^{n} u_{time,average}}{n}$

where

$u_{time,average}$	is the mean velocity, of the 3 or 5 minutes period, in the cavity determined from the measurements by the six velocity probes. [m/s]
n	is the number of probes

Since the cross sectional area of the cavity is assumed the same at the opening and at the position of the thermo anemometers, the following equation can be used to determine the volume flow rate, Q [m^3/s]:

Eq 5.4 $Q = u_{average} \cdot A$

where

A	is the cross sectional area [m^2]
$u_{average}$	is the mean of the time average velocity of the 6 probes

5.3. Comparison of tracer gas technique against thermal anemometer

To compare TG against TA, preliminary 16 experiments, with the outdoor model of the ventilated cavity were performed. Some of the results are shown in Table 5.1. The measurements were performed between 9:00 and 14:00 on the 11th and 14th of August 2000 for the experiments # 1-15, and on the 16th of October 2000 for the experiment # 16. Mean velocities for TG and TA are listed in Table 5.1.

Table 5.1 Velocity measured inside ventilated cavity with thermal anemometers (TA) and tracer gas (TG). Wind data measured 1.8 meter above roof height. The flow direction is observed from smoke that is spread near the openings and from tracer gas measurements.

Measure-ment #	Mean air velocity TA [m/s]	Turbulen-ce of TA [%]	Mean air velocity TG [m/s]	Mean wind speed [m/s]	Standard deviation wind velocity [m/s]	Mean wind direcection [°]	Standard deviation wind dir. [°]	Air flow direc-tion
1	0.17	17	0.19	1.77	0.69	268	26	upward
2	0.21	60	0.16	1.32	0.88	251	86	upward
3	0.18	59	0.18	0.91	0.61	287	37	upward
4	0.21	52	0.32	1.45	0.80	275	59	upward
5	0.19	45	0.19	1.71	0.66	265	22	fluc
6	0.19	47	0.23	1.79	1.01	262	69	fluc
7	0.22	46	0.22	1.98	1.03	265	25	upward
8	0.16	37	0.18	1.96	0.80	250	51	upward
9	0.18	44	0.24	1.90	0.87	252	50	upward
10	0.15	42	0.22	2.02	1.31	258	26	upward
11	0.12	37	0.17	0.69	0.52	148	59	upward
12	0.13	58	0.08	1.50	0.96	154	63	upward
13	0.13	66	0.08	1.48	0.85	156	53	upward
14	0.13	59	0.13	1.41	0.94	153	80	upward
15	0.14	61	0.3	1.20	0.68	157	71	upward
16*	0.17	80	0.08	2.12	1.21	98	57	fluc

**Experimental period of three minutes*

The turbulence of the air velocity is defined as the standard deviation divided by the mean velocity, and tells how even the velocity has been during the experiment.

The horizontal averaged value of the six inside thermal anemometer probes were used with Eq. 5.3, to calculate the mean air velocity TA in Table 5.1. The turbulence was calculated for the horizontally averaged velocity and listed in the Table 5.1. The mean air velocity TG from tracer gas measurement was calculated with Eq 5.1. The wind velocity and wind direction were measured simultaneously, and the mean values and the standard deviations were calculated for each run. The airflow direction in the cavity was observed with smoke and was also defined from the tracer gas measurements.

The air velocity was measured similar to Figure 4.6 in six positions in parallel with the wall. The collected data were analysed in order to identify the mean velocity, the standard deviation of the velocity and the turbulence intensity in the cavity flow, Table 5.1. For the rather narrow range of wind speed and direction the mean velocity measured in the cavity was in the range 0.12-0.22 m/s with thermal anemometers and range 0.08-0.32 m/s with tracer gas, while the turbulence intensity for the mean velocity (thermal anemometers) was from 17 to 80% (for the individual thermal anemometer probes the turbulence intensity was measured from 36-102%).

The results in Table 5.1 show that the outdoor conditions during the present experiments did not change in a wide range. The mean wind speed during the measurements was in the range 0.7 –

2.1 m/s while the mean wind direction was either around 260° (west) or 150° (south-east). The standard deviation of the wind direction during the experiments was from 22° to 86°. The airflow direction was mostly upward, with three observations of fluctuating direction.

The average air velocity measured with the thermal anemometer and with the tracer gas was compared in Figure 5.1. The comparison shows a good agreement between the two measurement methods. Only for some of the experiments, #4, #15 and #16, the agreement was poor. The differences were large especially for the experiments #4 and #15, where the average velocity determined by the tracer gas technique was more than 50 % higher than with the thermal anemometer. The discrepancy between TG and TA #16, could be due to fluctuating air direction, where the thermo anemometers were expected to estimate higher velocity than the tracer gas method. An reasonable explanation for divergence in #4 and in #15 was not found.

Nevertheless the systematic difference and the standard deviation of the difference in the average velocity determined by the two methods was low, 0.03 m/s. Thus it seems that the assumptions made for the determination of the average velocity by the thermal anemometer, the 2/3 criteria and the location of the maxim velocity in the middle of the cavity cross section, may be used in practice.

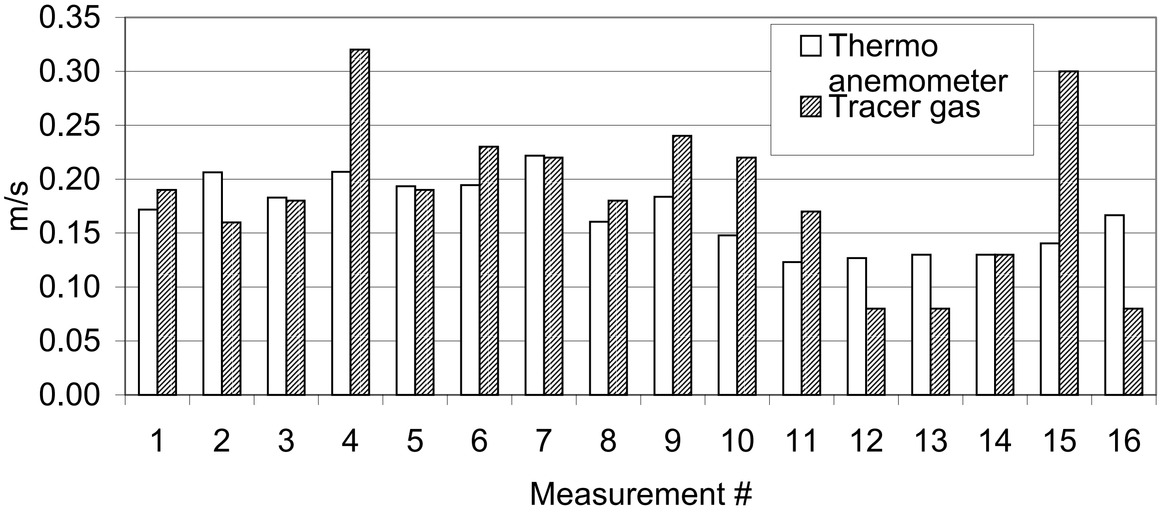

Figure 5.1 Mean air velocity inside the cavity measured by tracer gas and thermal anemometer

Both tracer gas method and thermo anemometers are methods that can be applied for air velocity measurements in a ventilated cavity. The tracer gas method can detect recycling of cavity air and the directional air velocity, but constant changes in air direction can be wrongly estimated as high air velocity, due to a long response time of the method. The tracer gas method is appropriate for long time measurements (days) where the average air velocity for a longer period and not the instantaneously air velocity is required. Besides the tracer gas analyser also measures the moisture content of the air, which can be used for estimation of the convective moisture transfer.

Thermo anemometers measure the instantaneously point air velocity with a high frequency. This is appropriate for investigation of fluctuations in the air velocity as well as for investigation of the velocity distribution in the flow field. The instruments are sensitive to moist and rain, and only appropriate for short time measurements (hours) in a dry weather period. The thermo anemometers are non-directional, and several measuring point are needed to estimate the horizontally average air velocity.

The two methods are supplemental where the tracer gas method is appropriate for long term measurements of the average velocity, where the thermo anemometers are appropriate for detailed investigations of the air velocity in the flow field.

Here the tracer gas method was tested under a narrow range of wind direction, wind velocity and temperatures. Even though the method was tested in the laboratory for air velocity in the range 0.02 to 1.4 m/s, it is recommended that the tracer gas method is further tested under a variety of wind directions, wind speed, and temperatures.

In practice the two different methods are supplemental. The thermal anemometer sensors are not robust towards humid weather exposure such as rain and fog, which makes them unsuitable for measurements during nights or over a longer period. However they have a low response time, which enables measurements with the frequency of the wind fluctuations. The tracer gas method has a slow response, but a stable run for long period measurements (days). The benefit from tracer gas method was an identification of low air change rate, i.e. low mean velocity, if air was recycled in the cavity.

6. Results from measurements on a ventilated wall

The objective of this chapter is to sum up experimental data of importance for model development and validation. First an analysis of wind data will be presented. Then measurements of the cavity airflow for different wind direction and wind velocity are presented, and finally the measured moisture transport through the ventilated cavity is reported.

Both tracer gas technique and thermal anemometers were used to measure air velocity in a ventilated cavity, on a test house exposed to real weather conditions, together with pressure difference measurements with pressure transducers, and wind data measurements with two ultra sonic anemometers at different heights.

Short time measurements with pressure transducers performed experimental data for estimation of the actual wind pressure coefficient, for later calculations of the wind pressure outside top and bottom opening of the test wall as a function of wind velocity. This estimation also provided the simultaneous wind velocity and wind direction, which were measured with an ultra sonic anemometer. The measured wind pressure coefficients were compared to similar computer-generated values. As two different ultra sonic anemometers at different heights made the measurements of the wind, the results were also analysed to characterise the surrounding area. However, due to surrounding buildings this turned out to be rather complicated.

The tracer gas measurements determine the airflow direction and the convective moisture transport. The thermal anemometer measurements was not only of benefit for validation of the tracer gas method, but also served for investigation of effect by fluctuating wind velocity on air velocity fluctuation.

6.1. Wind pressure coefficient

The wind pressure is one of the forces that drives the airflow. As the wind pressure depends on the wind velocity and wind direction, it was here chosen first to present the wind data. The wind pressure coefficient is specified for a reference height, and a function of the wind angle. Wind pressure coefficients must therefore have the same reference height for comparison. The wind pressure coefficients are used to estimate the wind pressure on a specific place on a building surface. When the reference height is different from the height of the available wind data, determination of the reference velocity can be performed, using parameters for roughness of the surrounding terrain.

6.1.1. Wind velocity and direction

The two ultra sonic anemometers, described in ‘Experimental set up, ventilated wall’, were used to measure the wind direction and wind velocity with a frequency of 0.3 Hz at 4.8 m above ground level (test house), and with 0.1 Hz at 20 m above ground level (weather station), where the height refers to ground level at the test house.

The measurements were averaged over a period of 3 minutes. The 3 minutes average wind velocities and directions were compared, and the ratio between wind velocity in 20 m height and 4.8 m height were calculated together with the difference in wind direction, see Table 6.1.

Table 6.1 Measured results from simultaneously measurements of the wind velocity and wind direction with two identical ultra sonic anemometers placed at height 4.8 and 20 m above ground level. The results are mean values for 3 minutes measuring period, measured with 0.3 Hz at 4.8 m and with 0.1 Hz at 20 m. The measurement marked '' was ignored, as the low velocity is connected to a high uncertainty.*

Date	Velocity 4.8m [m/s]	Dir. 4.8m [0°-360°]	Velocity 20m [m/s]	Dir. 20m [0°-360°]	Ratio velocity 20/4.8	Diff. in dir. [°]
06-sep	1.86	197	4.6	167	2.47	30
07-sep	1.05	167	3.46	127	3.30	40
08-sep	2.50	248	4.92	216	1.97	32
08-sep	2.05	228	5.68	198	2.78	30
15-sep	1.83	150	4.85	104	2.65	46
11-okt	2.73	150	6.77	116	2.48	34
12-okt	2.00	181	4.4	166	2.20	15
*13-okt	0.20	225	1.03	32	*5.18	*167
13-okt	0.75	266	1.04	258	1.38	8
16-okt	2.12	98	6.29	96	2.97	2
24-okt	3.67	237	6.65	215	1.81	22
30-okt	4.99	194	10.39	187	2.08	7
Average					2.4 (*2.6)	

The wind velocity at 20 m was found to be 2.4 times higher in average than at 4.8 m, with a standard deviation of 0.6. The difference in wind angle was in the range 2°-46° depended on the wind direction (excluding an extreme value of 167°).

The wind direction is sensitive to obstacles in the surroundings. Both anemometers were placed so they would be affected more or less from nearby obstacles, depending on the actual wind direction. The wind direction measured together with the wind velocity, at either 20 m or 4.8 m will be used together in the further analysis.

To compare wind velocity data measured at different heights and terrain roughnesses, the data have to be normalized to the same standard height. Swami and Chandra (1994) (see Chapter 3 'Basic theory') suggested a correlation between the velocity in two different heights, when the reference velocity is measured in one type of terrain and one height, and calculated according to another type of terrain in another height. In the actual case the terrain parameters are the same. The terrain around the test house was best described as 'Urban, industrials or forest area', where a_b=a_r=0.67 and b_b=b_r=0.25, meaning

Eq 6.1 $$V_{ref} = V_{vH} = \left(\frac{33}{h}\right)^{b_r} \cdot \left(\frac{H}{33}\right)^{b_b} \cdot \frac{a_b}{a_r} \cdot v_{rh}$$

Eq 6.2 $$V_{20} = \left(\frac{33}{4.8}\right)^{0.25} \cdot \left(\frac{20}{33}\right)^{0.25} \cdot \frac{0.67}{0.67} \cdot V_{4.8} = 1.4 \cdot \mathrm{V}_{4.8}$$

The *Table 6.1* show that the wind speed was in average 2.4 times higher in 20 m than in 4.8 m. This was high compared to the expected ratio of 1.4 from the theoretical estimate, Eq 6.2.

According to Hans Lund (2001) the ultra sonic anemometer at 20 m was placed so the air was pressed over the gable edge and increases the wind speed, meaning that the wind speed may be higher than the undisturbed wind speed at the same height. Accordingly the observed ratio between wind speeds may have been too high. This corresponds to the comparison between the theoretical ratio of 1.4 to the observed ratio of 2.4. Also the placement of the test house below a steep slope of 4 m is expected to cause a lee effect on the anemometer on the test house.

Using the equations from Simiu and Scanlan (1994) from Chapter 3 'Basis theory', the roughness length, z_0, was calculated from the measured parameters.

Reference wind speed u(20 m)= u(4.8 m)*2.4 [m/s], displacement height z_d=0, roughness length z_0= X m (unknown factor). The friction velocity, *u**, is found using

Eq 6.3 $$u(z) = \frac{u_*}{\kappa} \ln\left(\frac{z}{z_0}\right) \Rightarrow$$

Eq 6.4 $$u(20) = \frac{u_*}{0.4} \ln\left(\frac{20}{X}\right) \Rightarrow$$

Eq 6.5 $$u_* = \frac{u(20) \cdot 0.4}{\ln\left(\frac{20}{X}\right)}$$

With the expression for the friction velocity and the ratio between velocity in two different heights

Eq 6.6 $$u(4.8m) = \frac{u_*}{\kappa} \cdot \ln\left(\frac{z}{z_0}\right) \qquad \wedge$$

Eq 6.7 $$u(4.8m) = \frac{u(20m)}{2.4}$$

An estimate of the roughness length can be found by inserting Eq 6.5 into Eq 6.6, and set Eq 6.7 equal Eq 6.6:

Eq 6.8 $$\frac{u(20)}{2.4} = \frac{u(20) \cdot 0.4}{\ln\left(\frac{20}{X}\right)} \cdot \frac{1}{0.4} \ln\left(\frac{10}{X}\right) \Rightarrow X \approx 6.1m$$

If Eq 3.26 is used as suggested by Dyrbye and Hansen(1989) 4.8 is inserted in Eq 6.8 in stead of 10 and the roughness length is then estimated to X=1.73 in stead of X=6.1.

This is a surprisingly high roughness length. Comparing with the roughness classification in Chapter 3 'Basis theory', the measured roughness of 6.1 m is described as centre of large towns with mixture of low-rise and high-rise buildings, or irregular forests with many clearings. A visual observation of the area would estimate the roughness length to be 1 m.

The Figure 6.1 show the wind velocity as a function of the height above ground level after Orme et al.(1994), where z_d=0 as suggested by Simiu and Scanlan(1996). For the comparison the velocity profile is calculated for three different roughness lengths, when the velocity u(20 m)=5 m/s for all three cases.

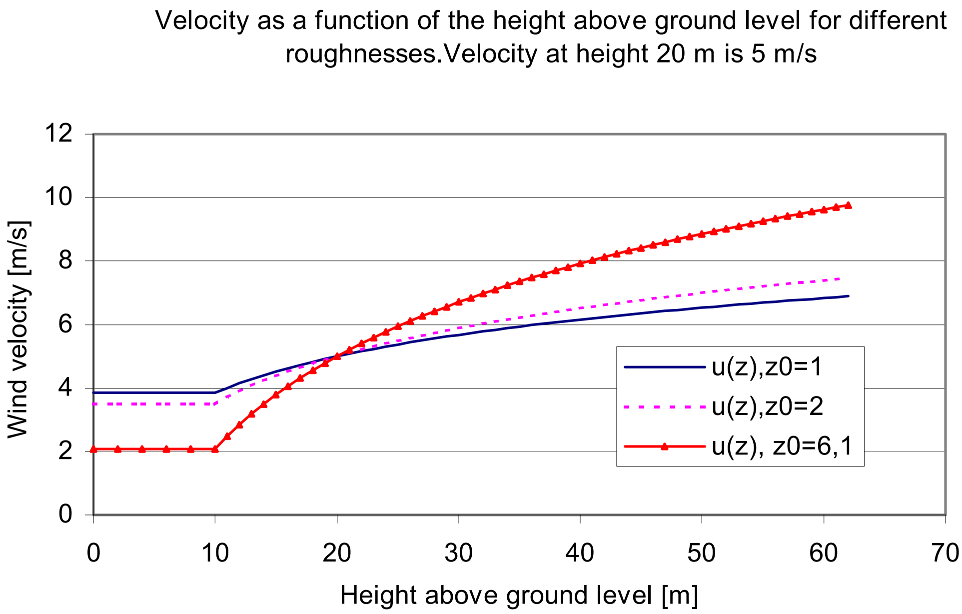

Figure 6.1 Wind velocity as a function of height above ground for different area roughness.

Orme et al. (1994) suggest that a displacement height is included in the Eq 6.6. For comparison between Simiu and Scanlan (1996), and Orme et al. (1994), the ratio of velocity at 20 m to velocity at 4.8 m for different roughness lengths was calculated with the methods proposed by each of them.

Orme et al. (1994) differ from Simiu and Scanlan (1996) by using a displacement height different from zero. The obstacles around the test house are approximately 4 m high, while the displacement height $z_d = 0.6 \cdot 4 = 2.4m$. For comparison of velocity change with height for different size of area roughness, calculations of the velocity in height 4.8 m were performed for a displacement height of 2.4 m and wind velocity of 10 m/s in height 20 m. The results are listed in Table 6.2.

Table 6.2 The velocity in 4.8 m is calculated for wind velocity of 10 m/s at 20 m, for different roughness lengths. Equations from Orme et al. (1994) and Simiu and Scanlan (1996).

	z_0	0.25	0.5	1	2	6.1
Orme et al. (1994)	u*	0.9	1.1	1.4	1.8	3.8
	u(4.8 m),z_d=2.4m	8.7	8.4	8.1	7.4	4.7
	Ratio u(20 m)/u(4.8 m) ,z_d=2.4m	1.15	1.19	1.23	1.4	2.1
Simiu and Scanlan (1996)	u*	0.9	1.1	1.3	1.7	3.4
	u(4.8 m) ,z_d=0	8.4	8.1	7.7	7.0	4.2
	Ratio u(20 m)/u(4.8 m) ,z_d=0	1.2	1.2	1.3	1.4	2.4

Table 6.2 shows that including the displacement height as proposed by Orme et al. (1994) do not affects the result much compared to Simiu and Scanlan (1996). Further it is seen that the theoretical ratio between velocities in different heights from Swami and Chandra (1994) is in accordance with the equations suggested by Simiu and Scanlan (1996) and Orme et al. (1994). The ratio of 1.4 correspond to a roughness length of 2 m, where the visual inspection estimated the roughness length to 1.

The results in Table 6.2 show that the difference in velocity is higher the more rough the area is, and that taller buildings and obstacles (higher displacement height) decreases the difference (ratio) in velocity change above the obstacles. Including the displacement height, using the measured wind velocities, showed that the roughness length was even higher that the first propose of roughness length of 6.1 m. To what extent the displacement height should be included has not been investigated further here.

For simulations the estimated roughness length of 6.1 m and displacement height of 0 were used together with data from the weather station, in accordance with the measured data. A theoretical roughness length of 1 is used elsewhere. This means that for simulations with wind data measured at the local weather station, the observed ratio of 2.4 between velocities at 20 m and 4.8 m was used, and for simulations with Design Reference Year data the theoretical ratio of 1.4 between velocities at 20 m and 4.8 m was used.

6.1.2. Wind pressure coefficient measurements

The pressure coefficients were calculated for a reference height of 4.8 m, i.e. the measured wind data from the reference point above the test house. The wind pressure coefficients were calculated from pressure difference measurements. The wind pressure coefficients outside the bottom and top vent were estimated from the measured pressure difference between the reference point and the points P_1 at the top, and P_2 at the bottom (see Chapter 4 'Experimental set up, ventilated wall'), using the following equation:

Eq 6.9 $$Cp = \frac{P - P_{ref}}{0.5 \cdot \rho \cdot u_{ref}^2}$$

From a measuring period of 3 minutes, the average Cp-value was matched with the average wind direction from the test house, see Figure 6.2.

Theoretical values for the wind pressure coefficients, as a function of the wind angle, have been calculated using the program 'Cp-Generator' (Knoll, 1996). Bas Knoll has most kindly performed these calculations, using detailed information of the test house and its surroundings.

The calculated wind pressure coefficients refer to a reference height of 20 m, similar to where the weather station was placed. To compare the measured and the calculated Cp-values, it was therefore needed to normalize to the same height. Here a reference height of 4.8 m was chosen, similar to the measuring height of wind data at the test house.

Changing the wind pressure coefficient in one height to another reference height, can be done when knowing the difference in wind speed at the two heights. The pressure at e.g. P_1 is the same for a given wind velocity and wind direction, independent of the used reference height. Therefore assuming the static reference pressure to be zero, the pressure can be determined from:

Eq 6.10 $$P = \tfrac{1}{2} \cdot \rho \cdot u_x^2 \cdot Cp_x$$

As the calculated pressure P is the same regardless of the reference height, the correlation between wind pressure coefficients with different reference heights 'a' and 'b' can be found as:

Eq 6.11 $$Cp_a \cdot u_a^2 = Cp_b \cdot u_b^2 \Leftrightarrow \frac{Cp_a}{Cp_b} = \frac{u_b^2}{u_a^2} \Leftrightarrow Cp_a = \left(\frac{u_b}{u_a}\right)^2 \cdot Cp_b$$

The wind pressure coefficient at height 'a' can then be found by multiplying the value for height 'b' by the square of the ratio between the 'velocity b' to 'velocity a'.

For comparison of the wind pressure coefficients, the reference height must be the same. As it was described earlier, the measured change in wind velocity by height did not follow what was suggested in the literature. It was believed that the observed ratio, of measured velocity at 20 m to velocity at 4.8 m, was overestimated due to wind pressed over the gable, where the ultra sonic anemometer for wind velocity measurement was placed. The generated values for the wind pressure coefficient with reference height of 20 m were therefore normalized for reference height of 4.8 m by multiplication by the theoretical value of 1.4^2. Also the generated wind pressure coefficients multiplied with 2.4^2 is seen in Figure 6.3.

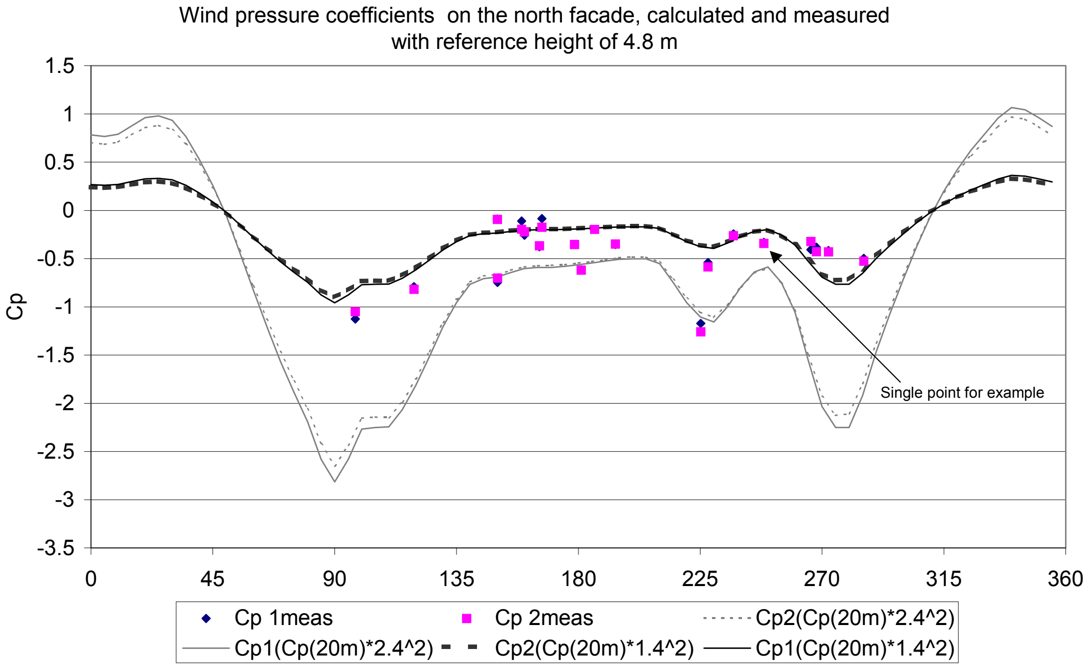

Figure 6.2 The curves of calculated wind pressure coefficients normalized to a reference height of 4.8 m using a theoretical and an observed factor, together with measured wind pressure coefficients.

Figure 6.2 shows the mean values of measured wind pressure coefficients for three minutes period together with theoretical generated values, which were normalized to the measured reference height by a theoretical (1.4^2) and a observed (2.4^2) factor. The curve normalized with the theoretical factor shows better accordance with the measured points than the curve normalized with the measured factor. The results also show a rather high variation of the measured wind pressure coefficients for approximately the same wind angle. This indicates that the uncertainty of the presented measurements was high.

The wind pressures were measured in a rather small interval of wind directions ranging from 92° to 273°, where the wind pressure coefficients were between –1.5 and 0. However, as seen from the generated values, the wind pressure coefficient can also be positive, when the wind direction turned into north. This means that the wind created pressure, when the pressure coefficients are positive. In the opposite, negative wind pressure coefficients means that the wind creates suction.

Each data point was the mean value of 3 minutes measurements, with 0.3 Hz. All the measured data, for a single three minutes period from Figure 6.2, are given as an example in Figure 6.3, together with the generated and normalized Cp-values.

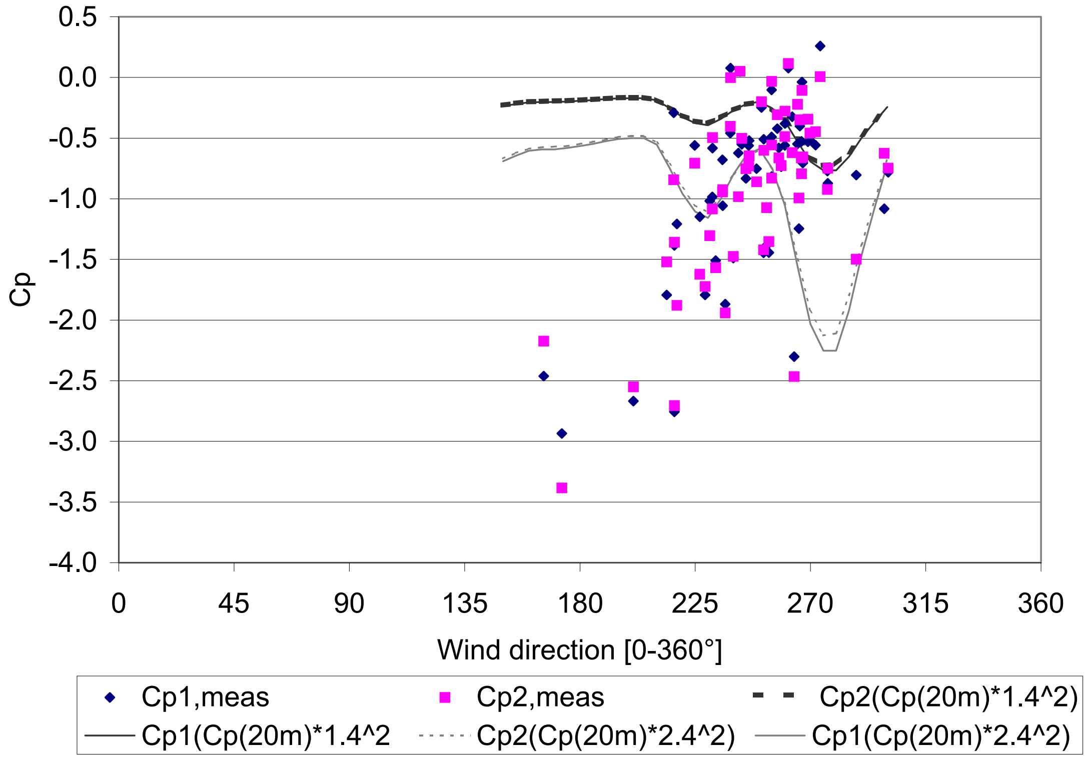

Figure 6.3 Wind pressure coefficient, with reference height of 4.8 m, showed as a function of the wind angle. The values were estimated from measured data in a three minutes period together with theoretical generated values (reference height changed by multiplication with 1.4^2 or 2.4^2). The results show that the wind direction and the wind pressure coefficient varied a lot over the relatively short time interval, and showed no clear correlation between the measured and generated values.

The measured Cp values with reference height 4.8 m in Figure 6.3, were compared to generated values from Bas Knoll. It is seen that the dispersion of the wind pressures are high, and that the measured values lie around the two curves. Due to the limit of data for different wind directions, it was chosen to use the generated wind pressure coefficients, normalised with 1.4^2 for the simulations later on.

Also the pressure difference between the outside points P1 and P2 were measured, and used for estimate of the 'Delta Cp' which is seen in Figure 6.4.

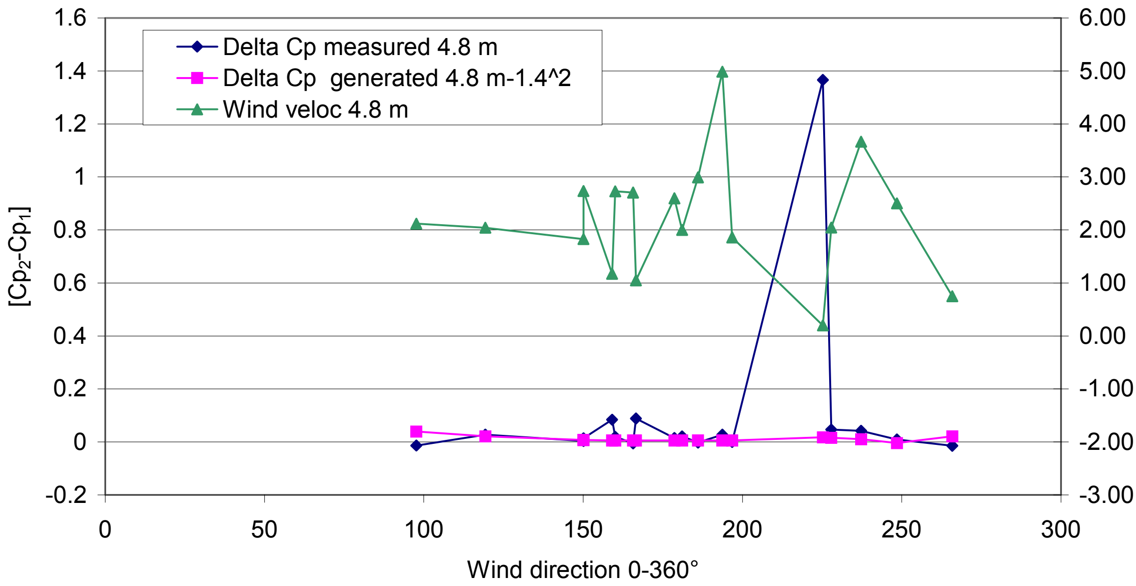

Figure 6.4 Measured and generated difference in wind pressure coefficient of point 1 and 2 as a function of the wind angle, together with the wind velocity shows that the wind velocity must be above 1.5 m/s (at height 4.8 m) to perform measurements. Positive values mean that the wind pressure support the buoyancy effect. For wind angle of 248° the generated difference in wind pressure coefficient is negative, but a positive difference was measured.

Figure 6.4 shows that the difference in measured and theoretical wind pressure coefficient was high for low wind speed. It was therefore concluded that the wind velocity at 4.8 m should be > 1.5 m/s for performing pressure measurements.

Not only the wind pressure coefficients, but also the difference in wind pressure coefficients is interesting in the analysis of wind pressure difference between vents.

The generated wind pressure coefficients were used for calculating the difference in wind pressure coefficients, between the bottom and top, see Figure 6.5.

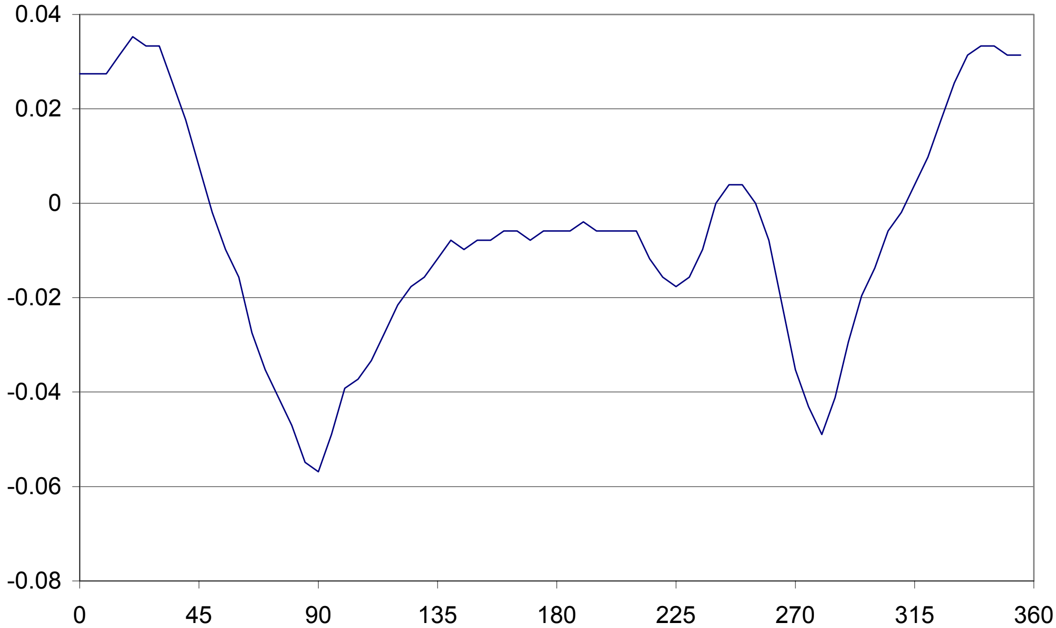

Figure 6.5 Difference in wind pressure coefficients outside the top and bottom vents, Cp1-Cp2. The positive values mean that the wind pressure opposes the buoyancy force, and negative values mean that the wind pressure supports the buoyancy force.

Buoyancy force can be both upward and downward, due to the sign of the temperturegradient. Sometimes it is called the stack effect, referring to warm air in a stack, that rises above the colder outdoor air. The buoyancy force is here defined as positive for upward direction of the force and negative for downward direction of the force.

The difference in pressure coefficients, between the positions of the top and bottom vents, is seen in Figure 6.5. The curve is positive when the wind pressure at the top is higher than the bottom pressure, so the wind pressure will oppose a positive buoyancy force. When the curve is negative the wind pressure at the bottom is higher than at the top, so the wind pressure supports a positive buoyancy force. From the Figure 6.5 it is seen that the wind pressure oppose a positve buoyancy force for wind directions from the north e.g. direction 0°-45° and 315°-355°, and for direction 240°-255°, i.e. west-south-west direction. It is also noted that the highest pressure-difference due to wind is obtained for sideward wind, coming from east (90°) or western direction (280°).

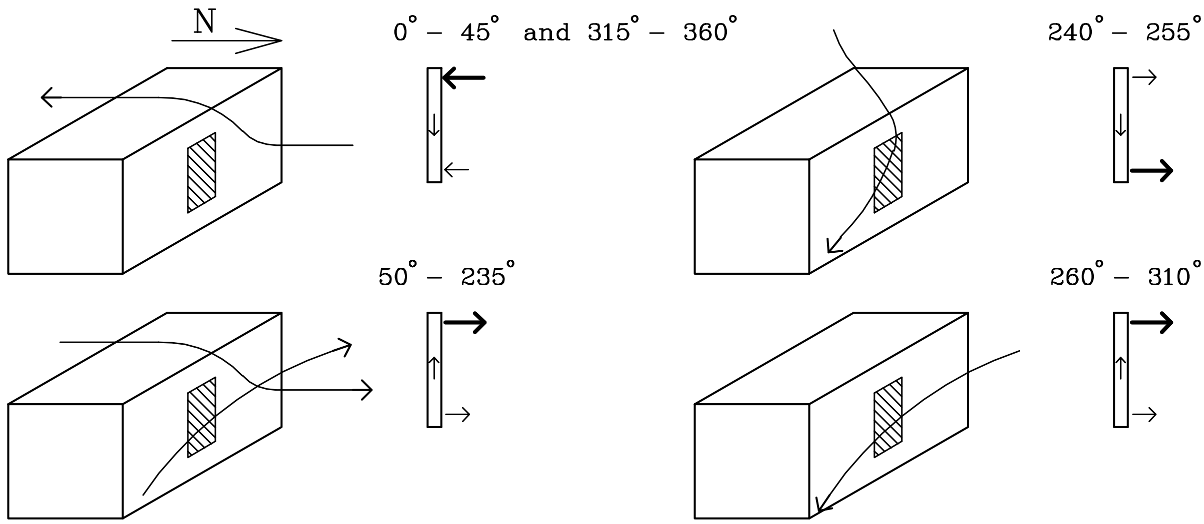

Figure 6.6 The test wall was placed on the north side. The wind influences the airflow differently depending on the wind direction. The arrow over the building shows the wind direction. The figures to the right show the wind pressure by direction and size relative to the bottom pressure. The arrow inside shows the resulting airflow due to wind pressure. The pressure is based on the wind pressure coefficients from Knoll(2000).

The interesting conclusions of this were, that sideward wind has more influence on the airflow than direct wind. Further it is interesting to note that wind can be affecting the airflow downward on the leeward side (see Figure 6.6 for wind angle of 240°-255°).

6.2. Direction of air flow

The test wall and the equipment were described in the Chapter 4 'Experimental set up, ventilated wall' followed by validation of tracer gas method for air velocity measurements in the Chapter 5 'Air velocity measurements'. The tracer gas measurements showed good accordance with simultaneous thermal anemometer measurements, as the air change over the cross sectional area was in accordance with the measured air velocity, meaning that the air was actual changed and not recycled, as proposed in the scope of Chapter 1 'Introduction'.

Measurements with thermo anemometers and tracer gas showed airflow both up and down, Table 5.1 in Chapter 5 'Air velocity measurements'. The wind direction was mainly in two directions, west (250°-287°) and southeast (98°-157°) during the experiments. Injection of smoke, gave the impression that the flow was either upwards or mixed up and down. Fluctuations in cavity air direction were observed for mean wind direction 265° (measurement #5) and 262° (measurement #6) however, measurement #7 with similar wind direction of 265° had upward air direction. Further fluctuation of air direction was seen for wind angle of 98°.

Thermal anemometers seem not to be more accurate for clear upward direction than for mixed up and down. The tracer gas method measures some very high velocities, which could be due to change in direction of the airflow, described in Chapter 5. It then indicates that the air was changed in the cavity during unstable flow direction.

Other measurements of the air velocity were performed, using tracer gas. These measurements were performed over longer periods, including night periods. The measured air velocity by tracer gas is seen together with the hourly mean wind direction (running average) and hourly mean wind velocity (running average) in Figure 6.7-Figure 6.11. The wind direction and wind velocity was measured at the weather station at 20 m above ground level. The air velocity was measured with an interval of 8 minutes.

The Figure 6.7-Figure 6.10 show longer periods (days) of air velocity measurements with tracer gas, performed in February 2001. The experimental data shown in Figure 6.11 are from August 2001.

Figure 6.7 shows a period where the air velocity was close to zero and a period where the velocity was very high. The period with low velocity was constantly negative, i.e. the flow was constantly downwards, this means that there was an air flow (no recycling), where the high velocity period meant that the airflow was changing direction, but with a change of air, i.e. no recycling here either.

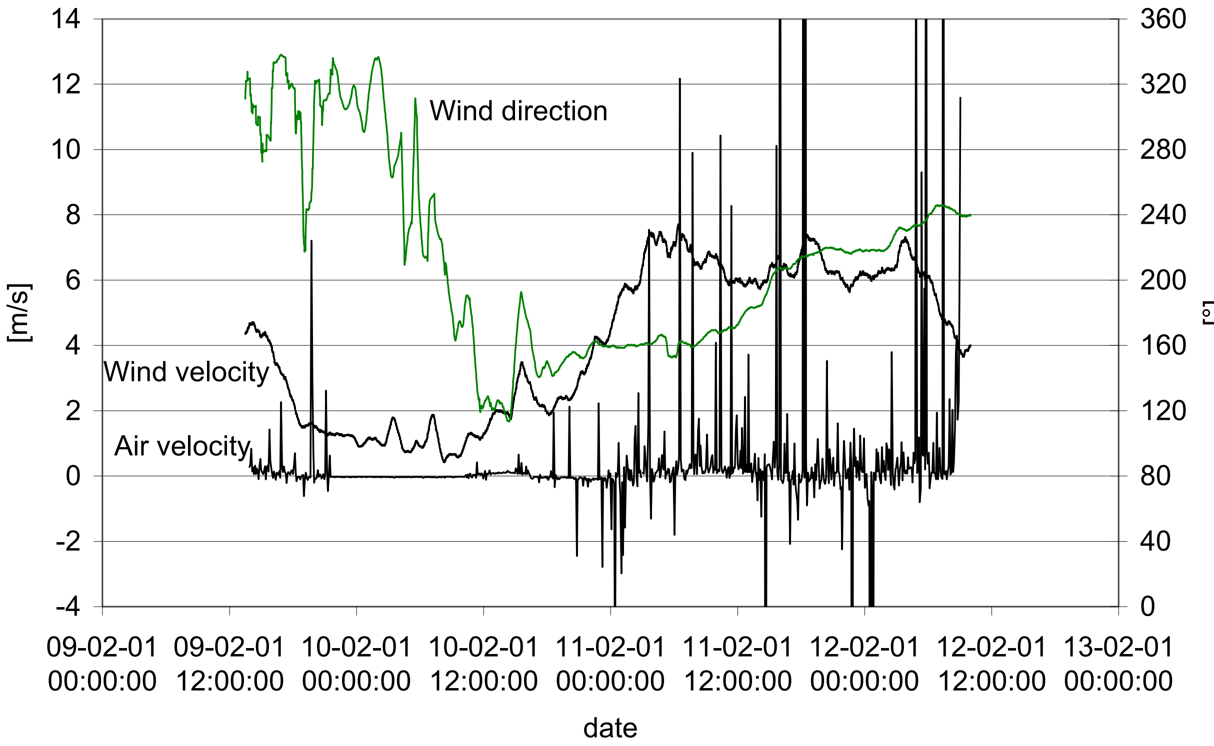

Figure 6.7 shows the air velocity measured by tracer gas in m/s, together with the wind velocity in m/s, and wind direction in degrees.

The low downward velocity in Figure 6.7 was correlated to low wind velocity,< 2 m/s. The airflow was driven by buoyancy force of cold air cooled by radiation heat loss at night, giving a downward airflow. From 11/2 at 3:00 to 12/2 at 2:00 the wind velocity increased from 4 m/s to 8 m/s, and the wind direction was in the range 160°-240°. In this period the airflow was unstable both in direction and in velocity. During the day with wind from 160°-240°, the buoyancy force and wind pressure difference were both expected to be upward, but the measurements did not indicate a stable flow direction.

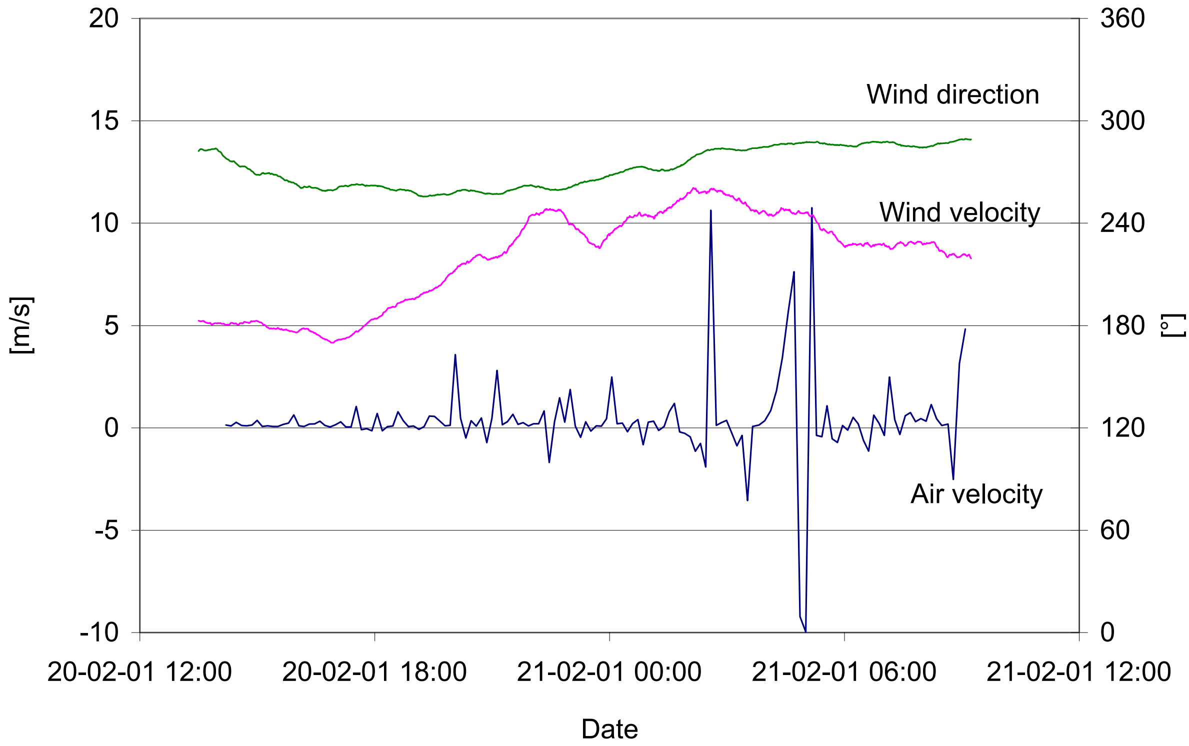

Figure 6.8 shows the air velocity measured by tracer gas in m/s, together with the wind velocity in m/s, and wind direction in degrees.

The airflow in Figure 6.8 was close to zero but positive in the beginning, where the wind velocity was stable around 5 m/s, followed by a period with changing direction and air velocity ranging between ±3 m/s, and at the end a period with high peaks of air velocity, measured during night time. The wind direction was stable from eastern direction (sideways to the test wall), where the wind velocity increased from 5 m/s to around 10 m/s during the experiment. It seems like the air velocity became unstable when the wind velocity increased, but as the only experiment, the air velocity was reasonable without extreme measured air velocity values.

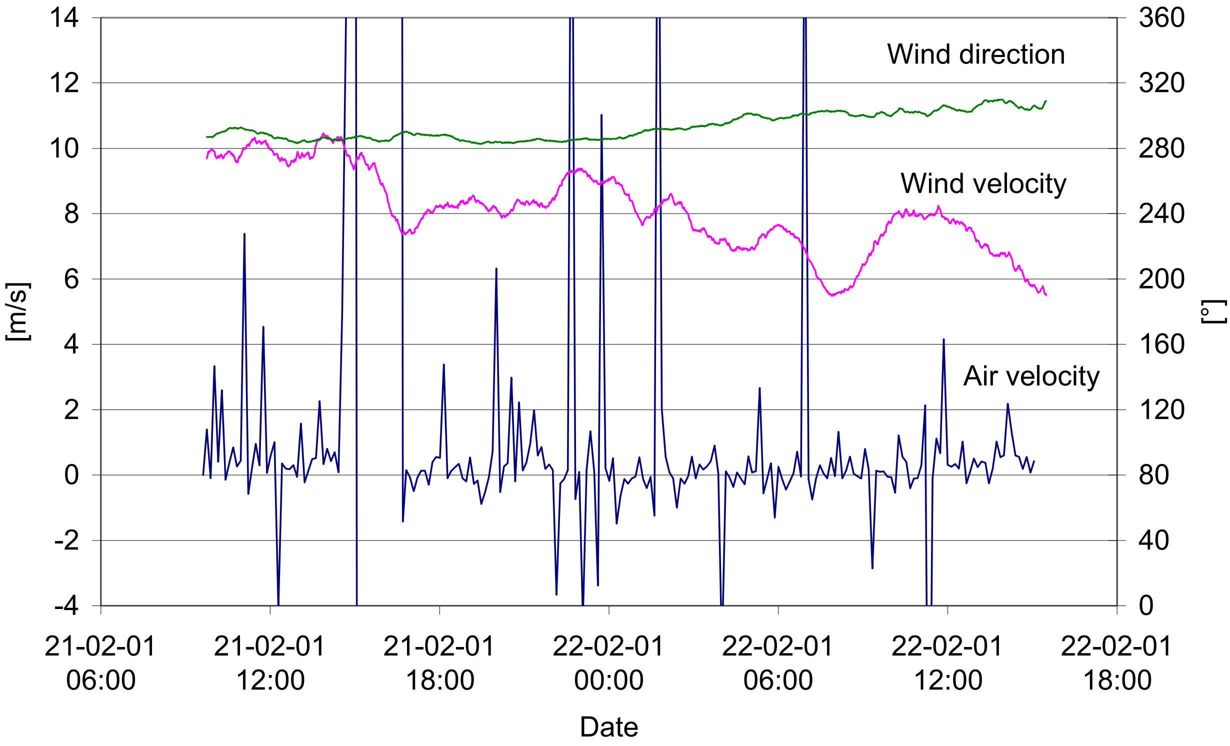

Figure 6.9 shows the air velocity measured by tracer gas in m/s, together with the wind velocity in m/s, and wind direction in degrees.

The measurements in Figure 6.9 show high fluctuations in the air direction, and an unstable period 21/2 in the afternoon with very high velocities. This period did not seem to be correlated to special wind velocity or special wind direction, although a sudden change in wind velocity was seen.

During the experiment shown in Figure 6.9 the wind direction was rather stable around 300° like for Figure 6.8, and the wind velocity ranged from around 10 m/s to 6 m/s. The air velocity showed changing direction mostly in the range ± 2 m/s, with some extreme values, and high air velocity the 21/2 around 16:00. The unstable air velocity seems to be correlated to a sudden change in the wind velocity from 10 m/s to 8 m/s. However, the decreasing wind velocity alone, can hardly explain such an impact on the air velocity. Similar sudden decreasing wind velocities were seen 22/2 in the afternoon, without resulting in measurements of very high air velocity.

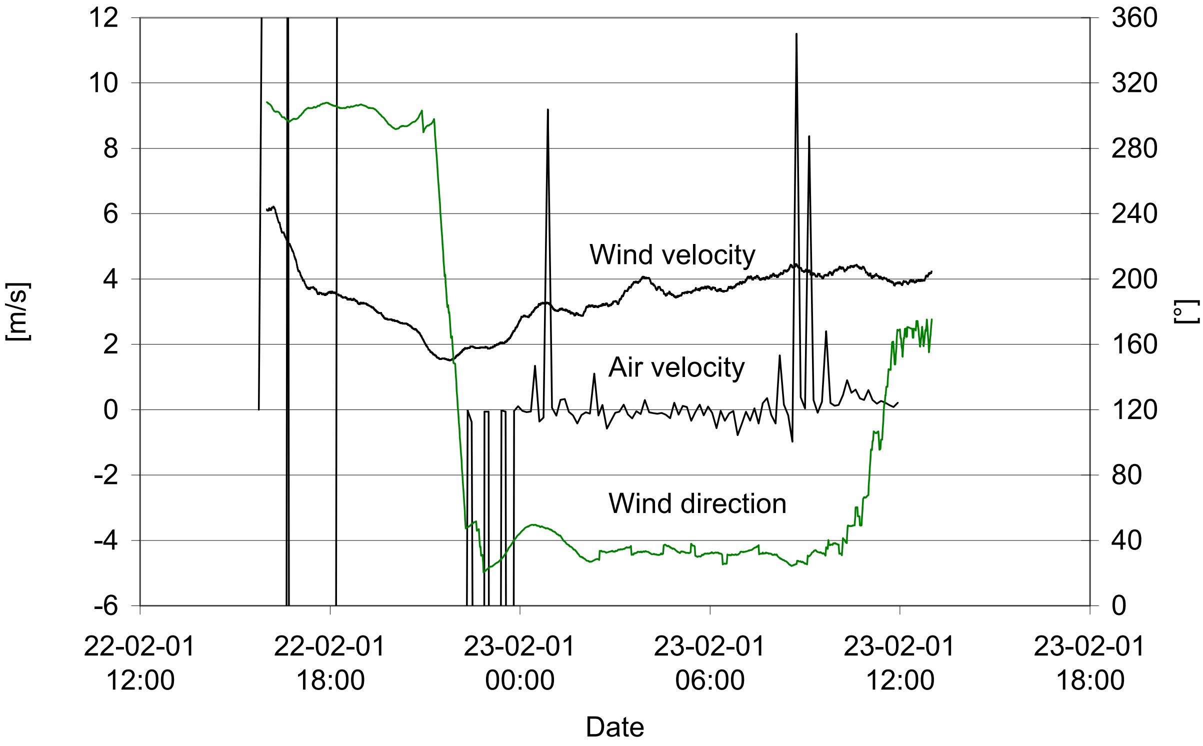

Figure 6.10 shows the air velocity measured by tracer gas in m/s, together with the wind velocity in m/s, and wind direction in degrees.

The last experiment from February is shown in Figure 6.10, where a very high velocity was measured in the first part until midnight, after where the flow was rather constant around zero with flow in both directions. The wind direction was around north, turning to south at the end of the observed period. A stable period during night and morning, when the wind velocity was from 3-4 m/s and the wind direction was constant near 35° (north). The low air velocity in both directions indicates recycling of ventilation air.

The presented measured periods, Figure 6.7-Figure 6.10, show that the direction of the cavity airflows was highly unstable, where the air velocity was very high in some periods and close to zero in others. The low air velocity in Figure 6.7 was correlated to low wind velocity (<2 m/s), where Figure 6.10 for a low wind velocity (<2 m/s) had very high air velocity. The different experiments were carried out for different wind directions, where the unstable air direction or air velocity didn't seem to be correlated to a specific wind direction.

It is not clear from the measured data, which external influences differentiate the stable and the unstable period.

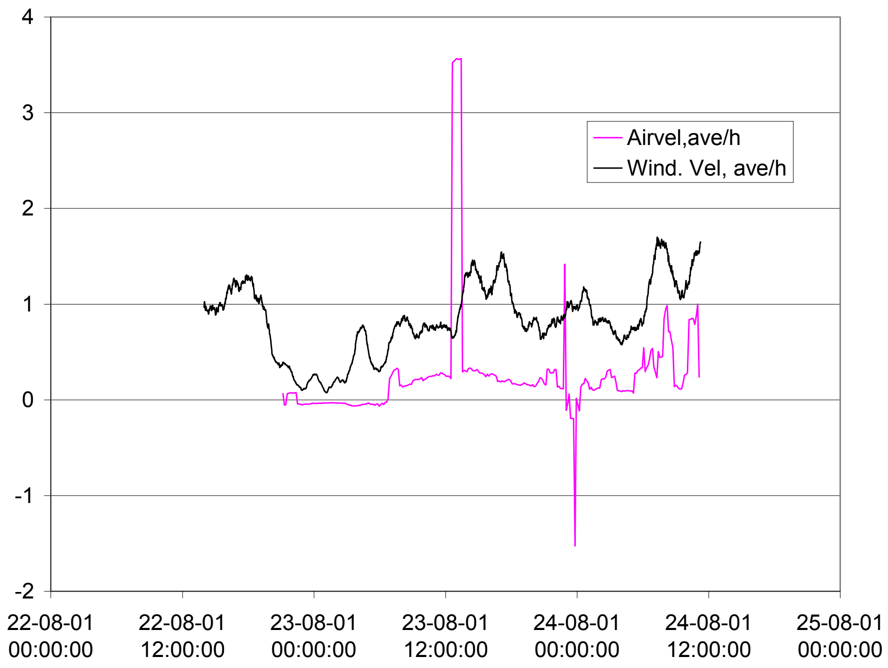

Figure 6.11 Air velocity and wind velocity as a function of time

Two days measurements in August, of the simultaneous air and wind velocity are shown in Figure 6.11. Air velocity was measured with an interval of 8 minutes and the wind velocity every minute, both curves are values of one hour running average.

Figure 6.11 shows measurement in the summertime, where the wind velocity was low, and the wind direction was constantly changing in all directions. The peaks in wind velocity seem to some extent to correspond with peaks in the air velocity.

It was not possible to determine a significant correlation between airflow direction and wind pressure. A possible theory was that wind suction and wind pressure either support or oppose the air velocity, some indication of correlation was suggested. For low wind velocity the buoyancy force dominates the airflow direction. For higher wind velocity the wind can either support or oppose the buoyancy force. Due to a limit number of experiments, it was not significantly shown that wind pressure difference opposing the buoyancy force gives fluctuation in the airflow direction.

6.3. Air velocity correlated to wind velocity

To find a correlation between air and wind velocity, the data from Figure 6.11 is plotted in Figure 6.12. In Figure 6.12 the air velocity is seen as a function of the wind velocity. The negative value of air velocity was by night, where the radiation decreases the temperature of the cavity air in a period with low wind velocity, and where the wind speed was low. Under these conditions the direction of the airflow became negative, i.e. flow from the top to the bottom. During daytime, or when the wind was stronger, the direction of the airflow became positive i.e. from the bottom to the top.

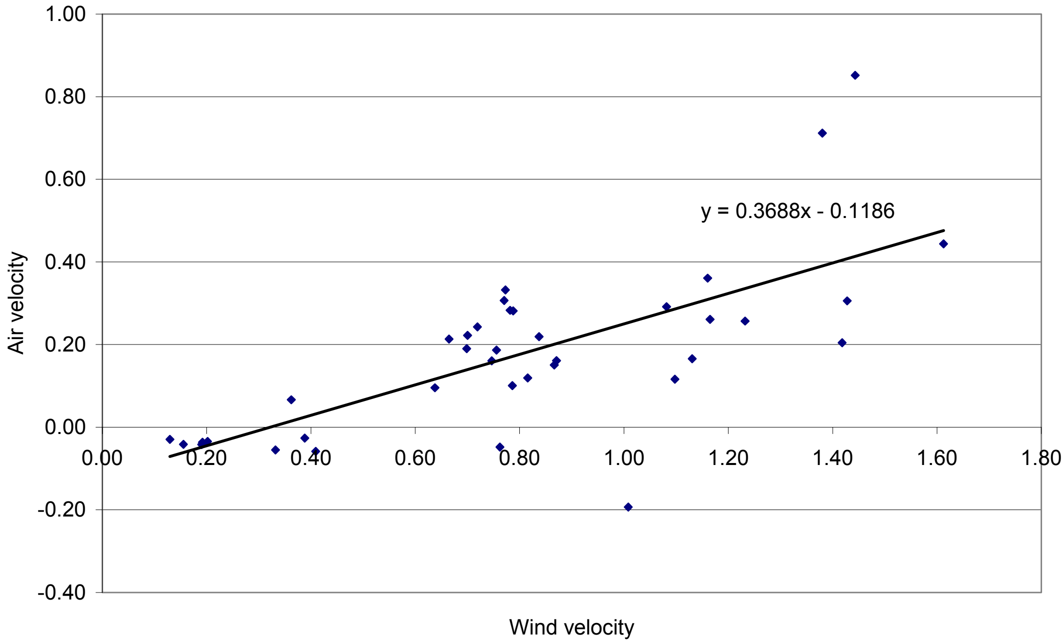

Figure 6.12 Hourly mean values of the air velocity measured with tracer gas against wind velocity with a first order regression model.

Table 6.3 Results of statistical analysis of the hourly mean air and wind velocity in Figure 6.12

	Coefficients	*Stand. dev.*	*P-value*
Intercept	-0.11863	0.054793	0.037083
Slope	0.368786	0.061452	6.92E-07

The wind velocity was measured every minute and the air velocity about every 8 minutes. The simultaneous wind and air velocities are therefore not available, while the nearest wind velocity has been used for statistical analysis. A poor correlation is found for ‘all data’, see Appendix D, but statistical analysis on the hourly mean air velocity, Figure 6.12, with the hourly mean wind velocity showed that both the slope and the intercept are significant, Table 6.3. It means that the air velocity is significantly correlated to the wind velocity, Figure 6.12.

The data for measured wind velocity and air velocity from Figure 6.7-Figure 6.10, is also analysed. In Figure 6.13 - Figure 6.16 the data are plotted together with a linear regression model. The statistical data for standard deviation and P-value for the regression model can be found in Appendix D.

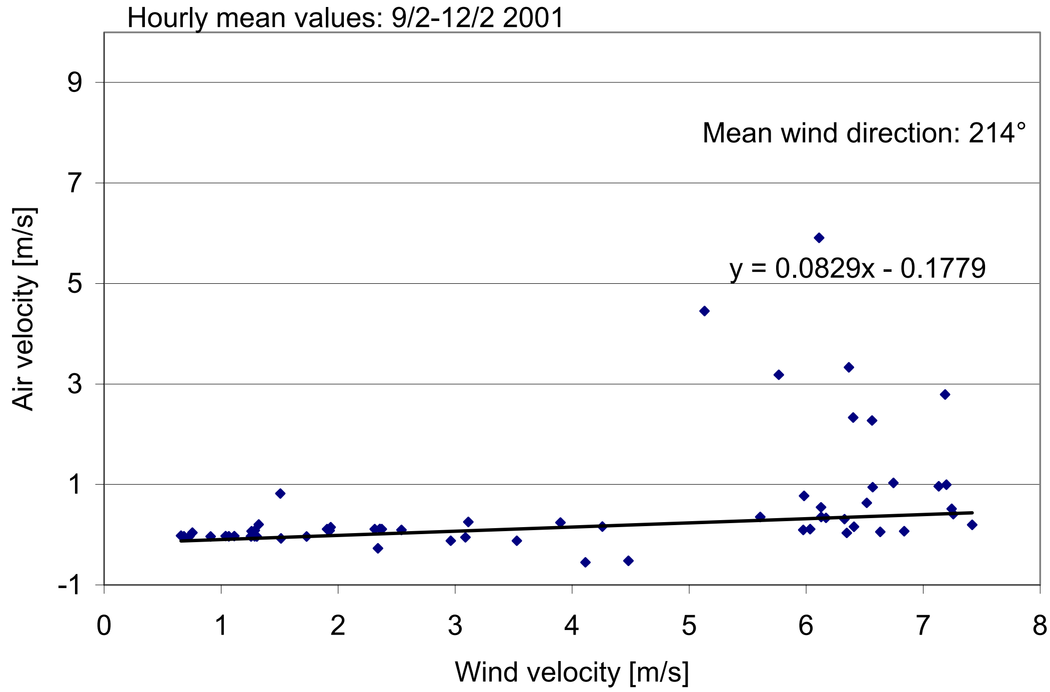

Figure 6.13 Hourly mean values of the air velocity measured with tracer gas against wind velocity with a first order regression model.

In Figure 6.13 the measured air velocity is seen as a function of the wind velocity. For wind velocity less than 5 m/s the measured air velocity was almost on a horizontal line, i.e. the wind did not influence the air velocity. For measurement with wind in the range 5 m/s to 8 m/s the dispersion was high, and no significant correlation could be stated.

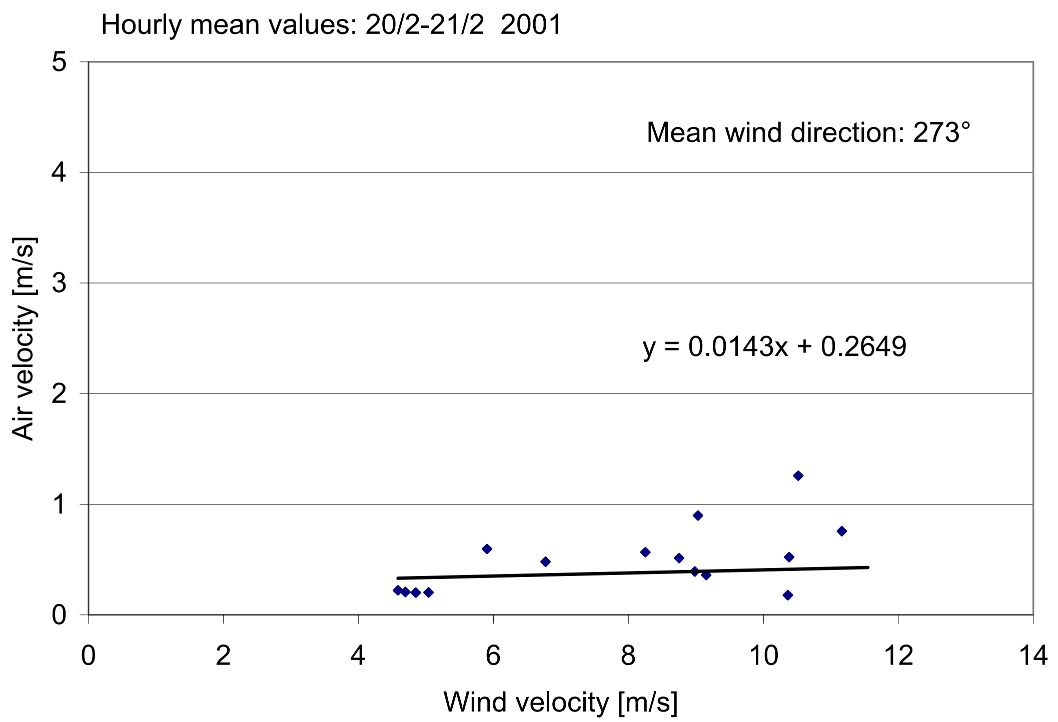

Figure 6.14 Hourly mean values of the air velocity measured with tracer gas against wind velocity with a first order regression model.

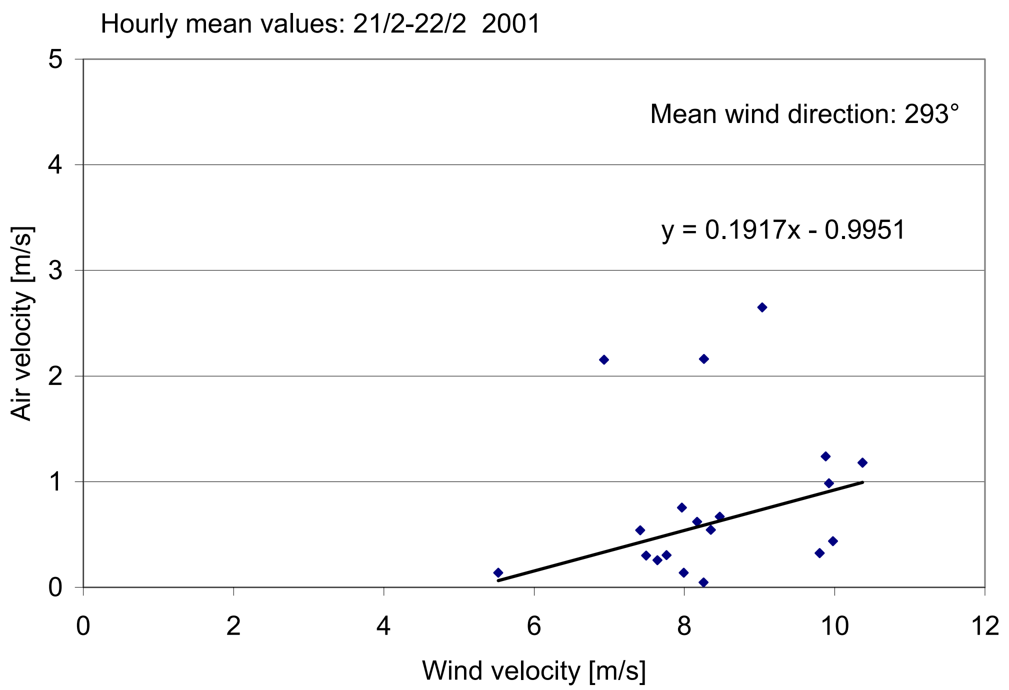

Figure 6.15 Hourly mean values of the air velocity measured with tracer gas against wind velocity with a first order regression model.

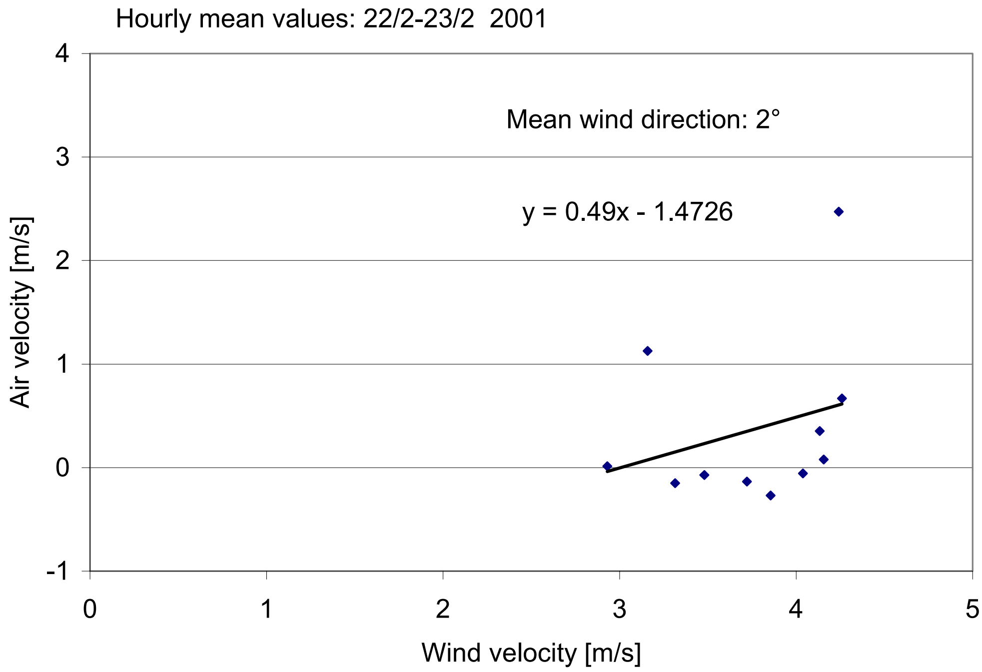

Figure 6.16 Hourly mean values of the air velocity measured with tracer gas against wind velocity with a first order regression model.

The plots of air velocity as a function of the wind velocity show very different results, and the scatter for the measured points are quite high. Only the slope in Figure 6.12 was considered significant on a 5% level (the P-values <0.05). Here the wind velocity was rather low and the wind direction was changing, coming from all directions.

6.4. Air velocity fluctuations in the cavity

The measurements in Figure 6.7 - Figure 6.11 showed fluctuations in the air velocity measured with tracer gas. These fluctuations were both due to changes in air velocity and due to change in airflow direction. Due to the rapid response, the use of thermo anemometers gave better measurements of the actual fluctuations in the air velocity.

The instantaneous velocity measurements in the cavity identified large velocity fluctuations in the six measuring points. Figure 6.17 shows an example of the instantaneous velocity measured over time by one of six themo anemometers, with a mean velocity of 0.29 m/s and a standard deviation of 0.15 m/s. The mean wind velocity was 1.3 m/s at height 4.8 m, and the direction 251° in average.

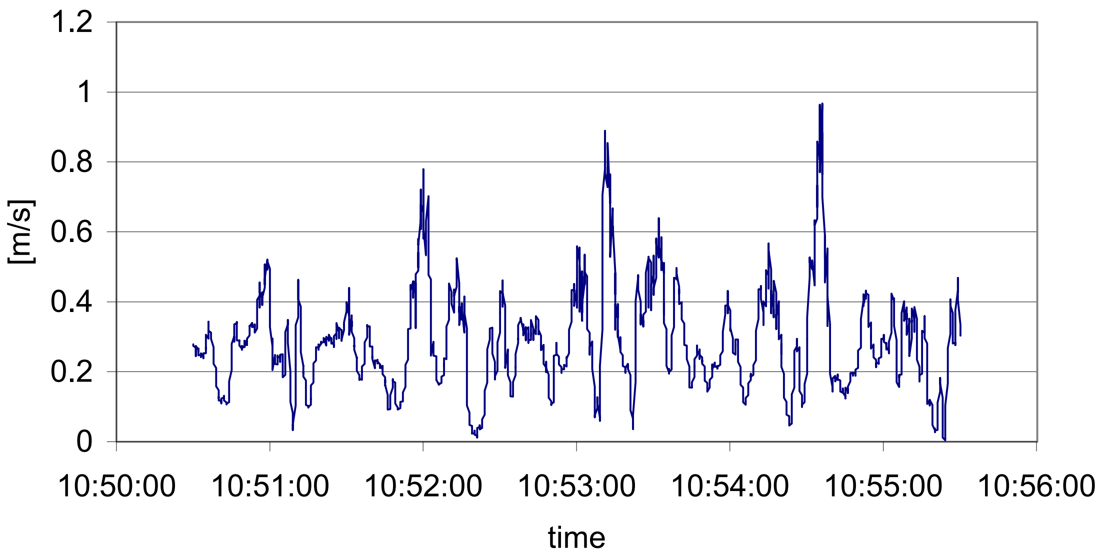

Figure 6.17 Instantaneous air velocity measured with thermo anemometer with 5 Hz, for a probe position 409 mm from the left edge.

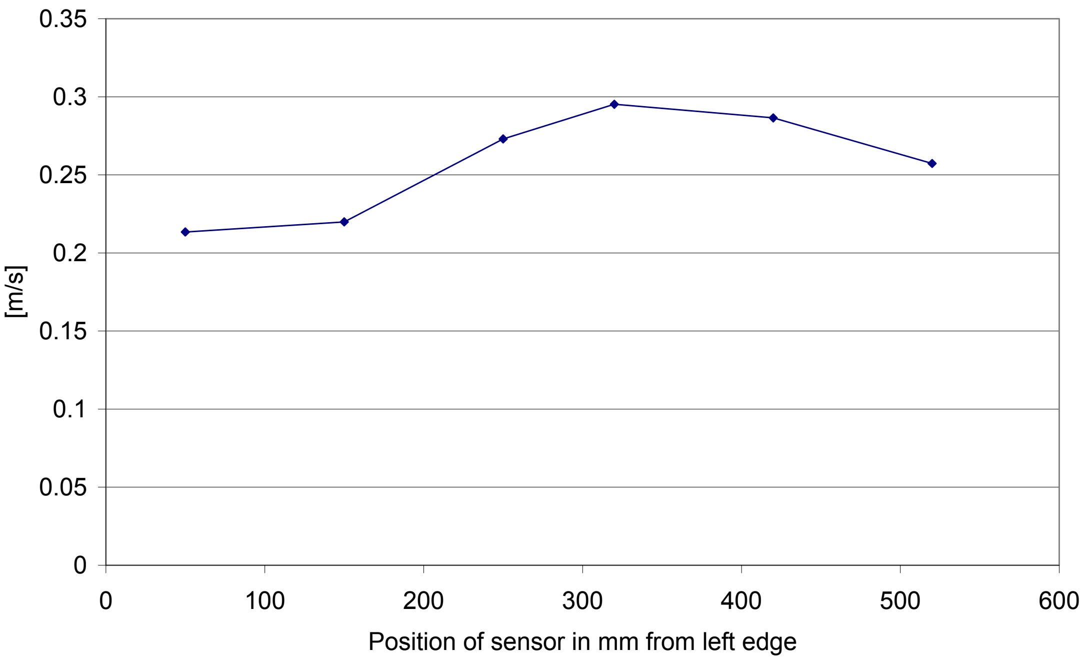

Figure 6.18 shows the average air velocity of an experimental period for each of the six positions. The experimental period was 5 minutes, where the mean wind direction was 251°(west) and the mean wind velocity was 1.3 m/s at height 4.8 m.

Figure 6.18 shows the velocity profile in parallel with the wall, where the velocity was highest near the centre and lowest at the sides. The velocity profile was affected by sideward wind; hence the profile was asymmetric around the centre. The figure shows that to determine the mean velocity over the cross-sectional area correctly, more than one measuring point was needed.

From measurements of the wind velocity and wind direction it was found that both were changing with a high frequency comparing to a normal sampling time of 10 min. for wind data. Changing air velocities inside the cavity were also observed by the thermal anemometer measurements, meaning that the wind fluctuation also affected the air velocity inside the cavity.

6.5. Moisture content

Together with the measurement of the tracer gas concentration, the gas analyser also measured the water concentration. This was primarily to compensate for the influence of water on accurate determination of the tracer gas concentration. The measured vapour concentration of the air was however, also used to determine the convective moisture transport. From the tracer gas concentration the air velocity and direction were found. From measurements of the water concentration in the outdoor air and in the cavity air, the difference in water vapour in g per volume air change was estimated, and with that the total convective moisture transfer per time, could be calculated.

An example of the convective moisture transfer during the measured period in August is seen in Figure 6.19. The data from the analyser were used for calculating the mean air velocity. This is used together with the measured water concentration upstream the dosing pint, and the water concentration of the outdoor air to find the accumulated convective moisture transport.

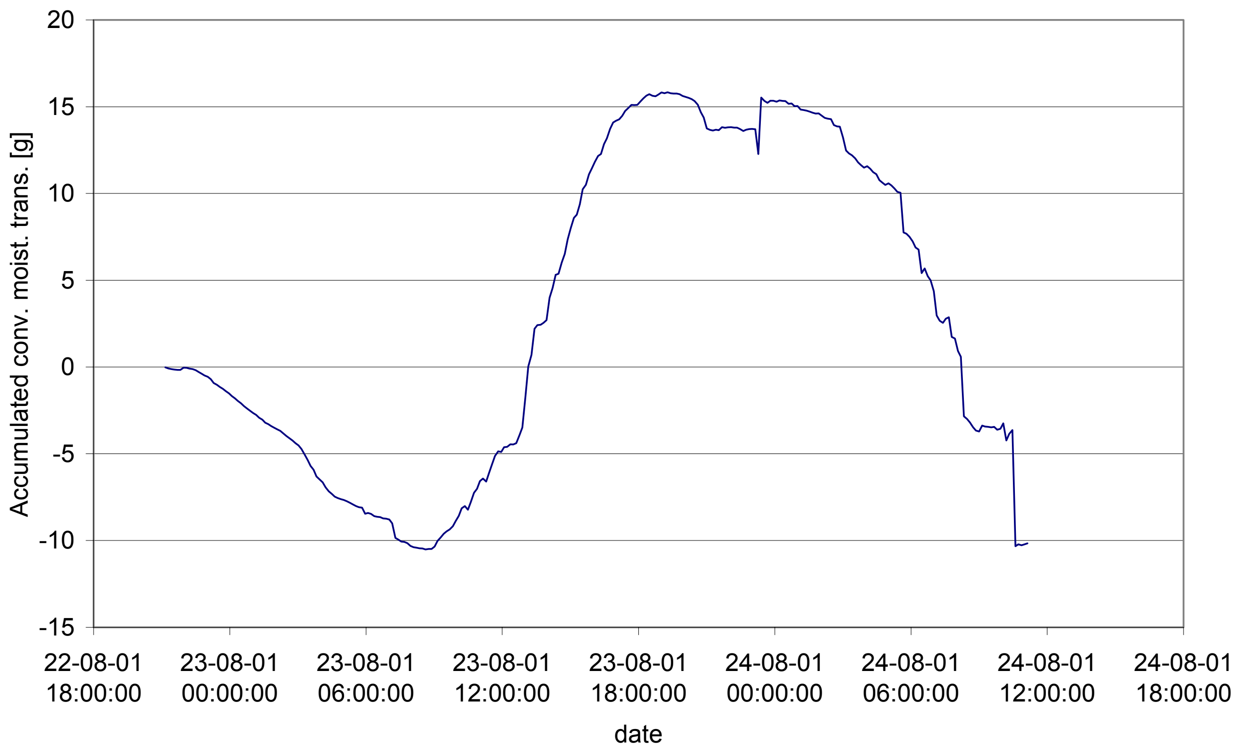

Figure 6.19 Measured accumulated moisture over a 2 days period, due to convection.

The Figure 6.19 shows the measured moisture transfer in [g], out of a ventilated cavity. Negative values means that the convection had wetted the structure since the start of the measurement, and positive values that the structure had been dried since the start of the measurement. The slope shows the size of convective water vapour transfer per time out of the cavity. It is seen that the ventilated cavity is wetted in the night period and dried during the day.

6.6. Summary

The numbers of experiments were too few to make significant statements or conclusions on the wind pressure coefficients and the airflow dependence on wind direction and wind velocity. Further a higher variety of wind direction and seasonable variations may be included. The buoyancy force should be known and included in future experiments.

The advantages of the two different velocity measurement methods have been used for different analyses. Where a high fluctuation in air velocity was found with the thermo anemometers but the gas analyser method showed that these fluctuations did not influence the mean airflow. Further the benefit of water vapour measurement with the tracer gas analyser was found to be utilizable for estimation of convective moisture transfer through a ventilated cavity.

It should be noted that the estimated difference in wind pressure coefficients by Knoll (2000) affected the cavity air in downward direction for the wind-directions in the intervals 0°-45°, 315°-360° and 240°-255°, see Figure 6.6. When the wind direction was 50°-235° or 260°-315° the wind pressure work in the upward direction. This meant that the wind and the stack effect works in the same direction most of the year for a north facing wall, where the wind-direction is mainly west and south, excluding the time where radiative heat loss make the buoyancy force downward.

7. Simulation model

Building simulations are widely used for research and investigation of thermal and moisture behaviour in the rooms and the materials of buildings. In traditional computer programs the source code is closed to the user, and missing flexibility makes it difficult to improve or make changes in the original code. Here it was alternatively chosen to work with an open source code.

The choice of simulation environment was the Simulink tool, which is a part of the MATLAB package(MATLAB, 2001). The interactive Simulink environment offers a long list of built-in blocks that implements commonly required modelling functions. It is a tool for simulating, modelling and analysing dynamic systems, using a set of integration algorithms based on the MATLAB ordinary differential equation solver. The Simulink tool was chosen due to the interactive user face, and the long list of built-in blocks, which facilitates exchange of models with other users. During the model building, a co-operation with Chalmers University in Sweden was started (Nielsen et al., 2002).

A computer model for simulation of the heat and moisture transport in a building envelope with ventilation was conducted, using the Simulink code in MATLAB. The model was built from smaller subsystems, which could be combined in general for description of hygro thermal conditions in virtually any kind of building envelope. For the present study of a ventilated wall the toolboxes were used to simulate the hygro thermal conditions in the wall material and cavity of a ventilated facade in order to find the yearly moisture transport by convection in the ventilated cavity, and to find the period length with critical moisture load for the air barrier, for different insulation thicknesses and different airflow rates.

7.1. Models in Simulink

A simulation model in Simulink will often contain several subsystems. Each subsystem consists of a variety of built in Simulink ‘source blocks’. The subsystem has a set of input and output variables. Using the same set of variables for all subsystems, by all users will, give access to easily exchange of subsystems, made by different users. A subsystem of e.g. the coupled heat and moisture transport in a material layer can then be copied and used in a variation of simulation models, where this part of a building envelope is to be simulated. The same subsystem of a material layer could, as an example, be included in a simulation model of a wall, a roof, or a floor.

With a set of general subsystems, it should in the future be easy and fast to set up a simulation model of any kind of a building envelope. The user can then improve some of the subsystems or implement his own subsystems in an existing model, without starting from scratch.

The exchange of subsystems has been tried with success in the following example of a ventilated wall. Here a model of a coupled heat and moisture transport in a material layer was made in co-operation with another Ph.D. project (Peuhkuri, 2000-b). The ‘Material Layer Subsystem’ was used in a simulation model of a ventilated wall, where also other subsystems were created and included. An existing subsystem ‘Config weather data’ (Noyé, 2000) for importing weather data was included in the model. This subsystem imports a weather data file for simulation of the outside weather conditions. While the ventilated wall model was created, the original Material Layer Subsystem was tested, validated and modified (Peuhkuri, 2001), and could now replace the original material layer subsystem.

From the experience of co-operation it was found that it is of benefit to agree on variable names for constants and material parameters. Another important topic was to agree on the use of the same data stream, so all toolboxes in the Building Physic library have the same vector of data streams, where the input and output data are the same. To coordinate this a working group was set up in connection to ‘CEN TC89 WG10 WI29-meetings’. With a set of variable names and their definitions a wide exchange of subsystems between universities could be possible in the future (Nielsen et al. 2002)

A Building Physics Toolbox was suggested by Hagentoft (2001) and under development between Chalmers University in Sweden and Technical University of Denmark. Subsystems are built and added to a library, from where they can be copied and used for simulations of all parts of the building envelope. An example is a model of one-dimensional heat transfer in a single material layer, which was developed and described by Hagentoft (2001). This thermal model was here copied and modified as a new model of the coupled heat and moisture transport in a material layer.

The Simulink subsystems, which were created and used as a part of this project, are listed in the Table 7.1. The models were made in order to simulate the coupled heat and moisture transport in a ventilated wall, but are considered as sufficiently flexible to simulate HAM transport in other building parts by replacing some of the subsystems with others. Simulations of a ventilated wall will later exemplify the use of Simulink subsystems for building envelope simulations.

Table 7.1 List of Simulink subsystems used for an example of Simulink simulation of a building envelope, Appendix E.

Name of subsystem	**Short description**	**Developer**
Indoor variable	Indoor RH and temperature, with a yearly cycle	Gudum
Matlayer	Coupled heat and moisture transport in a material layer, including heat conduction, moisture diffusion, thermo diffusivity	Gudum and Peuhkuri
Node	Coupled heat and moisture transport in a material layer, including heat conduction and moisture diffusion	Peuhkuri
Vapour retarder	Moisture transport over a water vapour resistance, but with no heat resistance	Gudum
Surf layer temp and moist	Moisture content and temperature at a surface of a material layer exposed to air. Inside the material the heat transfer by conduction and the moisture transport by diffusion are simulated. To the air the moisture transport by convection and the heat transfer by convection and radiation are simulated.	Gudum
Cavity temp and moist	Two coupled balances simulate temperature and moisture content in a ventilated air cavity. The heat balance includes a capacity, where the moisture balance is without capacity.	Gudum
Volumeflow	Airflow by volume through a cavity exposed to wind pressure and buoyancy force.	Gudum
Rain screen with heat cap	Temperature of a rain screen with an ventilated air gap on the inside, including convection and radiation on both sides.	Gudum
Outside temp and water vapour pressure	Calculates the outdoor temperature and water vapour pressure, from a file with reference climate data	Gudum
Config weather data	Reads and reformates weather data from a file.	Noyé
Dist. weatherdata	Transform the weather data to SI-units.	Noyé

A Simulink model of the moisture transport in a light weight wall with ventilated cavity was developed by connecting subsystems of the coupled heat and moisture transport in the wall, the heat and moisture transport in the ventilated cavity together with subsystems of the boundary conditions, seeFigure 7.2.

7.2. Ventilated wall model

To exemplify the Simulink tool and the use of it, a light weight ventilated facade was chosen as object for modelling and simulations. The rest of the chapter is detailed information of the equations behind the simulation model.

First is a presentation of the wall model with its subsystems. The equations behind are described separately for each subsystem in the following order: 'Indoor variable', 'Material layer', 'Vapour retarder', 'Surface', 'Cavity', 'Rain scren', 'Air flow', and 'Weather data.

The basis model of the modelled ventilated facade consist of an inside cover, a vapour retarder (if present), insulation material, air barrier, ventilated air cavity, and a rain screen, see Figure 7.1. The basis model is modified by e.g. excluding the vapour retarder or remove the ventilated cavity.

The simulation of exposure of the building envelope to outdoor weather conditions, was modelled by using a file with reference year of hourly data for the outdoor climate. Inside climate was simulated by two sinusoidal expressions of temperature and relative humidity with a yearly cycle.

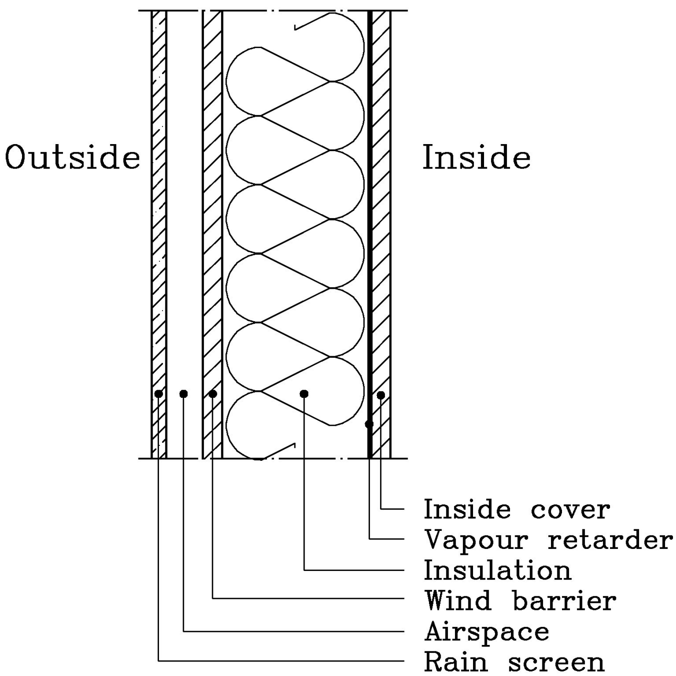

Figure 7.1 The material layers in a ventilated wall, which has been object for modelling the coupled heat and moisture transfer using Simulink.

The simulation model describes the coupled heat and moisture transport in a multi layer wall in one dimension, with a ventilated air layer on the outside. The moisture transport through the wall is considered as diffusion only, and moisture transport in the ventilated cavity by convection only.

The model uses detailed calculations of the wind pressure, and requires detailed wind pressure coefficients, from measurements, qualified estimates or from computer calculations.

The simulation model of the wall was created by subsystems of the different physical parts of the wall. Each material layer was represented by at least one subsystem, in which the heat and moisture transport were solved. The insulation layer was e.g. simulated as two separate material layers, and the surface of the wind barrier was in a subsystem different from the subsystem of the wind barrier material. In connection there were other subsystems for the ventilated cavity, the rain screen, and the boundary conditions. See Figure 7.2.

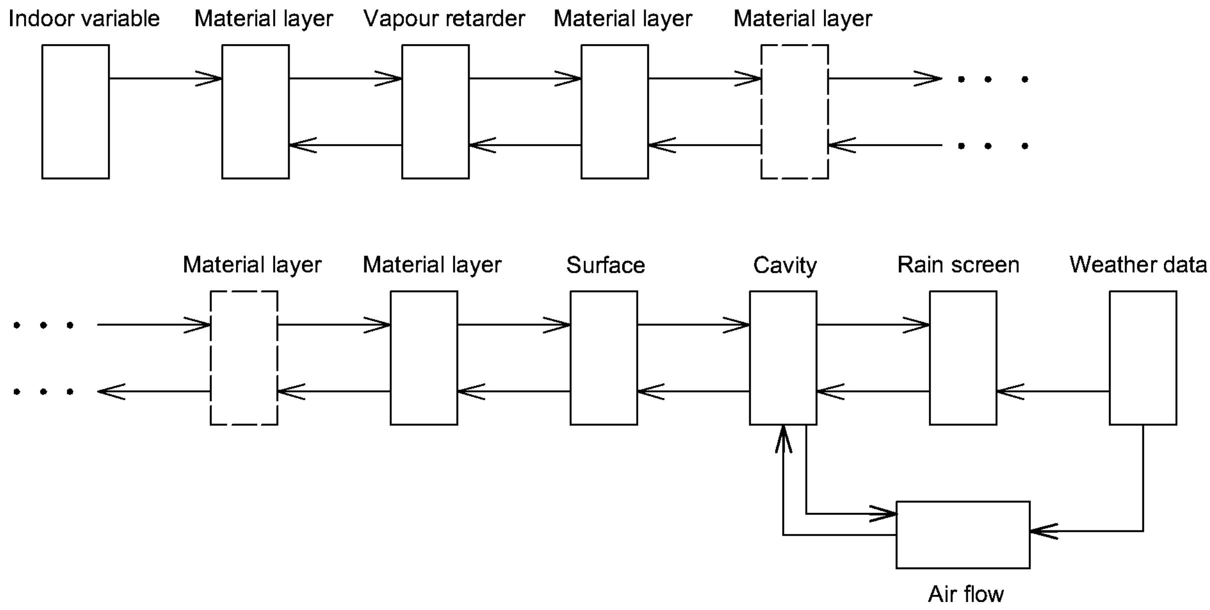

Figure 7.2 Subsystems in a Simulink model of a ventilated wall, where the arrows show the data streams. Each physical part of the ventilated wall was described by at least one subsystem.

7.3. Indoor boundary conditions

The indoor variables which were considered to influence the HAM transport were the relative humidity and temperature.

For indoor climate conditions Rode (1996) suggests constant monthly mean values for temperature and relative humidity, with temperature variation from 21°C to 23°C, with minimum in wintertime, and with relative humidity from 40% in February to 66% as maximum in September. Similarly Andersen (1993) suggests a smooth curve in a diagram, with monthly mean values close to the ones suggested by Rode. Here two sinusoidal equations, which follow the monthly values, are suggested to simulate the indoor conditions for the simulation.

Eq 7.1 $$Temp = 22 - \sin\left(\frac{2\pi \cdot hour}{365 \cdot 24} + 1.57\right)$$ [°C]

Eq 7.2 $$RH = 53 - 13 \cdot \sin\left(\frac{2\pi \cdot hour}{365 \cdot 24} + 0.75\right)$$ [%]

The constants included in the Eq 7.1 and Eq 7.2, were empirical values estimated to fit the indoor climate data from (Rode, 1996) and Andersen (1993). Figure 7.3 shows the indoor relative humidity and temperature from (Rode, 1996) and Andersen (1993), together with the results from the fitted equations.

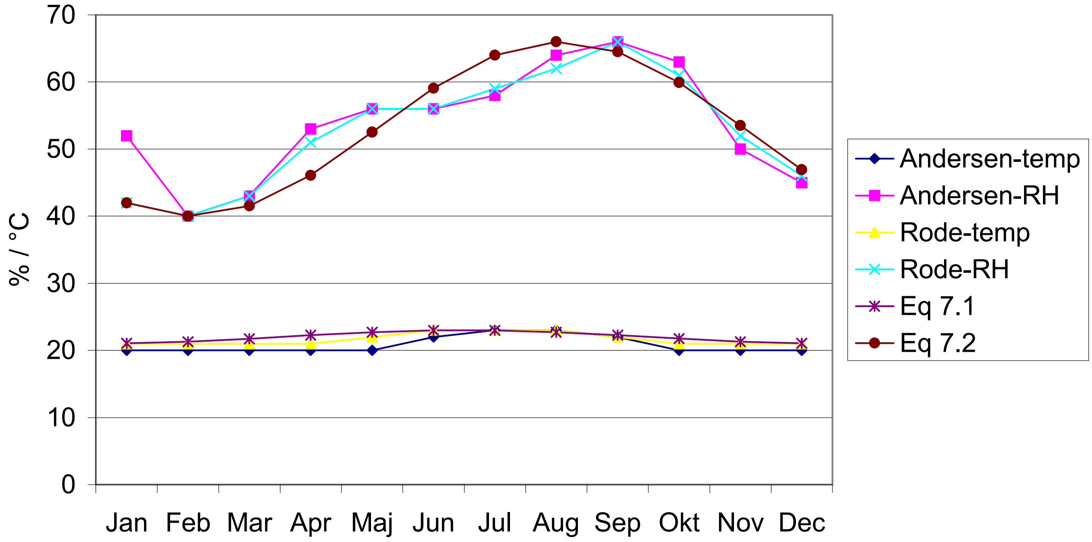

Figure 7.3 Curve through monthly mean values for indoor temperature and relative humidity suggested by Rode (1996) and Andersen (1993), and the values using equations Eq 7.1 and Eq 7.2.

The equation estimates a lower relative humidity from March to May, and a higher from June to August compared to (Rode, 1996) and Andersen (1993). The temperature is highest with the equation but rather close to the suggestion of Andersen(1993). It was chosen to use the equations, in order to have a simple and continuous curve for the simulations.

7.4. Material layer

On the basis of a one-dimensional heat transfer subsystem by Hagentoft (2001), a model of a coupled heat and moisture transfer was developed. Here each layer was considered homogeneous and isotropic, and the thermal and moisture capacity were lumped and localized in a node in the middle of the layer (Hagentoft, 2001). Two subsystems, one for heat transport and one for moisture transport formed the coupled heat and moisture transfer model. The model of thermal conductivity was prepared for considering influence of both the moisture content and temperature, and the moisture diffusivity was prepared for considering influence of the moisture content. In practice missing material properties limited the use of this.

Two coupled differential equations, Fourier's law and Fick's law, described the heat conduction and moisture diffusion.

Fourier's law of heat conduction

Eq 7.3 $\rho_0 c_p \frac{\partial T}{\partial t} = \frac{\partial}{\partial x}\left(\lambda(u,T)\frac{\partial T}{\partial x}\right)$

where

ρ_0	is the dry density of the material	[kg/m^3]
c_p	is the specific heat capacity of the material	[J/kgK]
T	is the temperature	[K]
t	is the time	[s]
x	is the coordinate	[m]
$\lambda(u,T)$	is the thermal conductivity, function of temperature and moisture content	[W/mK]

Fick's law of moisture diffusion

Eq 7.4 $\rho_0 \frac{\partial u}{\partial t} = \frac{\partial}{\partial x}\left(\delta_p(u)\frac{\partial p}{\partial x}\right)$

where

ρ_0	is the dry density of the material	[kg/m^3]
u	is the moisture content, kg water per kg dry material	[-]
t	is the time	[s]
x	is the coordinate	[m]
$\delta_p(u)$	is the vapour permeability, as a function of moisture content with water vapour pressure as driving potential	[kg/(Pa s m)]
p	is the water vapour pressure	[Pa]

Either the water content of the material or the water vapour pressure can be used as driving potential for moisture. Traditionally, in HAM models for wood, the water content is used, but it has the disadvantage of discontinuity across different material borders. In contradiction the water vapour pressure is continuerly across material borders. The problem with water vapour pressure is that a maximum pressure occurs for saturation, and that the amount of water must be calculated and controlled besides the water vapour calculations.

The vapour permeability with water vapour pressure as driving potential was used. Available data of permeability for different RH was listed in a table, where linear interpolation between the data was assumed. Here the influence of temperature on the permeability was not considered.

A more complex model for the HAM transport in materials, including liquid transport and thermo effusion, is suggested by Rode (1998), see Appendix F.

The thermal diffusion is described by (Nevander, 1994): A mix of gases with different molecule weight in a temperature gradient field will result in separation of the gasses. The concentration of the lighter gas will increase in the area with the highest temperature and the heavier gas will increase its concentration in the area with lower temperature. For humid air, the water vapour becomes the lighter gas and therefore moves towards the area with the highest temperature.

A model with thermal diffusion but without liquid transport was tested and was found to give results of moisture content approximately as without thermal diffusion. As the further simulations with a cavity model gave problems with long simulation time and unstable time steps, it was chosen to simplify the model to Eq 7.3 and Eq 7.4. It was also assumed that the sorption curve was independent on the temperature and that liquid transport does not take place. However, a subsystem of the coupled HAM transport in a material layer including latent heat and liquid transport is in the progress of development (Peuhkuri, 2001).

7.4.1. Material properties

The thermal conductivity of a material is defined as the ratio between the density of heat flow rate and the magnitude of the thermal gradient in the direction of the flow. Thermal conductivity is a practical definition of a resultant of conduction, radiation from the pore surfaces and convection within the pores. If the material is wet, heat transferred by moisture add to the density of heat flow rate and change the thermal conductivity (IEA,1996). Also the mean temperature of the material seems to affect the thermal conductivity.

The (EN)ISO 10456:1999(E) standard suggests that conversions of thermal values from one set of conditions to another are carried out according to the expression:

Eq 7.5 $\lambda_2 = \lambda_1 \cdot F_T \cdot F_m \cdot F_a$

where

F	is a conversion factor with respect to either Temperature, moisture or age.

Pedersen (1990) suggest that the thermal conductivity of a material as a function of moisture content and temperature is described by the equation:

Eq 7.6 $\lambda(u,T) = \lambda_{dry,10} + u \cdot f_{\lambda,water} + (T - Tref) \cdot f_{\lambda,T}$

where

λ	is the thermal conductivity for dry material at 10°C
$f_{\lambda,water}$	is the water content correction coefficient [W/mK]
$f_{\lambda,T}$	is the temperature correction coefficient [W/mK°C]
u	is the moisture content in [kg water/kg dry material]
T	is the temperature [K]
T_{ref}	is the reference temperature 283.15 [K]

For the simulations the Eq 7.6 was chosen, due to most available data (Rode, 1996) for a list of different common building materials.

The heat capacity increases with the moisture content (Rode, 1998) (IEA, 1996)

Eq 7.7 $c_p(u) = c_{p,0} + u \cdot c_{p,w}$

where

c_p	is the specific heat capacity for the dry material, subscript ‘$_0$’, or water, subscript ‘$_w$’.
u	is the moisture content in kg water/kg dry material.

The water vapour pressure can be estimated by an empirical equation using the temperature and the relative humidity. The relative humidity is defined as the partial water vapour pressure divided by the water vapour saturation pressure:

Eq 7.8 $\varphi = \dfrac{p}{p_s}$

The saturation water vapour pressure is given by the empirical equation by Kjerulf–Jensen (Chapter 3 'Basic theory'):

Eq 7.9 $$p_s(T) = \exp\left(23.5771 - \frac{4042.90}{T - 37.58}\right)$$

where

T is the temperature [K]

Measured values of the equilibrium water content and relative humidity for the materials used in the simulations were found in the literature (Rode, 1996). According to Økland (1998) it has been common not to include the hysteresis effect in simulation models, but instead use the average adsorption and desorption isotherm. An exception from this is *MATCH* (Pedersen, 1990). Also Berit Time (1998) has found by measurements that the effect is not negligible for wood. For simulation, the mean value from absorption and desorption was calculated and used as sorption curve. The simulation model makes linear interpolation between the available sets of data, and linear extrapolation.

When saturation in a material takes place relative humidity is 100%. For practical use of the sorption isotherm a default value of water content above the hygroscopic zone, >98% relative humidity is added to the data. In this way the relative humidity does not exceed its limit of 100% even though the material is saturated.

7.5. Vapour retarder

As the vapour retarder is very thin, the thermal resistance of it was neglected. The moisture resistance is high for the vapour retarder and the vapour resistance of the neighbour materials are unimportant, compared to the vapour resistance of the vapour retarder. Only the vapour resistance of the vapour retarder was included in the simulation of vapour transport over the vapour retarder, and the thermal resistance was excluded, see Appendix E. This is illustrated in Figure 7.4.

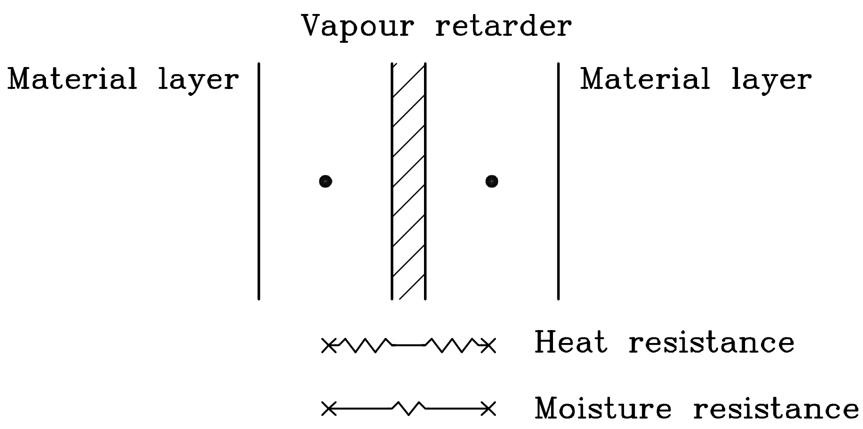

Figure 7.4 The vapour retarder had an insignificant heat resistance, but a dominant vapour resistance, while the vapour resistance in the neighbour material layers are excluded in the simulation model.

7.6. Surface conditions

At the surface between air barrier and cavity heat loss is due to convection and radiation, and moisture transport is due to convection, see Figure 7.5. Therefore the temperature and moisture content at the surface of the air barrier are calculated, for correct simulations of radiation and convection from the surface. Furthermore, both the heat and moisture transfer coefficients were assumed dependent on the air velocity.

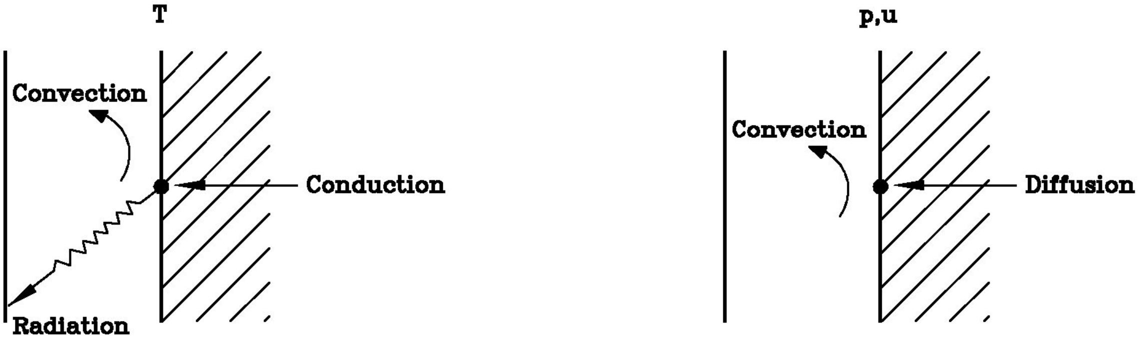

Figure 7.5 The transport mechanisms included for the outer surface of the wind barrier for simulation of the temperature, water vapour pressure and moisture content.

7.6.1. Heat transfer by convection

As described in the Chapter 3 'Basic theory', the ventilation can be in the natural, mixed or forced regime according to the forces that drive the flow. To estimate the heat transfer coefficient for the inside of a ventilated building component e.g. a ventilated cavity, the choice of estimate will depend on whether the natural, mixed or forced ventilation is dominating the air flow.

ASHRAE (1997) suggests the heat transfer coefficient for laminar flow in the natural ventilation region, given by Eq 7.10:

Eq 7.10 $$h_{surface-air} = 1.42 \cdot \left(\frac{T_{surface} - T_{cavity}}{L} \right)^{\frac{1}{4}}$$

where

L	is the length of the plate in the flow direction
$T_{surface}$	is the temperature of the surface of either the wall or the rain screen
T_{cavity}	is the temperature of the air in the cavity

Andersen (2000) and Hagentoft (2001) suggest a heat transfer coefficient for a ventilated cavity for laminar air flow inside the cavity:

Eq 7.11 $$h_{surface-air} = 2.0 \cdot \left(T_{surface} - T_{cavity} \right)^{\frac{1}{4}}$$

Straube and Burnett (1995) suggest (from Kays and Crawford, 1980) that the equation for the heat transfer coefficient for forced convection of air in the laminar flow regime between parallel plates is:

Eq 7.12 $h_{surface-air} = 3.66 + \dfrac{0.104 \cdot \mathrm{Re} \cdot \mathrm{Pr} \cdot d / L}{1 + 0.016(\mathrm{Re} \cdot \mathrm{Pr} \cdot d / L)^{0.8}}$

where

L	is the length of the flow path [m]
Re	is the Reynolds number [-]
Pr	is the Prandtl number [-]
d	is the distance between the parallel plates [m]

Prandtl number $\mathrm{Pr} = \dfrac{\mu \cdot c_p}{\lambda}$

μ	is the dynamic viscosity [kg/s m]
c_p	is the heat capacity [J/kg K]
λ	is the thermal conductivity [W/m K]

Andersen (2000) and Hagentoft (2001) indicate by their suggestion, Eq 7.11, with an exponent of 0.25 that the airflow is in the natural flow regime (ASHRAE, 1997). In opposition to this Straube and Burnett (1995) assume that the airflow in a ventilated wall cavity is forced convection. They all agree that the airflow should be treated as laminar flow.

According to the measurements of air velocity in a ventilated cavity, presented in this thesis, the wind had an impact on the airflow, where the fluctuations in air velocity was explained by the effect of wind. Whether the flow should be treated as mixed or forced was not determined. Still it may be argued that airflow regime in some cavities is in the natural regime and in others are considered in the forced. This will depend on the design of the vents and the geometry of the cavity.

For the calculation of heat transfer coefficient the suggestion by Straube and Burnett (1995) Eq 7.12, of a forced convection was followed, due to the observed influence of forced convection by wind, from the airflow measurements.

7.6.2. Heat loss by radiation to rain screen

The energy exchange by radiation between bodies depends on the absolute temperature, emissivities, the areas, and the viewfactors. Here the more practical use of the theoretical radiation formulas is described.

In order to retain the simplicity of linear equations, a radiation heat transfer coefficient, h_r, is defined. The heat transfer by radiation in between two surfaces 1 and 2 gets the form:

Eq 7.13 $q_r = h_r \cdot (T_2 - T_1)$

Duffie and Beckmann (1991), Hagentoft (2001) and Andersen (1989) suggest that when T_1 and T_2 are close:

Eq 7.14 $h_r = 4 \cdot \varepsilon_{12} \cdot \sigma \cdot T_m^3$

where

Eq 7.15 $T_m = \dfrac{T_2 + T_1}{2}$ and

Eq 7.16 $\dfrac{1}{\varepsilon_{12}} = \dfrac{1}{\varepsilon_1} + \dfrac{1}{\varepsilon_2} - 1$

Andersen,(2000) suggests an even more simpler expression for the radiation heat transfer coefficient:

Eq 7.17 $h_r = 5.7 \cdot \varepsilon_{ca}$

where

ε_{ca} is the emissivity of the surfaces of the materials (assumed identical to ε_{12} in Eq 7.16).

The emissivity of the cavity surfaces are both assumed to be 0.9, so ε_{12}=0.82. The temperature independent radiation heat transfer coefficient, Eq 7.17, $h_{ca,ra}$=4.7 W/K, and the temperature dependent radiation heat transfer coefficient, Eq 7.14, varies from 3.4 to 4.9 W/m^{2}K for temperatures between –10°C and 25°C. See Figure 7.6.

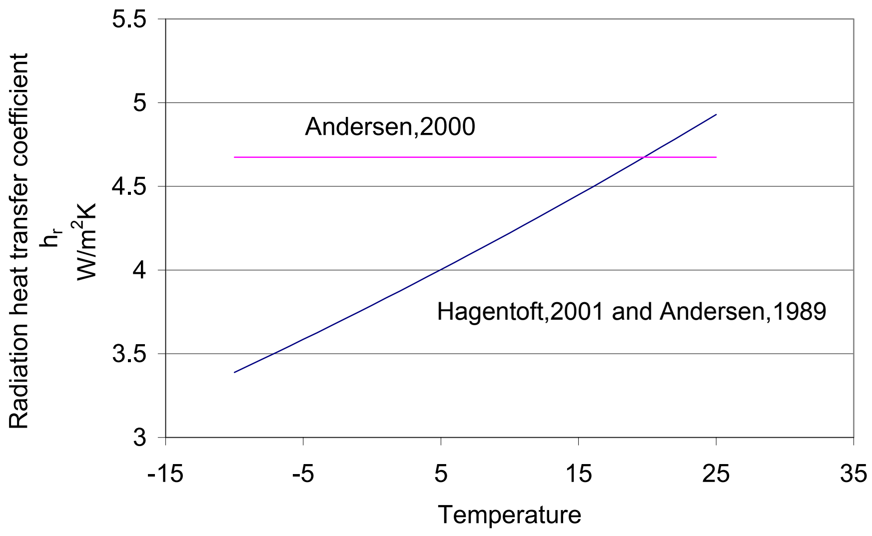

Figure 7.6 Radiation heat transfer coefficient as a function of the mean temperature, between two parallel plates with emissivity of 0.9, using Eq 7.14 (Hagentoft (2001) and Andersen (1989)) and Eq 7.17 (Andersen, 2000).

For the simulations the Eq 7.14 was chosen, due to its more accurate estimate of heat change by radiation.

7.6.3. Moisture transfer coefficient from surface

Moisture transport from the surface to the cavity air, g, [kg/s] is described analogue to heat transfer, with a convection mass coefficient:

Eq 7.18 $$g = \beta \cdot \left(p_{surface} - p_{air}\right) \cdot A$$

where

β	is the mass transfer coefficient [kg/(m^2 s Pa)]
p	is the partial water vapour pressure on the wall surface or in the air [Pa]
A	is the area of the wall surface [m^2]

The importance of including a vapour resistance between air and wall depends on the problem. Nevander (1994) suggest that the resistances on both the outside and inside can be set to zero. Nielsen (1980) suggest that for unknown air velocity the mass transfer coefficient is set to

β_{inside}=2.8·10^{-3} m/s=2.1·10^{-8} kg/(m^2 s Pa)
$\beta_{outside}$=17·10^{-3} m/s= 12.6·10^{-8} kg/(m^2 s Pa)

For more detailed analysis the mass transfer coefficient can be considered dependent on the air velocity. The flow of air over a surface increases the transfer of moisture from a wet surface to dry air (Burnett and Straube, 1995). The accelerated drying caused by air flowing over a surface can be calculated by using a mass transfer analogy to heat transfer, known as Lewis correlation, Eq 7.19. The surface vapour flow resistance, *β*, can be defined in terms of the convective heat loss coefficient, $h_{surface\text{-}air}$:

Eq 7.19 $$\beta = \frac{h_{surface-air}}{R_v \cdot T \cdot \rho \cdot c_p} \quad \text{[kg/(s Pa m}^2\text{)]}$$

where

R_v	is the gas constant for water vapour	[461.5 J/kg K]
T	is the absolute temperature	[K]
ρ	is the air density	[kg/m^3]
c_p	is the specific heat capacity of air	[1003 J/kg K]

The moisture transfer coefficient as a function of air velocity, Eq 7.19, was used for the further analysis, to obtain more accurate simulation results.

7.7. Cavity

The temperature and moisture content in the cavity was lumped and localised in a single node, to represent the temperature and moisture content for the cavity air, see Figure 7.7. The temperature and moisture content of the air was calculated from an energy and moisture balance, respectively.

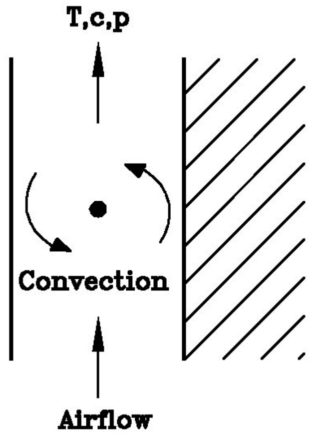

Figure 7.7 The transport mechanisms included for the heat and moisture transport in a ventilated cavity for estimation of the temperature and moisture content of the air.

Figure 7.7 shows the convective heat transfer and convective moisture transfer from the rain screen and the air barrier to the cavity air in balance with the outdoor ventilation air, which were included for simulation of the temperature, water vapour pressure and moisture content of the cavity air.

The mean temperature of the air cavity was found from a thermal balance of the cavity. The balance includes energy entering and leaving the cavity by the volume airflow, and heat transfer by convection from both the air barrier and the rain screen. The heat conduction in the air was considered negligible.

The heat balance becomes:

Eq 7.20 $q_{airflow,in} - q_{airflow,out} + q_{conv,innersurface} + q_{conv,rainscreen} = 0$

The energy carried by the volume airflow for the incoming air is shown in

Eq 7.21 $q_{airflow,in} = c_{p,air} \cdot V \cdot \rho_{air} \cdot T_{outdoor}$

where

c_p	is the heat capacity for the air [J/kg K]
V	is the mean volume air flow [m^3/s]
ρ_{air}	is the air density by volume [kg/m^3]
$T_{outdoor}$	is the outdoor temperature [K]

Similar the energy leaving the control volume due to airflow, is:

Eq 7.22 $q_{airflow,out} = c_{p,air} \cdot V \cdot \rho_{air} \cdot T_{cavity,exit}$

where

$T_{cavity,exit}$	is the air temperature at the exit of the cavity [K]

The temperature of the exit air can be expressed by $T_{cavity,top}=2T_{cavity,mean}-T_{outdoor}$, assuming that the cavity temperature varies linearly over the vertical distance between the vents (Andersen,2000). It was assumed that the temperature estimate of exit air can be used for both upward and downward airflow.

To estimate the convective heat transfer coefficient from respectively the rain screen and the air barrier, to the cavity Eq 7.12 was used, as described for the 'surface conditions'.

Similar to the heat balance, a moisture balance was used to calculate the moisture content of the cavity air. The transport phenomena were the convective moisture transfer between the air and both the rain screen and the air barrier, and furthermore the difference in moisture content for air entering and leaving the cavity; and from these the moisture balance were made. It was assumed that airflow in the wall layers did not take place, and that rain was not present behind the rain screen as should be provided by correct design and correct workman ship. Therefore, the moisture balance can be written in steady state as:

Eq 7.23 $$c_{out} \cdot Q + g_{air-barrier} + g_{rain-screen} = c_{air} \cdot Q$$

where

c_{out}	is humidity by volume in supply, i.e. outdoor air [kg/m^3]
Q	is the air change in the cavity [m^3/s]
$g_{air-barrier}$	is the moisture evaporation from the surface of the air barrier [kg/s]
$g_{rain-screen}$	is the moisture evaporation from the inside of the rain screen [kg/s]
c_{air}	is humidity by volume in exit air [kg/m^3]

The mean moisture content in the cavity air was calculated as:

Eq 7.24 $$c_{cav,air} = c_{out,air} + \frac{g_{air-barrier} + g_{rain-screen}}{Q_v}$$

The corresponding water vapour pressure in the cavity air, was then:

Eq 7.25 $$p_{wv} = c_{cav,air} \cdot R_v \cdot T$$

where

$c_{cav,air}$	is the water concentration by volume in the cavity air [kg/m^3]
T	is the absolute temperature of the cavity air [K]
R_v	is the gas constant for water vapour, 461.5 [J/kg K]

Eq. 7.24 express the moisture concentation in the cavity, or more correctely the moisture concentration at the exit of the cavity. It can be argued that the equation should be:

$$c_{cav,air} = c_{out,air} + \tfrac{1}{2} \cdot \left(\frac{g_{air-barrier} + g_{rain-screen}}{Q_v} \right)$$

By this it is assumed that the concentration change linearly through the cavity. The error followed is that the moisture concentration is calculated to high, and therefore the difference in moisture content between cavity air and surface, i.e. the driving potential for moisture transport, is calculated to small.

7.8. Rain screen

The temperature of the rain screen was depended on the convective heat loss to the cavity and the outdoor air, and on the heat loss by radiation to both the air barrier and the surroundings. The heat resistance of the rain screen was considered negligible, meaning that the temperature over the screen was considered constant. This assumption might not be correct for materials with low thermal conductivity, but for a model with a thin layer of one material, like wood or Plexiglass as rain screen, it is considered acceptable, (Duer, 2001).

The moisture balance included convective moisture transport between the rain screen and the cavity air and the outdoor air respectively.

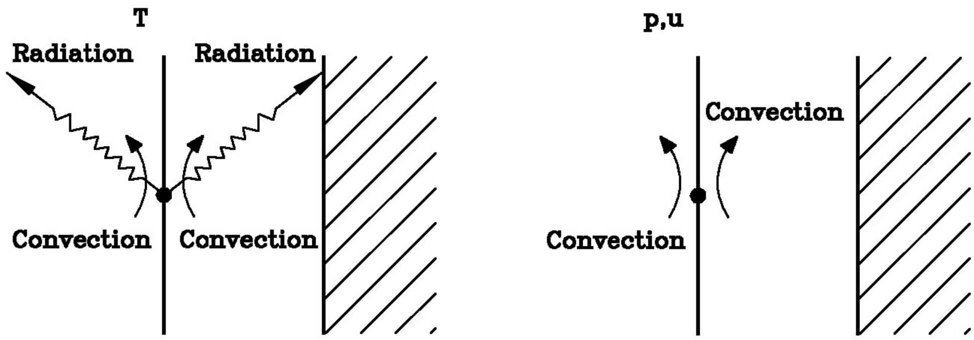

Figure 7.8 Heat balance for the rain screen included radiation and convection to the air barrier and the surroundings. The moisture balance included convective moisture transfer to the cavity air and to the outdoor air.

The heat balance of the rain screen included heat loss by convection to the outside, influenced by the wind velocity, heat loss by convection to the inside, influenced by the air velocity. Furthermore the heat balance included radiation between the rain screen and the air barrier, and radiation between the rain screen and the surroundings, including radiation to both the sky and the ground. The heat loss by conduction was considered insignificant compared to the heat loss by convection and radiation.

7.8.1. Outside convective heat transfer coefficient

Different approaches to estimate the convective heat transfer coefficient at the outer surface are possible. From fluid mechanics it is known that the heat transfer coefficient over a surface changes with the air velocity. The air velocity is not homogeneous over a building surface and depends on the wind (i.e. direction and velocity) and the temperature gradient between the surface and the surroundings.

Most of the correlations for practical use, are related to the wind or air velocity, and estimates an overall convective heat transfer coefficient. A commonly used correlation to estimate the convective heat transfer coefficient, h_c [W/m^{2}K], is given by ASHRAE(1997):

Eq 7.26 $h_c = 5.62 + 3.9 \cdot v$ for v < 5 m/s

Eq 7.27 $h_c = 7.2 \cdot v^{0.78}$ for 5 ≤ v < 30 m/s

where

v is the wind speed [m/s]

However, wind tunnel experiments by Sparrow et al. (1979) and from field measurements of the heat transfer coefficient for walls by Jayamaha et al.(1996) indicate that the heat transfer coefficient tend to be overestimated by Eq 7.26 and Eq 7.27. Jayamaha et al. (1996) measure that the convective heat transfer coefficient in the field, for the central area of a vertical wall varies from about 6 to 10 W/m^{2}K for wind speed in the range 0-4 m/s. They find that the heat transfer coefficient is correlated to the wind velocity but insignificantly changing with the wind direction. Jayamaha et al. (1996) find, from their measurements, a correlation for the heat transfer coefficient in the central region of a vertical wall :

$$h_{center} = 1.444 \cdot v + 4.955$$

From wind tunnel experiments of Sparrow (1979), the average heat transfer coefficient is estimated to be about 1.18 times the value in the central area, therefore Jayamaha et al.(1996) suggest that the convective heat transfer coefficient is:

Eq 7.28 $h_c = 1.18 \cdot (1.444 \cdot v + 4.955)$

Other researchers suggest different convective heat transfer coefficients as functions of wind or air velocity. Nevander (1995) and Andersen (2000) suggest different functions composed of two equations.

Nevander (1995) suggests:

Eq 7.29 $h_c = 5 + 4.5 \cdot v - 0.14 \cdot v^2$ at windward side for v<10 m/s

Eq 7.30 $h_c = 5 + 1.5 \cdot v$ at leeward side for v<8 m/s

Andersen(2000) suggest:

Eq 7.31 $h_c = \begin{cases} 3.5 \cdot (T_{surface} - T_{outdoor})^{\frac{1}{3}} & v \le 0.5 \quad m/s \\ 3.0 + 5.0 \cdot v_s & v > 0.5 \quad m/s \end{cases}$

where

T is the temperature at the surface and for the outdoor air [K]
v_s is the wind velocity by the surface [m/s]

The equation from Nevander distinguishes between the leeward and windward side, where Andersen uses the temperature difference between surface and environment to estimate the heat transfer coefficient for wind velocity below 0.5 m/s, and wind velocity for higher wind speed.

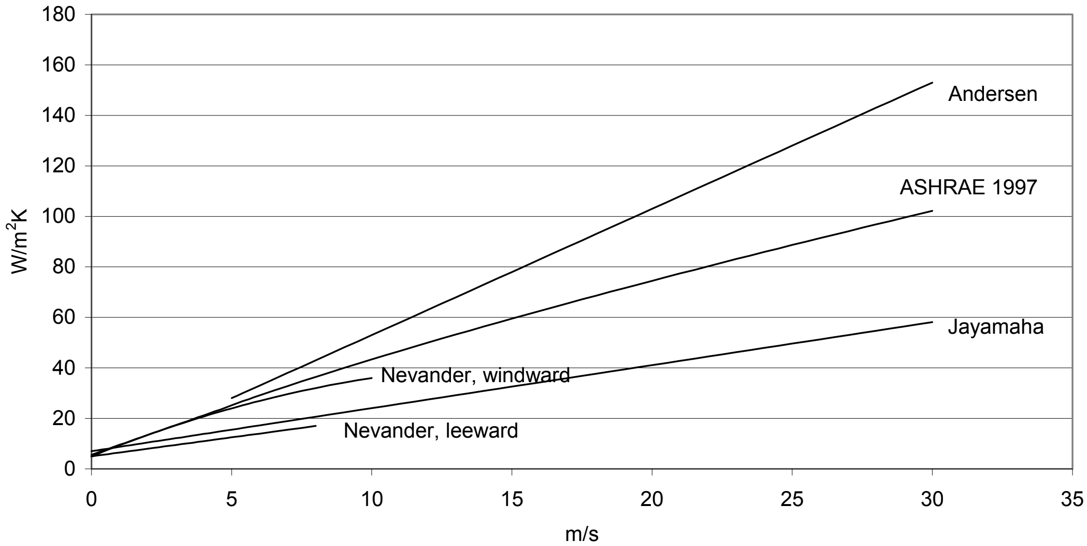

Figure 7.9 Outside convective heat transfer coefficient as function of wind velocity.

The estimated heat transfer coefficient by Jayamaha et al. (1996) is between the leeward and windward values from Nevander (1995). The estimates by Andersen (2000) is the highest followed by ASHRAE (1997), see Figure 7.9 .A disadvantage for simulations with Andersen (2000) is that it cannot be considered continuous for wind velocity around 5 m/s, due to the use of either temperature difference or wind velocity.

Here the function by Jayamaha et al. was chosen, for the simulations. The choice was due to its form of a single equation, and that the correlation was found for a vertical wall under outdoor conditions similar to a facade wall, and furthermore it is corresponding well with Nevander (1995).

The convective heat transfer coefficient for the cavity side of the rain screen was the same as used for the convective heat transfer coefficient of the air barrier Eq 7.12.

7.8.2. Heat loss by radiation to surroundings

For the radiation heat transfer from the outer building surface to the surroundings Kragh (1998) suggests that the general radiation balance at the building surface is the direct solar radiation absorbed by the surface, the long wave radiation from the surroundings and the long wave radiation to the surroundings.

The balance may be written as

Eq 7.32 $$q_{r,net} = \alpha G + \varepsilon L - \varepsilon \sigma_s T_s^4$$

where

$q_{r,net}$	is the net radiance at the building surface [W/m^2]
L	is the incident long-wave radiance [W/m^2]
G	is the incident solar radiance [W/m^2]

α	is the solar absorptivity
ε	is the emissivity of the surface
σ_s	is the Stefan-Boltzmann constant, $5.6697 \cdot 10^{-8}$ [W/m^2K^4]
T_s	is the surface temperature [K]

In order to include the incident solar radiation, knowledge of the orientation of the surface, and the shadow during the day over the year, must be included. For simplicity it was decided to model a north-facing wall, where the incident solar radiance can be excluded. The direct sun radiation may however, be included in future improvement of the model.

The incident long-wave radiance from the firmament, *L*, (diffuse radiation) on a horizontal plane is listed in the weather data file in W/m^2, (Jensen and Lund, 1995).
(See section 'Weather data' later in this chapter)

According to Hadvig (1986) it can be assumed that:

Eq 7.33 $L = \sigma_s \cdot T_{sky}{}^4$

where

L	is the measured long wave radiation from the firmament [W/m^2]
σ_s	is the Stefan-Boltzmann's constant $5.6697 \cdot 10^{-8}$ [W/m^2K^4]
T_{sky}	is the sky temperature [K]

For a sloped surface the radiation heat transfer is both to the sky and to the surroundings. The radiation heat transfer from the surface to the surroundings (sky and obstacles) was weighted by the view factors of the surfaces and depends on the surface temperatures. The radiation heat transfer from surface 1 to m surfaces:

Eq 7.34 $q_{r,net} = \varepsilon \cdot \sigma \cdot \left[\left(\sum_{n=2}^{m} \left(F_{1,n} \cdot T_n \right) \right)^4 - T_{surface}{}^4 \right]$

where

$F_{1,n}$	is the view factor from surface 1 to surface n	
T	is the absolute temperature	[K]
ε	is the emmisivity of surface 1	
σ	is the Stefan Boltzmanns, $5.6697 \cdot 10^{-8}$	[W/m^2K^4]

For a vertical wall the radiation to the surroundings was considered as radiation to the sky and ground only, radiation to other obstacles was not considered. The view factors between the facade surface and the sky and ground respectively were estimated to ½ for both.

The temperature of the surroundings was an average temperature between the sky and ground, weighted by the view factors of ½.

Eq 7.35 $T_{surroundings} = \frac{1}{2} \cdot \left(T_{ground} + T_{sky} \right)$

The sky temperature was calculated from the long wave sky radiation on the ground Eq 7.33, listed in the reference year. The ground temperature was assumed equal to the air temperature; this can cause some error especially on sunny days or clear nights. On sunny days the ground temperature is higher than the air temperature and on clear nights the ground temperature becomes colder than the air temperature.

However, it was chosen to replace the temperatures of the surroundings in Eq 7.35 with the air temperature:

Eq 7.36 $T_{surroundings} = \frac{1}{2} \cdot \left(T_{air} + T_{sky}\right)$

The radiative heat exchange between the vertical surface and the surroundings was simplified to:

Eq 7.37 $q = \varepsilon \cdot \sigma \cdot \left(T^4_{surroundings} - T^4_{surface}\right)$

Eq 7.32 can then be written as:

Eq 7.38 $q_{r,net} = \varepsilon \cdot \sigma \cdot \left(\left(\frac{T_{air} + T_{sky}}{2}\right)^4 - T_s{}^4\right)$

As an alternative Andersen(2000) suggests that the outside radiation is estimated as

Eq 7.39 $Q = h_{out,ra} \cdot A \cdot \left(T_{surroundings} - T_{rainscreen}\right)$

where

$h_{out,ra} = 4.0 \cdot \varepsilon_{rainscreen}$

For typical building materials the emmisivity is around 0.9, which gives $h_{out,ra}$=3.6 W/K.

The radiation heat transfer for the cavity side of the rain screen to the air barrier is known from Eq 7.14.

The most accurate would be to use Eq 7.38. However, the more simple expression Eq 7.39 was used. This was in order to avoid run time error during simulations. When the rain screen has a low heat capacity, the time step decreases below a minimum step size, which in practise means that the simulation stops.

7.9. Air flow

The airflow by volume in the cavity with two vents depends on the difference in total pressure between the ventilation openings. The sum of the difference in wind pressure between the vents and the stack effect is used as total pressure difference between the vents.

It was assumed (Eq 3.13), that the flow characteristic follows a power law in which

Eq 7.40 $Q = C_D \cdot A \cdot \left(\frac{2 \cdot \Delta P}{\rho}\right)^n$

where

Q is the air flow rate by volume [m^3/s]

C_D	is the discharge coefficient (comprise of the contraction coefficient and the velocity coefficient)
n	is the flow exponent (for fully developed flows, n=1.0 for laminar flow and 0.5 for turbulent flow)
ΔP	is the pressure difference between the vents (Walker and Forest 1995) [Pa]

Walker and Forest (1995) have shown that the power law can be used to describe the ventilation rate in attics. The pressure difference, ΔP, is an addition of the difference in wind pressure at the two ventilation openings and the stack effect, due to temperature difference between the outside air and the cavity air. The definitions of the pressures are described in Chapter 3 'Basic theory'.

Li and Delsante (2001) derive analytical solutions for calculating natural ventilation flow rates and air temperatures in a single-zone building with two openings when no thermal mass is present. They base the air flow rate on the power law equation for turbulent flow (n=0.5). Straube and Burnett (1995) also use a power law with n=0.5 for their estimation of the airflow in the cavity for ventilated façade.

For the estimation of the convective heat transfer coefficient between air barrier and cavity air, the airflow was assumed laminar by Andersen (2001), Hagentoft (2001) and Straube & Burnett (1995). Without counting on the conflict they suggest for the airflow through the vents an exponent n=0.5, which is used for turbulent flow.

Here it was assumed that the airflow in a ventilated facade follows a power law for turbulent flow (n=0.5), too.

7.9.1. Resistance coefficient for duct, entrance and exit.

The discharge coefficient is the square root of the total resistance multiplied by the contraction factor (= 0.7), see Chapter 3 'Basic theory'. For a ventilated cavity this includes resistance through the cavity, resistance at the entrance, and resistance at the exit.

Straube and Burnett (1995), Andersen (2001) and Kronvall (1980) suggest the resistance factors differently. An example was made for comparison between the discharge coefficients. The example was airflow through a smooth pipe with sharp edges at both the inlet and exit. The duct has the width of 0.559 m and depth of 0.025 m, further the flow path length, *L*, is 1.65 m and Reynolds number was 1000. The calculations can be found in Appendix G, where the results for resistance factors and the resulting discharge coefficient, C_D are listed in Table 7.2.

Table 7.2 Comparison of discharge coefficients with different estimates of the friction factors, see appendix G.

Method of:	$\xi_{entrance}$	$\xi_{pipe/sloth}$	ξ_{exit}	C_D
Burnett & Straube	0.5	3.17	0.88	0.47
Kronvall	1.80	3.17	0	0.45
Andersen	0.4/0.5	3.456	0.1	0.50/0.50

It was found that the discharge coefficient was about the same, though the single resistances vary between the authors. Kronvall (1980) determines the entrance resistance as a function of the air velocity, where Andersen (2001) and Straube and Burnett (1995) choose constant values. Andersen (2001) makes detailed calculation of the resistance in the pipe where the others use a more simple expression.

7.9.2. Wind pressure

Straube and Burnett (1995) report that wind pressure is often more significant for ventilation than thermally induced pressures. The simulation here of the wind pressure was performed by using estimated wind pressure coefficients for the actual wall, generated with Cp-generator (Knoll et al.,1996). The wind pressure coefficients were given for every 5°, at positions corresponding to the outside of the ventilation openings of the outdoor test model.

The wind pressure difference between two vents is given by:

Eq 7.41 $\Delta P_{wind} = \frac{1}{2} \cdot \rho \cdot V^2 \cdot (Cp_2 - Cp_1)$

where

ρ	is the air density
V	is the reference wind velocity
Cp	is the wind pressure coefficient corresponding to the reference height

The wind pressure is a function of the air density, i.e. the temperature and moisture content of the climate have impact on the pressure load. This could be included in a future improved model, but is not included in the existing model.

7.9.3. Buoyancy force

Buoyancy force is due to difference in air density between the cavity air and exterior air. When the air is heated in the cavity the density decrease and the lighter warm air rises above the cold air with a higher density, equal to a difference in pressure.

Water vapour is lighter than atmospheric air, which means wetting of the ventilation air will increase the stack effect due to change in density of the air.

The air density changes with the temperature, relative humidity, and barometric air pressure. (Hansen et al. 1992) suggest:

Eq 7.42 $\rho = 0.0034837 \cdot \frac{P}{T} - 0.0013169 \cdot \frac{p_d}{T}$

where	P	is the barometric pressure	[Pa]
	T	is the absolute temperature	[K]
	p_d	is the partial pressure of water	[Pa]

The pressure difference generated by the difference in density is:

Eq 7.43 $\Delta P_{stack} = g \cdot \Delta h \cdot (\rho_{outdoor,air} - \rho_{cavity,air})$

Burnett and Straube [1995] suggest that the density of dry air [kg/m^3] varies as:

Eq 7.44 $\rho = \frac{351.99}{T} + \frac{344.84}{T^2}$

where

T	is the average temperature of the air [K]

For calculation of the buoyancy force the density of the cavity air was found from Eq 7.44. This choice was made to stabilise the simulation by having only the temperature, T as variable, instead of the water vapour pressure, p_d, the barometric pressure, P, and the temperature, T. However, as atmospheric air is almost an ideal gas, the second part of Eq. 7.44, has a minor influence.

For calculations of the volume air flow, the Eq 7.40 becomes:

Eq 7.45 $$Q = C_D \cdot A \cdot \left(\frac{2 \cdot (\Delta P_{stack} + \Delta P_{wind})}{\frac{351.99}{T} + \frac{344.84}{T^2}} \right)^{0.5}$$

7.9.4. Weather data

Typical outdoor weather conditions are represented by a test reference year (TRY) or a design reference year (DRY). Where both reference years are based on real measured data. The advantage of DRY is a more realistic description of the extremes. In DRY the values for some key values (temperature, relative humidity, wind speed and solar radiation) have been modified, so the highest monthly value corresponds to the mean value of the highest measured monthly value from a 15 years period. Here the weather data from the Danish Design Reference Year (DRY) (Jensen and Lund, 1995) was used for yearly simulations. A table with the parameters included in DRY can be found in Appendix H.

The air temperature, relative humidity, wind direction and wind speed are given by hourly mean values. The barometric air pressure is available for every 3 hours. Further the effect of long wave radiation from the firmament per area, q_{sky}, is listed every hour, and is used for determine an equivalent sky temperature (Noyé, 2000).

Eq 7.46 $$T_{sky} = \sqrt[4]{\frac{q_{sky}}{\sigma_s}}$$

where

σ_s is the Stefan-Boltzmanns constant, $5.6697 \cdot 10^{-8}$ [W/m^{2}K^4]

The diffuse long wave radiation from the sky, is listed every hour. This was included in the model for calculation of radiation heat loss for the rain screen. It should be noted that the long wave radiation values listed in the reference year are valid for a horizontal plate.

To estimate the heat loss by radiation from the rain screen to the surroundings, the mean temperature seen by the vertical surface is calculated by Eq 7.36, and is used for finding the radiation heat loss to the sky by Eq 7.39:

Eq 7.47 $$q_{radiation} = h_{ra} \cdot \left(T_{rainscreen} - \frac{T_{air} + T_{sky}}{2} \right)$$

where

$h_{ra} = 4.0 \cdot \varepsilon_{rain\ screen}$

8. Validation of Simulink model

A Simulink model for simulating the coupled heat and moisture transfer in a light weight ventilated wall was validated stepwise. The comparison was with another computer model and by comparison of simulation results against measurements. The computer program *MATCH* (Pedersen, 1990), which simulates the coupled heat and moisture transfer in typical building materials, was used for comparison.

First the ‘Air flow’ subsystem of the model, which simulates the airflow through the ventilated cavity, was compared to measurements. Then a simplified model of the coupled heat and moisture transfer in a wall with multiple layers excluding radiation was compared with a similar *MATCH*-model. Finally a full simulation model of the coupled heat and moisture transfer in a light weight ventilated wall, was compared with outdoor measurements of moisture content and temperature in different test walls.

The subsystem of heat and moisture transfer in a material layer, ‘Material layer’, was tested and validated with good agreement with a similar *MATCH* model, (Peuhkuri,2001). No further validation of the ‘Material layer’ subsystem was performed here.

Field measurements were compared with simulation results. Measurements of temperatures and relative humidity from five different façade walls were compared to Simulink simulations. The measurements were made by the Danish Building and Urban Research, for different examples of vented walls and a compact wall, (Nicolajsen and Hansen, 2001). For the comparisons with measurements the simulations were using measured weather data as outdoor boundary conditions. The initial condition for the simulations were the available measured values or 10°C and 50% RH.

8.1. Simulink ‘Airflow’ subsystem compared to measurements.

The ‘Air flow’ subsystem in the Simulink model calculates an air velocity in the ventilated cavity. Simulations were performed with the weather data logged at the test house and compared with simultaneous measurements of the air velocity measured with tracer gas.

The ventilated facade was, as described in chapter 4, from the inside made of 13 mm gypsum board, vapour retarder of 0.1 mm PE-foil, 100 mm mineral wool insulation, 13 mm gypsum board, 25 mm air space, and 10 mm Plexiglass, see Figure 4.2. The equipped facade was placed on the north side of a low rise building with flat roof, where the direct solar radiation could be eliminated. The facade was sheltered from the wind by nearby buildings and trees. As wind pressure coefficients outside the vents, the values from Knoll (2000) were used.

On the test facility, measurements of the airflow in the cavity were measured simultaneously with the wind direction and wind velocity above the test house. The temperature and relative humidity was recorded by a nearby weather station. The temperature of the cavity air was estimated from available data of temperature measured on the inner side of the rain screen, at about 200 mm from each opening. The uncertainty of the temperatures inside and outside the cavity was high, meaning that the stack effect was poorly estimated.

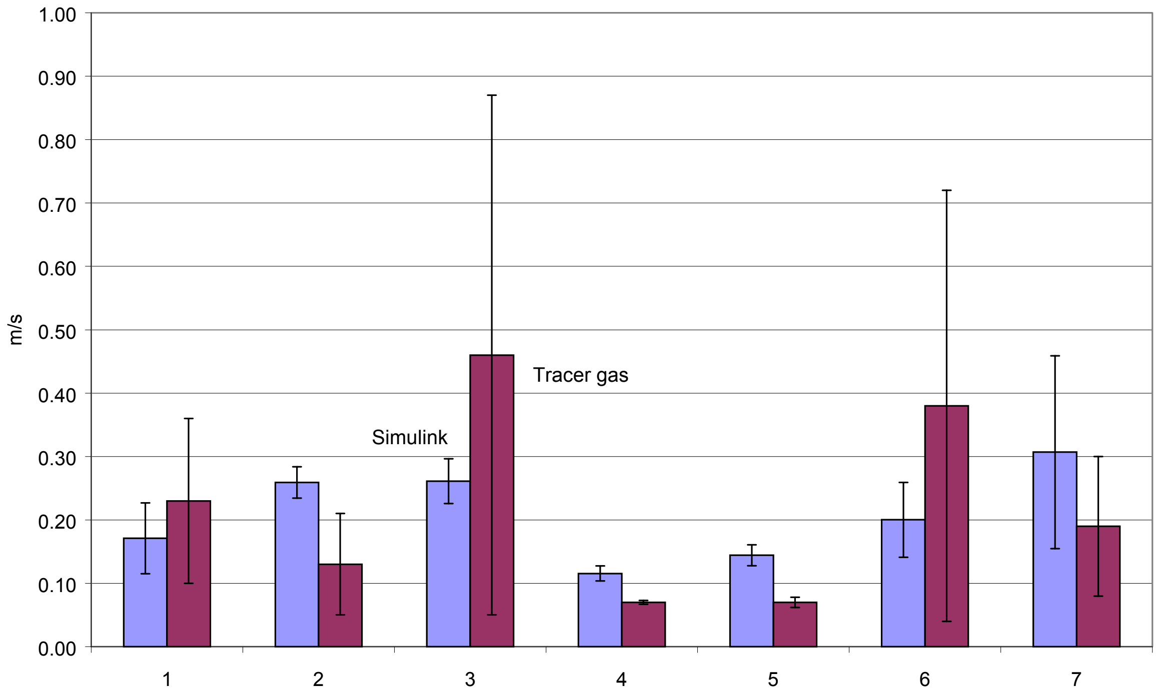

Figure 8.1 Mean velocity from 9 minutes simulation with Simulink compared to mean value of two tracer gas measurement, for experiment 1-7. Lines show the standard deviation for either the measured or simulated values for the experiment.

The results in Figure 8.1 show that the simulations of air velocity are in the same range as the measurements. It is also seen that the standard deviation is rather high especially for some of the measurements. This was due to a relative short measured period compared to the time constant of the tracer gas measurement technique. The simulations on the other hand were influenced by uncertainty of temperature in the cavity and the wind pressure coefficients. Other uncertainties were the estimate of discharge coefficients for the vents and slide, and the flow pattern(laminar and/or turbulent) as well.

8.2. Comparison between 'Multiple layer' Simulink model and *MATCH* model.

A simple model of a multiple layer wall without ventilation or air gap was simulated with *MATCH* and with Simulink. The simulation case consisted from the inside of 13 mm gypsum, 0.1mm PE-foil, 200 mm mineral wool, 13 mm gypsum, and 20 mm pine, see Figure 8.2. Boundary conditions were on the inside constant 21°C and 60% relative humidity, and on the outside hourly mean values from the design reference year (DRY).

The Simulink model of the rain screen, was built from a material layer, with a thermal resistance inside the material layer, in order to make a model identical to *MATCH*. (Without ventilated cavity this did not increase the simulation time, where the Simulink model of a façade with ventilated cavity had to be simplified in order to limit the simulation time.)

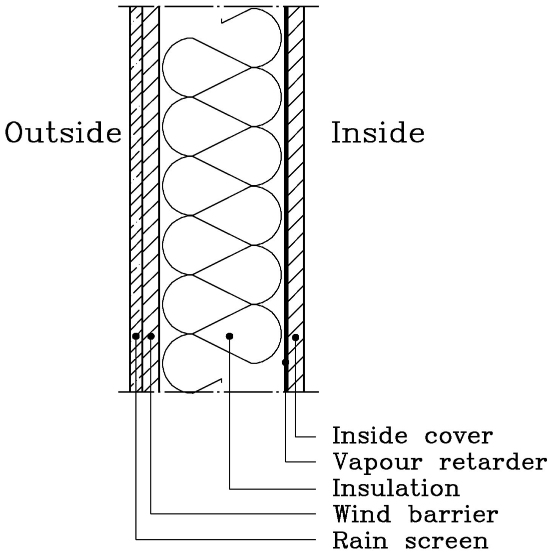

Figure 8.2 Material layers in the multiple layer wall simulated with Simulink model and MATCH model.

The material properties, and the equations for the heat and moisture transfer coefficients were identical between the models. Radiation for the outer surface was excluded, as the temperatures for the sky and surroundings are simulated differently for the Simulink model and in *MATCH*.

The temperatures in the middle of the rain screen for the two simulations were in accordance, see Figure 8.3. The numerical difference between temperatures simulated by the Simulink-model and *MATCH* -model was in average 0.09°C for the whole year.

MATCH can approximately simulate a ventilated layer, this part of the model has however not been validated. It was chosen not to include a comparison here.

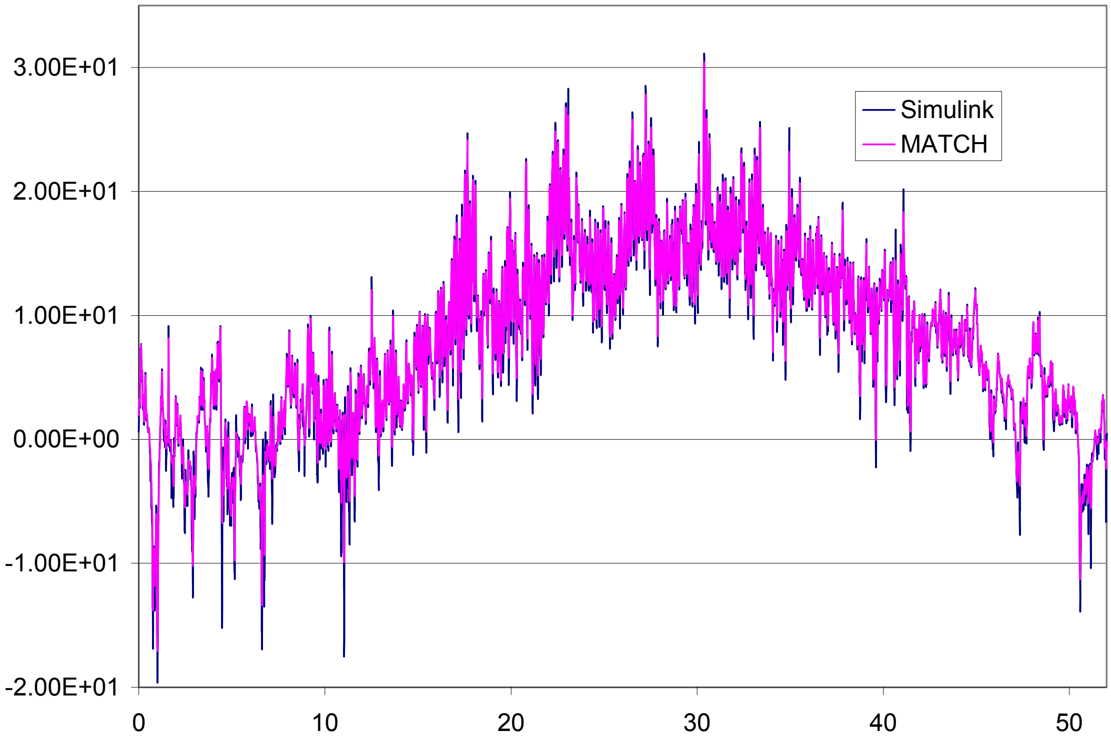

Figure 8.3 Temperature in the middle of the rain screen simulated with Simulink model and MATCH model.

The moisture content in the middle of the rain screen show a systematic but small difference in moisture content, with a higher or identical moisture content simulated with Simulink than with *MATCH*. See Figure 8.4. The curves were identical in the spring and the difference between them was highest in the fall.

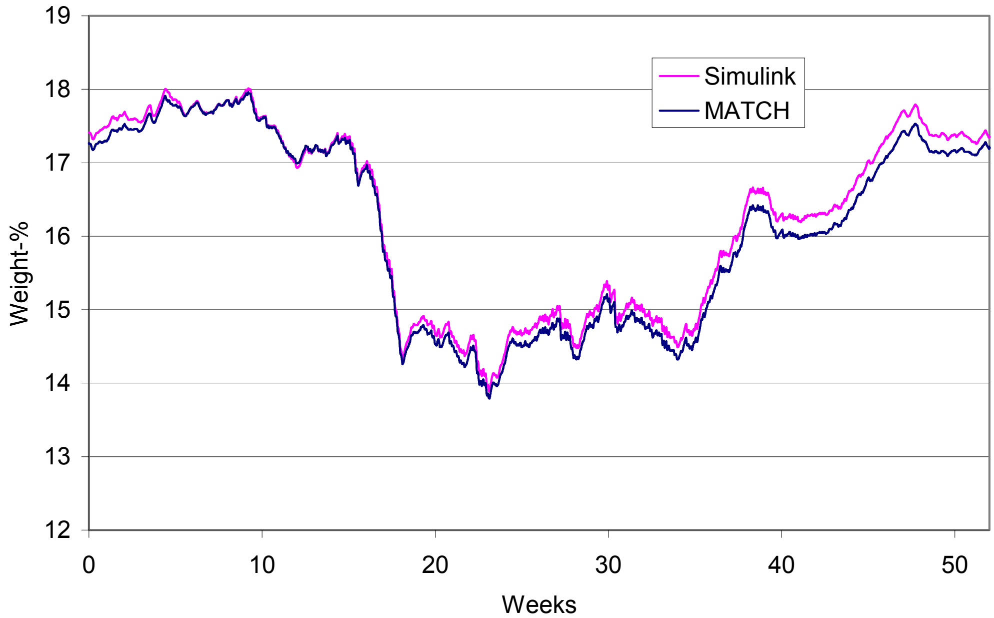

Figure 8.4 Moisture content in the rain screen show a good accordance between the MATCH simulation and the Simulink model.

The moisture content simulated with Simulink and *MATCH* in the other layers is seen in Figure 8.5. Here the simulation results for the two models were identical for the inside cover and the two insulation layers, and a difference in moisture content for the air barrier was observed similar to what was seen for the rain screen.

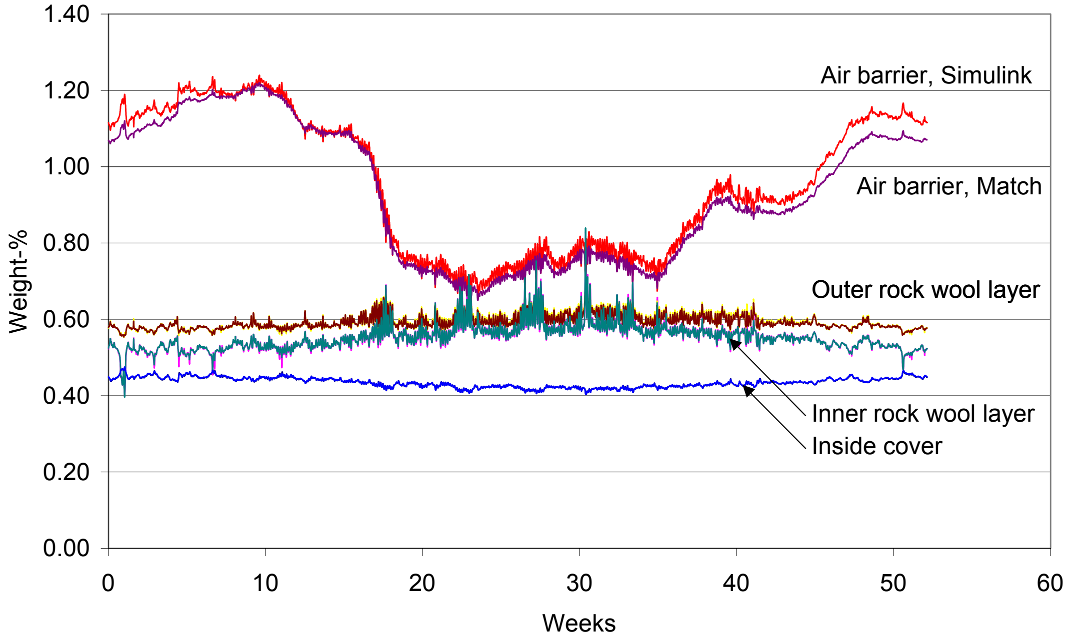

Figure 8.5 Moisture content by weight-% within the material layers simulated with Simulink and MATCH. It shows that the moisture content for the two models were in good accordance for the inner layers, and acceptable for the air barrier.

The reason for the differences seen in the simulation results of the temperatures and moisture content with the two models was not found. It may be due to the different numerical solvers used for the simulations.

8.3. Measured moisture content compared to Simulink simulations

Measurements of the moisture content and temperature at different locations in different light weight facade walls have been carried out at the Danish Building Research Institute (Nicolajsen and Hansen, 2001). Data was logged every 12 hour during a long period. Measurements from one year were compared to simulations.

Simulink simulations were compared with 5 variations of north facing facades. Four walls were with a ventilated cavity and one was a compact wall without air cavity.

The moisture contents were measured by wood-dowels of beech and the temperatures by thermistors. The moisture content measurements were temperature compensated, and the corresponding relative humidity was found by a sorption curve for beech. Appendix I.

It should be noted that the wood-dowels has a time constant of 12 hours, and special attention must be paid for thin hygroscopic materials, due to the dowels physical size of 1 x 2 cm. In a 9 mm thick gypsum material, a hole was drilled and the dowel inserted, meaning that the measurement was performed for the whole material and parts of the neighbour material (here referred to as behind the air barrier). Moisture content below 11 weight-% was not registered, as the measurement technique has a high uncertainty below this level. (Andersen et al. 2001). The uncertainties of the moisture content for the dowels are approximately 5 % by weight (Peuhkuri, 2001-b).

The simulated and measured relative humidity behind the air barrier were compared for each of the test walls. The air barrier was chosen as assumed the best measuring place for the comparison. The rain screen was affected by driving rain, which was not considered in the simulation model; and the air was changing rapidly compared to the time constant for the dowels, while the measuring behind the air barrier was found to be of preference for comparison.

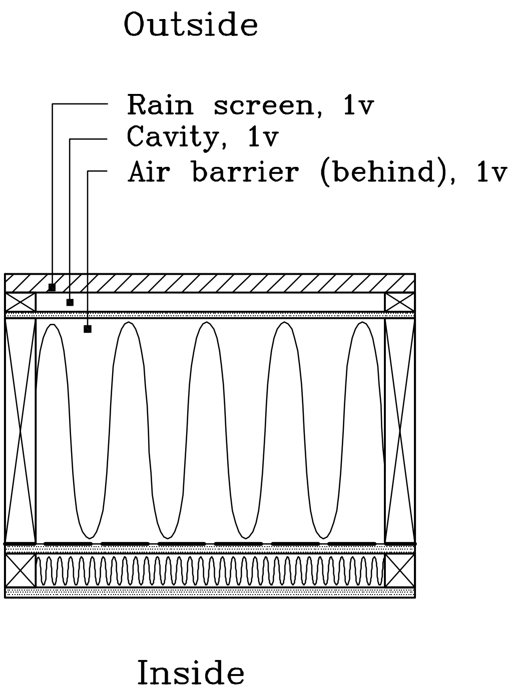

Figure 8.6 Test wall (1V) was from the inside made of 13 mm gypsum, 45 mm Rock wool, 13 mm gypsum, PE-foil, 240 mm Rock wool, 9 mm gypsum, 25 mm ventilated cavity, 20 mm pine bevel lapped siding. The points show where thermistors and dowels were placed.

The wall, 1V, was ventilated through an open slide at the bottom and one at the top, where the one in the top was protected from direct rain by a projection cap of metal some few centimetres above the slide. In the bottom of the slide was an asphalt felt to drain driving rain. The rain screen was a pine bevel lapped siding.

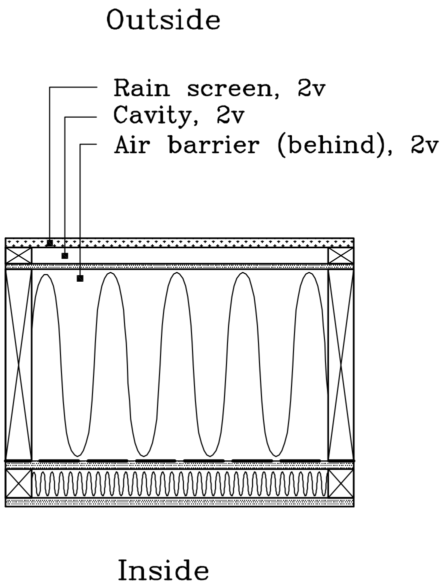

Figure 8.7 Test wall (2V) was from the in side made of 13 mm gypsum, 45 mm Rock wool, 13 mm gypsum, PE-foil, 240 mm Rock wool, 9 mm gypsum, 25 mm ventilated cavity, 15 mm plywood. The points show where thermistors and dowels were placed.

The wall, 2V, was ventilated through an open slide at the bottom and one at the top, where the one in the top was protected from direct rain by a projection cap of metal some few centimetres above the slide. In the bottom of the slide was an asphalt felt to drain driving rain. The rain screen was a plywood plate.

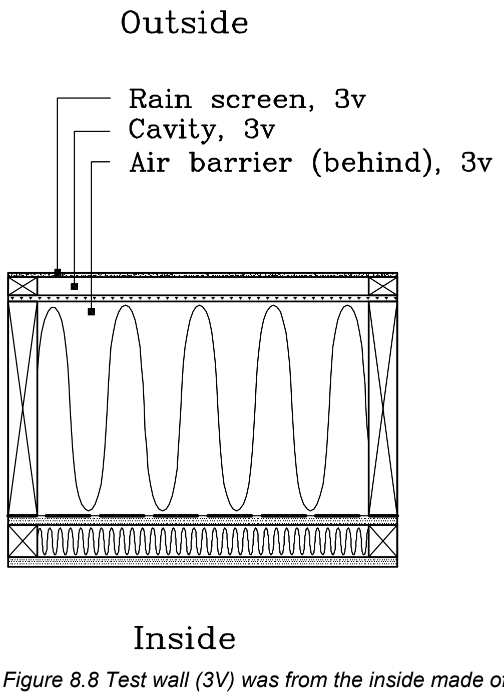

Figure 8.8 Test wall (3V) was from the inside made of 13 mm gypsum, 45 mm Rock wool, 13 mm gypsum, PE-foil, 240 mm Rock wool, 12 mm plywood, 25 mm ventilated cavity, 8 mm cembrit. The points show where thermistors and dowels were placed.

The wall, 3V, was ventilated through an open slide at the bottom and one at the top, where the one in the top was protected from direct rain by a projection cap of metal some few centimetres above the slide. In the bottom of the slide was asphalt felt to drain driving rain. The rain screen was a cembrit plate.

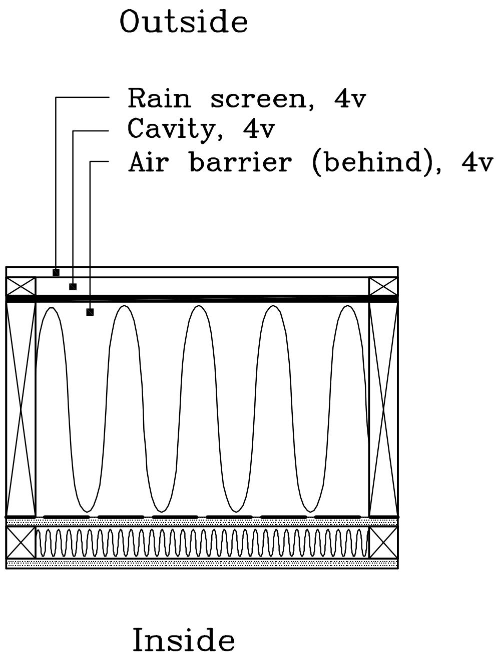

Figure 8.9 Test wall (4V) was from the in side made of 13 mm gypsum, 45 mm Rock wool, 13 mm gypsum, PE-foil, 240 mm Rock wool, 12 mm asphalt impregnated fibreboard, 25 mm ventilated cavity, 15 mm plywood. The points show where thermistors and dowels were placed.

The wall, 4V, was ventilated through an open slide at the bottom and one at the top, where the one in the top was protected from direct rain by a projection cap of metal some few centimetres above the slide. In the bottom of the slide was an asphalt felt to drain driving rain. The rain screen was an asphalt impregnated fibreboard plate.

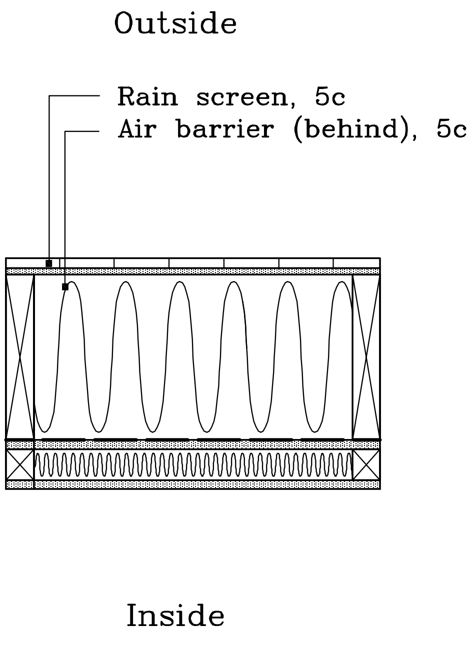

Figure 8.10 Test wall (5C) was from the inside made of 13 mm gypsum, 45 mm Rock wool, 13 mm gypsum, PE-foil, 240 mm Rock wool, 9 mm gypsum, 22 mm pine tongue and groove wood panelling. The points show where thermistors and dowels were placed.

The wall, 5C, was a compact wall without air cavity. It was protected from direct rain by a projection cap of metal. The rain screen was a pine tongue and groove wood panelling.

Simulations of the temperature and relative humidity for a period of one year for the 5 test walls were made with a Simulink wall model. The coefficient C_D was modified to obtained simulation results in accordance with the measured values, see Figure 8.17. The discharge coefficients for the ventilated test walls were assumed low, C_D= 0.03, due to the overhang at the top and the asphalt felt at the bottom. However, for the models 3V and 4V a discharge coefficients of C_D= 0.47 was found better. The wind pressure coefficients for the test house at Danish Building and Urban Research was unknown, and the values from the DTU test house was used, as both facades were north facing.

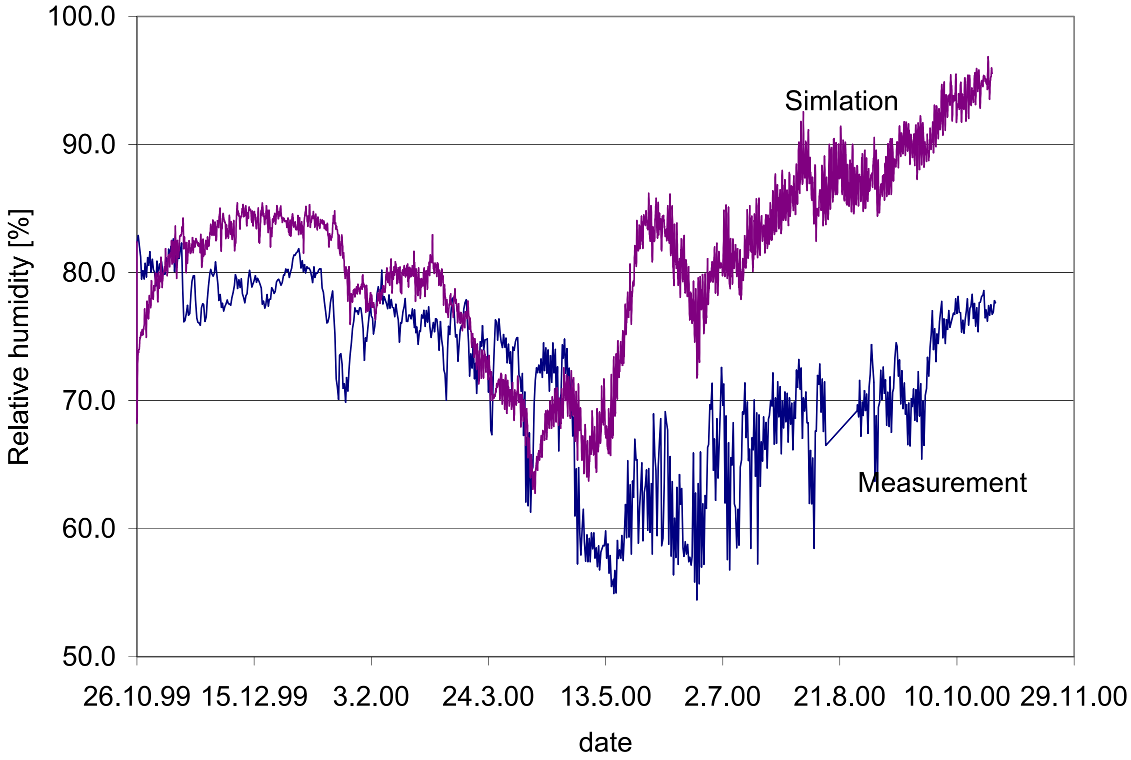

Figure 8.11 Relative humidity behind the air barrier, simulated and measured for the ventilated wall 1V. Dischargecoefficient of 0.03.

Figure 8.11 shows a good agreement between measurement and simulation of the relative humidity behind the air barrier until May, where the measured and simulated results seem to diverge. At this time the data logger for recording weather data was changed and it was later discovered that it was measuring with a constant error of about +2-3°C and +2-3% relative humidity, (Mossing, 2001). The simulations have therefore been performed with wrong weather data from May to October. The results showed that the simulation of the relative humidity behind the air barrier was in accordance with the measurement when the correct weather data was used until May, but the correspondence became poorer for the rest of the period simulated with the wrong weather data.

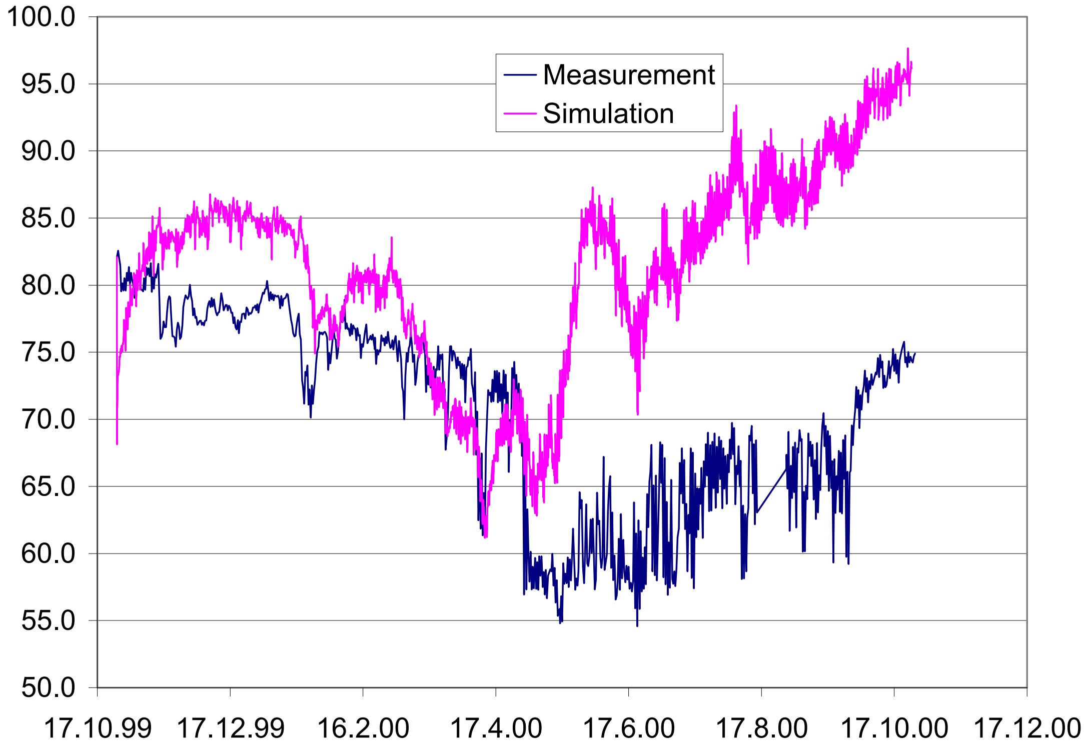

Figure 8.12 Simulated and measured relative humidity in the insulation behind the rain screen of a ventilated facade with plywood rain screen, 2V. Dischargecoefficient of 0.03

For 2V a good agreement between simulation and measurements of the relative humidity behind the air barrier was found too, see Figure 8.12. Similar to the case 1v, the less accordance was seen starting from May.

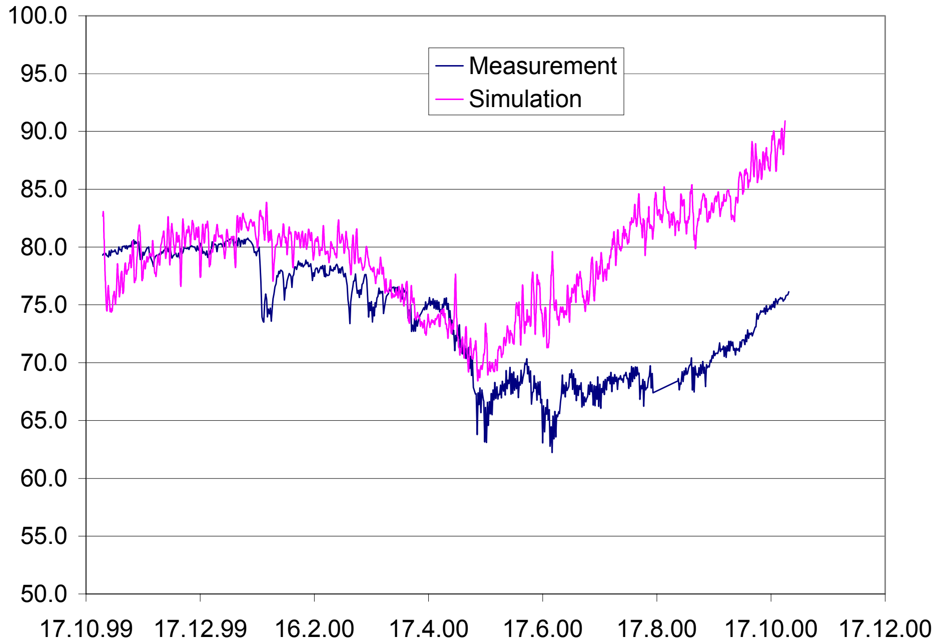

Figure 8.13 Measured and simulated relative humidity in the insulation behind the rain screen of a ventilated facade with cembrit rain screen, model 3V. Where the simulated results are running average with a period of 24 hours. Discharge coefficient of 0.47.

The calculated relative humidity results were fluctuating considerably for the simulation in Figure 8.13. Therefore the running average, with a period of 24 hours, was shown. The fluctuation was due to more rapid change in temperature with the cembrit rain screen than with wood based rainscreen (not shown). The specific heat capacity of cembrit is 850 J/kg K (Nicolajsen and Hansen, 2001), which is lower than the specific heat capacity for fibreboard1300 J/kg K (Rode, 1996).The cembrit is also less hygroscopic and has a lower diffusivity than wood. The temperature of the cembrit will therefore change more rapid with change of temperature in the outdoor climate than wood. This also affected the temperature of the air barrier, and thereby the relative humidity, another factor was the higher discharge coefficient, which was earlier found to increase the fluctuations.

The difference between model 3V and model 4V is the rainscreen material, as they were simulated with the same dischargecoefficient. While the fluctuation for model 3V was suggested as due to difference in heat capacity and difference in capacity for moisture.

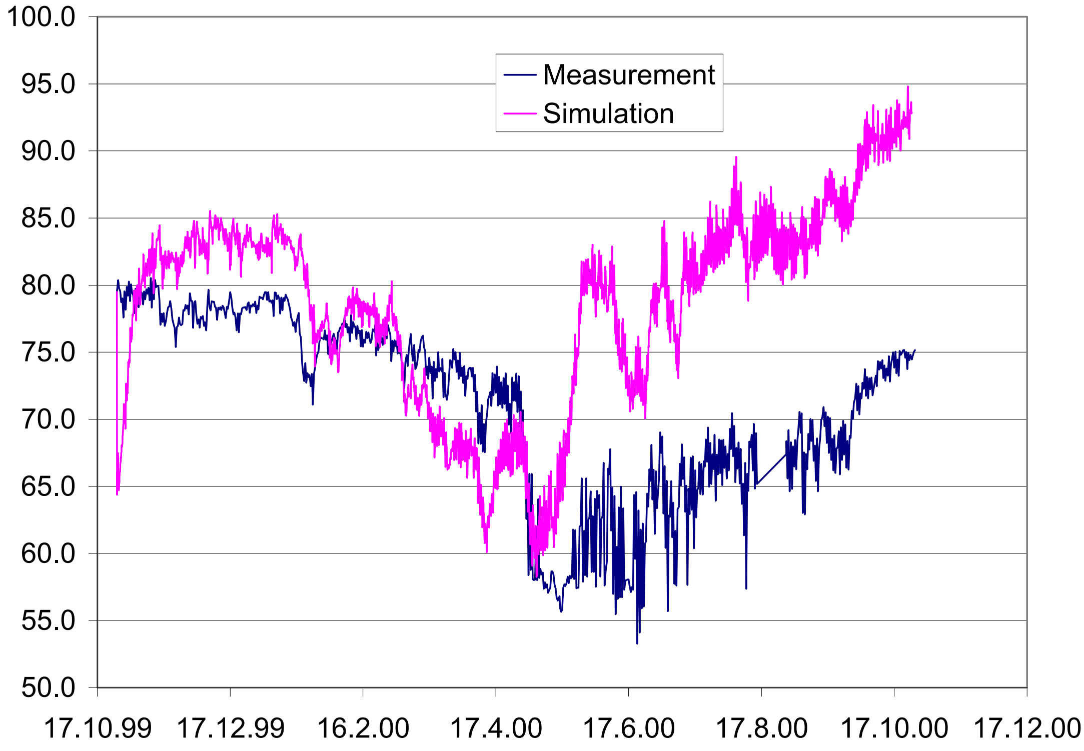

Figure 8.14 Measured and simulated relative humidity in the insulation behind the rain screen of a ventilated facade with plywood rain screen and air barrier of asphalt impregnated fibreboard, 4V. Discharge coefficient of 0.47.

For 4V a good agreement between simulation and measurements of the relative humidity behind the air barrier was found too, see Figure 8.14. Similar to the case 1V and 2V, the less accordance was seen starting from May.

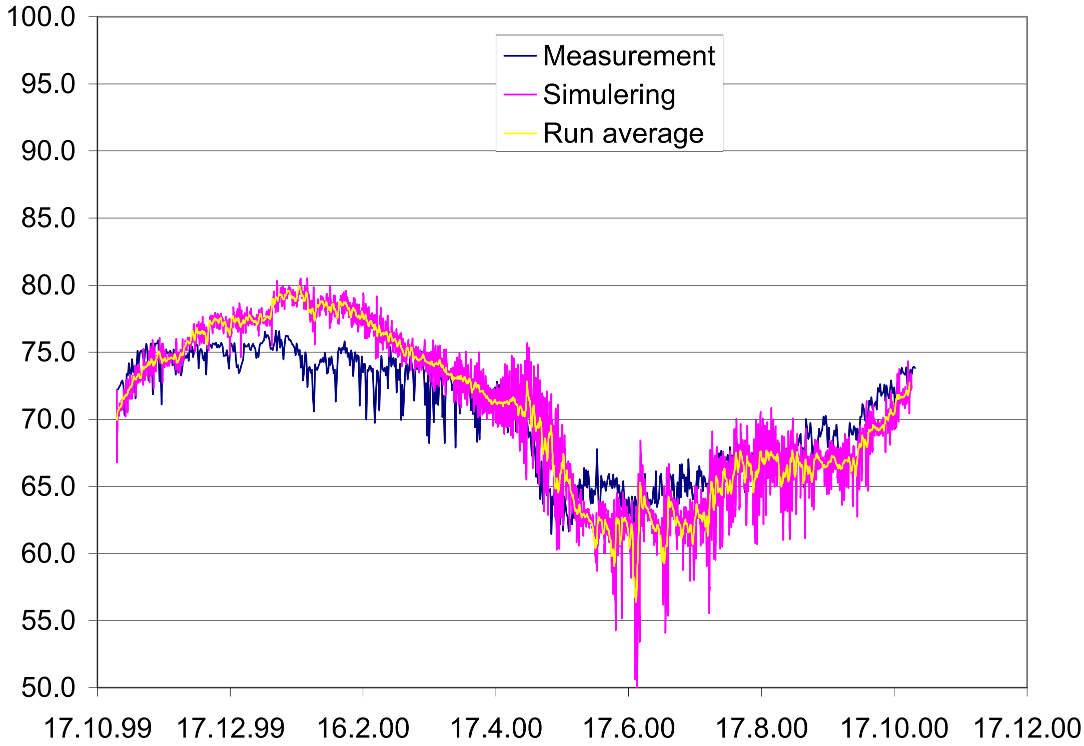

Figure 8.15 Measured and simulated relative humidity in the insulation behind the air barrier of a compact facade with wood panelling as rain screen, 5C.

For the compact wall the disagreement between simulation model and measurement starting from May was not seen. The compact model was not ventilated and therefore the air barrier was less affected by the outdoor climate. It was however, surprising that the curves were so similar.

The first four models 1V-4V seen in figures 8.11-8.14 were ventilated construction. Figure 8.15 shows results for a compact model 5C, which was not ventilated. For all the five cases the measurement point behind the wind break are compared. This means that the ventilated examples are in nearer contact with the outdoor air compared to the compact and not ventilated construction.

Simulations of 1V were made with a different set of wind pressure coefficients. The difference in Figure 8.16 shows the effect of using wind pressure coefficients available in the literature, which does not count for the obstacles in the surroundings compared to more detailed coefficients. Comparison of simulations with wind pressure coefficient values estimated from Jensen (1959) and Knoll (2000) is seen in Figure 8.16.

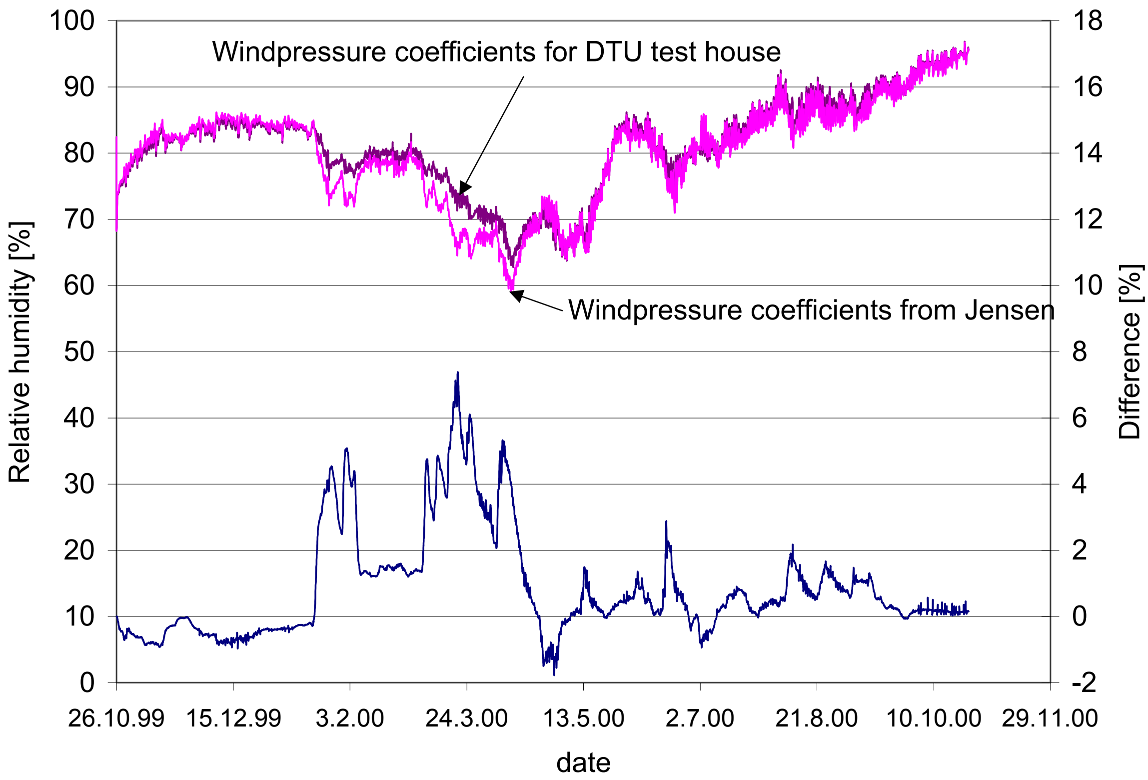

Figure 8.16 The effect of different estimates of wind pressure coefficients on the relative humidity behind the air barrier. The simulations are performed using the wind pressure coefficients for the DTU test house generated with Cp-Generator (Knoll, 2000) or tabled values from Jensen (1959). Further is the difference between the two curves seen.

Simulation of 1V with two different sets of wind pressure coefficients show no difference in relative humidity behind the air barrier most of the year, and slightly higher relative humidity with values from Knoll (2000) than with Jensen (1959).

Figure 8.16 shows that the influence of wind pressure coefficients was of the same size or less than the difference between measurements and simulations. Most of the time the difference was within ±2%-points relative humidity, but in some periods a difference of up to 8%-points relative humidity was seen. The difference in simulated relative humidity due to different wind pressure coefficients showed that general wind pressure coefficients may be chosen from the literature for simulations.

The effect of discharge coefficient was investigated too. Simulations with model 1V were made with different discharge coefficients, and the relative humidity in the air barrier were compared. The simulations were made with different values for the discharge coefficients of 0.47, 0.1, 0.07, 0.03 and 0.01. The relative humidity behind the air barrier is seen in Figure 8.17.

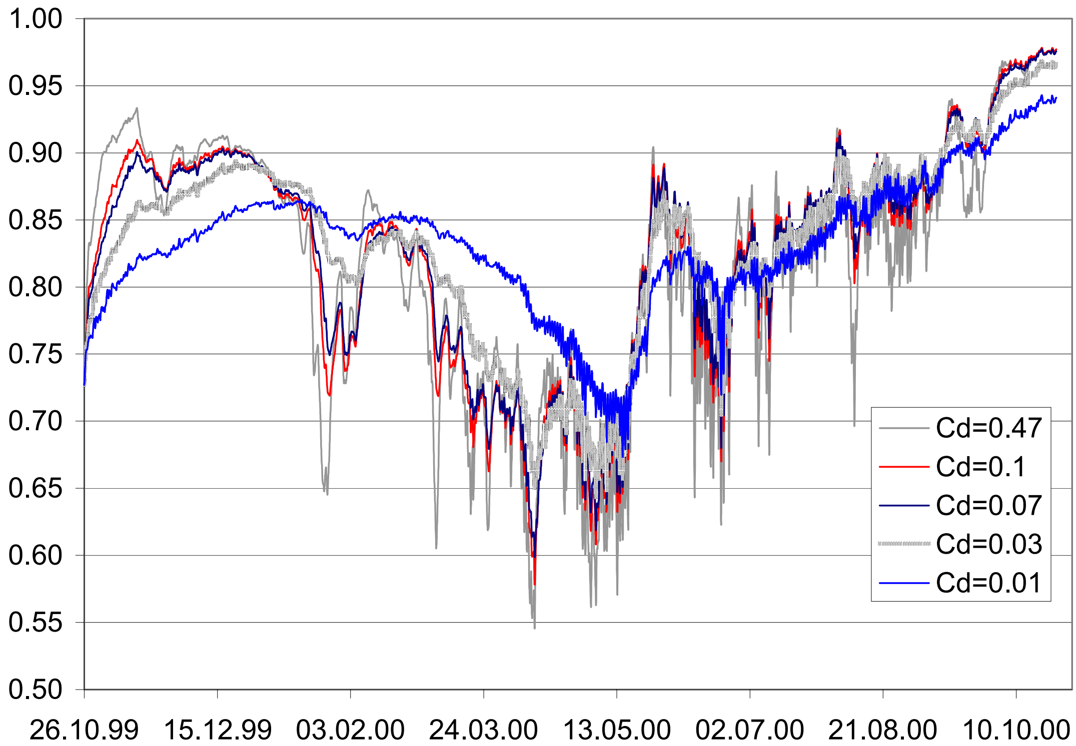

Figure 8.17 Simulation of relative humidity in air barrier for model 1V with different discharge coefficients.

The discharge coefficient that was found to fit best were 0.03, seen in Figure 8.11, corresponding to rather closed vents. The effect of increasing the discharge coefficient from 0.01 to 0.03 was rather significant. The higher the discharge coefficient the more outdoor air is passing through the structure, which results in higher changes in the relative humidity.

For both 1V and 2V a discharge coefficient of 0.03 was found best, where it for 3V and 4V were a discharge coefficient of 0.47 that was best. The difference may be due to different construction and materials and distance to corners. The rain screen of cembrit in 3V was properly smoother than a wood siding like 1V. The rain screen of 2V and 4V were both plywood, but the air barrier was asphalt-impregnated fibreboard for 4V and gypsum for 2V. The asphalt paper may also be placed a bit differently between the test models.

8.4. Summary

Simulations with a Simulink subsystem for simulation of the air flow in a ventilated cavity was in accordance with measurements. There was a high standard deviation for the measurements and the simulations, and the difference between measurements and simulations were rater high but smaller than the standard deviation of the uncertainty of the measurements. However, the difference seems not to be systematic, and the air velocity was in the same range.

Good accordance for temperature and relative humidity in materials between *MATCH* and Simulink simulations were seen, for a multi layer wall model. The temperatures were almost identical layer by layer, where the moisture content for the Simulink model was slightly higher than with *MATCH*. The difference in moisture contents was not significant, and the difference was mainly for the rain screen. Whole year simulation of the moisture content showed that for the rain screen the difference was highest in the winter.

A difference between the measurements and simulations were the logging interval of the results. The simulations logs data every simulated hour, where the experiments log data every 12 hours. Another difference was the hysteresis of the wood dowels. The simulations seem to overestimate the fluctuation for the relative humidity.

The simulation of relative humidity in the air barrier follows the measurements well. A separation is clearly seen when the boundary has been measured incorrectly, and therefore the input for the simulations have been wrong. However, this was not observed for the compact model without ventilation.

Simulations with detailed wind pressure coefficients and with general values were made. It showed that the effect on the relative humidity of the air barrier were minor compared to use of less detailed wind pressure coefficients. The difference was most of the year ±2%-points but higher up till 8%-points in February and March. This show that the use of general wind pressure coefficients can be used for simulations with hourly mean values for the wind data. If the fluctuations in the wind are included in the future, this might not be true.

9. Parameter studies by simulations

A ventilated façade was used as an example of a qualitative analysis of the hygro thermal conditions in a ventilated building envelope by the use of a Simulink model. This chapter includes a discussion of comparison between different wall designs, and a definition of critical moisture conditions. Some parameters were varied to compare different cases, these parameters and the cases were described. Simulations of the different cases were performed, and the simulation results are presented and discussed.

9.1. Scope of parameter studies

The optimum airflow for a ventilated building envelope was here defined as the airflow giving the shortest time of critical moisture conditions inside the materials of the structure. Critical moisture condition was defined as a combination of temperature and relative humidity in a material, which is favourable for mould growth. The most critical position with respect to moisture has been determined from experiments. Measurements have shown, that for Danish weather conditions, the facades have the highest moisture content just behind the air barrier (Nicolajsen and Hansen, 2001). Therefore the relative humidity and temperature in the air barrier were compared for comparison of different variations of a light weight facade.

When the relative humidity is higher than 80% and the temperature is above 5°C mould growth may occur (Hukka and Viitanen, 1999). The occurrence of mould growth also depends on the length of period with critical moisture conditions and temperature level. A study by Sedlbauer (2001) shows that the conditions for mould growth highly depend on the various fungus species. However, it also seems like the criteria by Hukka and Viitanen (1999) were on the safe side, and were applied here.

The acceptable length of a period with critical moisture conditions has also to be defined. Studies of ventilated attics find that plywood sheathings in traditional attics, before the energy crises, had a moisture ratio at its highest between 15% (73% RH) to 17% (80% RH) by weight during 25 % of the time (Larsson, 2001). The attics were dry and safe to mould growth due to heating from the dwelling. Such poorly insulated attics tend to have fewer problems than modern attics with heavy insulation. This indicates, that we might accept a continuous period of 8-10 weeks (15-20% of the time) where the relative humidity is above 80% and the temperature higher than 5°C. Sedlbauer (2001) finds that with the optimum conditions, the fungus growth may start after only a few days, but that for a common species, such as Aspergillus, the temperature should be above 10°C and the relative humidity higher than 90% for 64 days for start of mould growth. In accordance with both Larsson (2001) and Sedlbauer (2001), Viitanen (1997) finds that around the lowest critical conditions allowing the growth, several weeks or months of exposure can be accepted. Here a period length with exposure of critical moisture condition is therefore accepted for up till 10 weeks.

For general use of the present Simulink model of a ventilated façade, the actual wind load and the pressure drop through the vents are often unknown, meaning that a simulation of moisture content often will be too inaccurate to determine whether a structure passes or fails a certain durability criteria. However, the simulations will be used for investigation of whether a building structure can benefit from increased insulation thickness and/or changed ventilation rate.

The simulation estimates the hours of critical moisture load in the air barrier of gypsum. The period will rarely be continuously. However, the results will be analysed as if it was continuously, i.e. the worst case.

The optimum airflow rate, which keeps the moisture content at a minimum, is expected to be individual for each structure, depending on the indoor moisture load, the material layers and their thickness, but also poor workmanship will have a major influence on the actual heat and moisture transport. However, in practice some guidelines are needed, and some general rules of thumb for the ventilation of façade walls should be given, even though it might not be the optimum for a specific façade.

9.2. Analytical parametric variation

Recent trends in modern buildings are increasing insulation thickness for reducing energy consumption, use of compact wall with wood siding, and wish of 'breathable houses' without vapour retarder. Therefore the parameters studied were: Insulation thickness, ventilation rate, and walls with and without vapour retarder.

The change in the Danish building regulation allowing the use of wood cladding of facades up to four stories high, providing the wall is compact without ventilation or air cavity. This change makes it of general interest, to investigate the change in moisture load for not ventilated facades walls, compared to a traditionally ventilated wall.

The facade studied was north facing, and was in principle from the inside made of 13 mm gypsum board, vapour retarder of 0.1 mm PE-foil (if included), mineral wool insulation 100 mm-300 mm, 13 mm gypsum board, 25 mm air cavity (if included), and a wood based rain screen, see Figure 9.1 for the case #1.

The model had a width of 0.559 m and height of 1.65 m, with an open slide at the top and bottom. The surroundings were assumed to be the same as for the outdoor test building at DTU, described in Chapter 4 'Experimental set up, ventilated wall', with the wind pressure coefficients generated with the Cp-Generator (Knoll,1996). The boundary conditions were the DRY at the outside and sinusoidal temperature and relative humidity with a yearly cycle on the inside, as described in the Chapter 7 'Simulation model'.

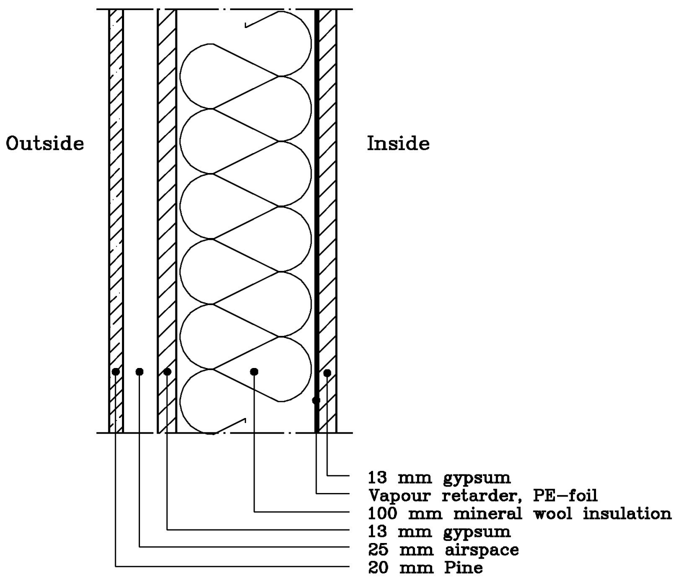

Figure 9.1 Material layers of ventilated facade model case # 1.

Table 9.1 shows the used parameter combinations. Changing the insulation thickness and the area of vent openings, altering the stack and the wind effect, changed the ventilation rate. Varying the discharge coefficient corresponded to varying the ventilation opening area. For a duct width of 0.025m the discharge coefficient was found to be approximately 0.47. Reducing the width to 1/4 i.e. width of 0.006 m (called scattered) reduces the discharge coefficient to 0.26

(Appendix G). For simulation of a compact wall, a modified model without the cavity subsystem was used.

To get realistic initial conditions for a simulation, a one year period was simulated with DRY as boundary conditions, and the final values of temperatures and moisture contents were used as start values for the ”real” simulation.

9.3. Simulation results of parameter variations.

The results are shown in Table 9.2, and used for investigation of the following hypotheses:

1)Light weight wall structure with normal moisture load (i.e. with vapour retarder) does not need ventilation, i.e. the wall can be accepted both for fire and moisture perspective.
2) With heavy moisture load, the ventilation helps the structure to dry out.

The total yearly convective moisture transport within the ventilated cavity and the moisture content in outer gypsum are the analysed results, that are compared between the cases, in order to investigate the effect of:

A. Insulation thickness. Case 1+2+3, Case 8+9
B. Ventilation opening area. Case 2+4+5
C. Absence of vapour retarder. Case 7+8+9
D. Absence of ventilation. Case 2+4+6

Table 9.1 Parameter variations of the different simulated cases

Case #	Insulation thickness [mm]	Discharge coefficient	Vapour retarder
1	100	0.47 max open	Yes
2	200	0.47 max open	Yes
3	300	0.47 max open	Yes
4	200	Closed	Yes
5	200	0.26 scattered	Yes
6	300	Closed	Yes
7	200	Closed	No
8	200	0.47 max open	No
9	300	0.47 max open	No

Table 9.2 Simulation results of yearly convective moisture transport out of a ventilated cavity, time of relative humidity above 80%, and time of critical moisture load in air barrier for different facades, case 1-9. The time is given as a number of hours and a percentage of time.

Case #	Convective moisture transport out of the cavity in kg/year	Hours per year, where the relative humidity is above 80%, for the outer gypsum layer (% of time).	Hours per year, where the relative humidity is above 80 % and temperature is above 5°C (% of time).
1	0.114	1217 (14%)	715 (8%)
2	0.113	3463 (40%)	1358 (16%)
3	0.113	4132 (47%)	1563 (18%)
4	-	3987 (46%)	846 (10%)
5	0.113	3408 (39%)	1304 (15%)
6	-	4066 (46%)	853 (10%)
7	-	8040 (92%)	4611 (53%)
8	10.192	6028 (69%)	2961 (34%)
9	8.295	5920 (68%)	2740 (31%)

The convective moisture transport out of the cavity is the amount of water in kg per year, that was carried out of the cavity by ventilation air. A positive value means that the ventilation reduced the moisture content of the structure more than it wetted it.

9.3.1. Influence of thermal insulation thickness

The results from case 1,2 and 3 in Table 9.2 and Figure 9.2 showed results for a ventilated façade with a perfect vapour retarder and insulation thickness of 100 mm, 200 mm and 300 mm. It is seen in Table 9.2, that the total convective moisture transport was limited but positive, meaning that the structure was dried due to convection. The moist source, in the walls with vapour retarder, was mostly outdoor air wetting the structure which were later dried out. The period of critical moisture conditions was seen to increase with the insulation thickness, which was due to lower temperature in the air barrier, which increases the relative humidity although the lower temperature for the thicker insulation also results in more time where the temperature was below 5°C.

Overall the period length with critical moisture load was acceptable, where the worst case was for thick insulation of 300 mm, which had critical moisture load 18% of the time, where the acceptable period was up to 15%-20%.

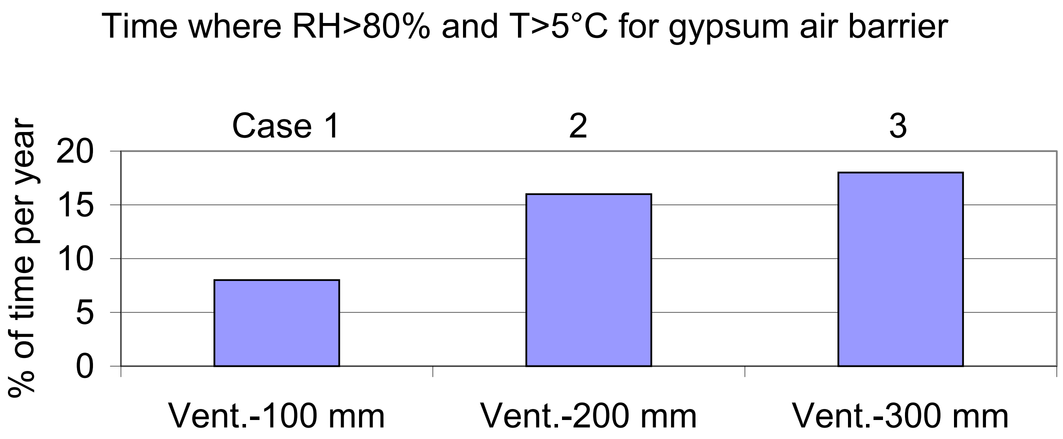

Figure 9.2 The period of critical moisture load increased with the insulation thickness for a ventilated façade with perfectly sealed vapour retarder.

9.3.2. Opening area

Comparison of case 4 (no ventilation), case 5 (limited ventilation) and case 2 (normal ventilation), Figure 9.3 shows the effect of reducing the discharge coefficient for a normal (200 mm) insulated structure with perfect vapour retarder. This means that the wind effect was varied. From Figure 9.3 it is seen that the time with critical moisture conditions decreased with decreasing ventilation for a ventilated façade with perfect vapour retarder, although the difference between case 2 and 5 was minor.

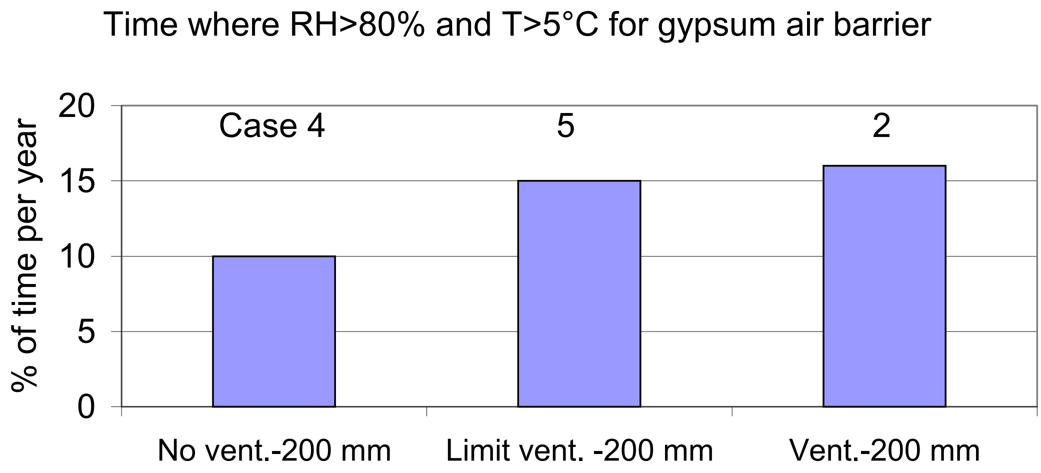

Figure 9.3 The period with critical moisture load increases with increased vent opening for a ventilated wall with perfectly sealed vapour retarder.

The ventilation had a negative impact on the moisture load on the façade. This was due to a rather low inside moisture load, which meant that the average water vapour pressure in the air barrier was lower than for the outdoor air in the ventilated cavity, and that the air barrier was actually wetted by the ventilation air for some periods of time.

9.3.3. Wall without vapour retarder.

Figure 9.4 shows the time of critical moisture load in the air barrier, when there was no vapour retarder in the wall. Here it was seen that the moisture load was much higher than compared to models with vapour retarder. Further it was seen that the ventilated design had considerably less hours of critical moisture conditions, case 8, than the non-ventilated model, case 7, meaning that for a wall with heavy moisture load the ventilation was of benefit. The Figure 9.4 also shows that here, without vapour retarder, the increased insulation thickness was positive for the façade (case 8 and 9), where it was negative for the wall with vapour retarder, Figure 9.2. Further the Figure 9.4 shows the convective moisture transport was high and positive out of the cavity.

The simulations showed more time with critical moisture conditions for thicker insulation with vapour retarder, and less time of critical moisture conditions for thicker insulation in the absence of vapour retarder. Even though the difference between case 8 and case 9 was minor, about 1% difference in time with critical moisture load, the simulated phenomenon was discussed.

For the wall without vapour retarder the moisture source was the inside environment. From the theory it is known that the temperature of the inside surface layer in case 8 (200 mm) will be lower than the temperature in case 9 (300 mm) (in winter). The theory also tells that the diffusivity decreases with increased temperature, for the equation used in the simulation.

Eq 9.1 $\delta_p = \dfrac{\delta_c}{R_v \cdot T}$

where

δ_p	is the diffusion coefficient [kg/m s Pa]
δ_c	is the diffusion coefficient [m^2/s]
R_v	is the gas constant for water vapour [461.5 J/kg K]
T	is the absolute temperature [K]

For the wall without vapour retarder the limit for moisture diffusion may be the diffusion through the inside gypsum. As the temperature of the inside gypsum was lower for case 8 than for case 9, the moisture transport by diffusion (through inside gypsum) should be higher for case 8 than for case 9. Furthermore the vapour resistance of the insulation layer, even though it is small, will also be higher for the thicker layer in case 9 than for case 8. All in all a slightly higher vapour transport by diffusion for case 8 than for case 9. When furthermore the criteria of temperature above 5°C was included, the difference in hours with critical moisture load was increase to 3% for case 8 compared to case 9.

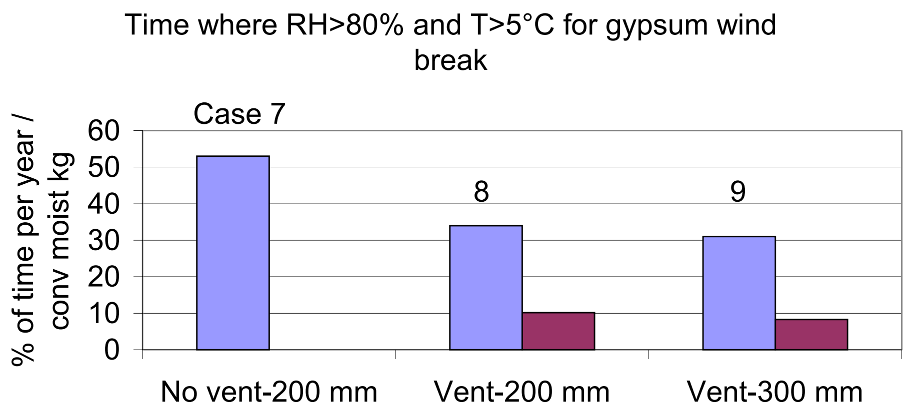

Figure 9.4 Percent of time per year with critical moisture conditions in the air barrier of a façade wall without vapour retarder, and with different insulation thickness (light/blue) , together with the yearly convective moisture transport out of the ventilated cavity (dark/red).

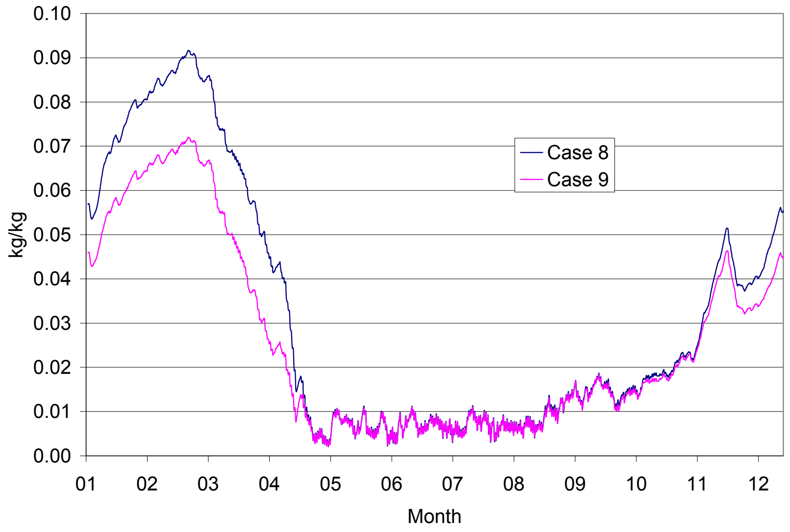

Figure 9.5 Moisture content in the gypsum air barrier, simulated for case 8 (200 mm) and 9 (300 mm). 80% relative humidity for gypsum is approximately 0.0093 kg/kg.

The moisture content in the air barrier of gypsum for a ventilated wall without vapour retarder is seen in Figure 9.5 for case 8 with 200 mm insulation and for case 9 with 300 mm insulation. It is seen that both case 8 and case 9 exceeded the limit for critical moisture load (80% relative humidity (RH) for gypsum is approximately 0.0093 kg/kg) most of the year except for the summer period.

The simulations showed that the designs without vapour retarder became very wet and the drying potential by the outdoor air was high. The thicker insulation lowered the air barrier temperature so the air barrier surface temperature for case 8> case 9.

9.3.4. Absence of ventilation

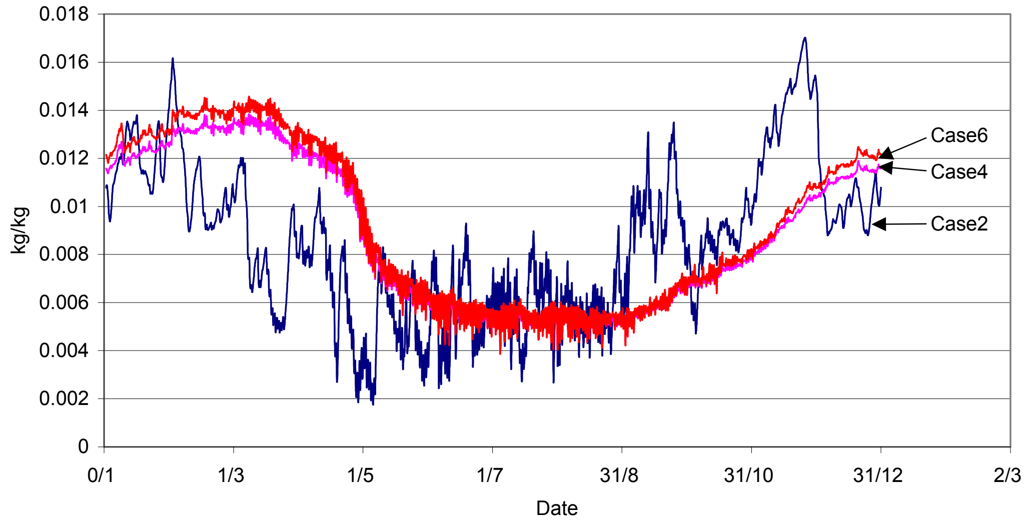

Figure 9.6 Simulated moisture content in the gypsum air barrier for 3 different wall models. Case 2 with 200 mm insulation, vapour retarder and maximum vent opening. Case 4 was also with 200 mm insulation and vapour retarder, but without ventilation. Case 6 had vapour retarder like case 2 and 4, but it had more insulation (300 mm) and is without ventilation.

Figure 9.6 shows that the absence of ventilation dampened the variation of the moisture content i.e. dampened the effect of exposure to the weather. The ventilation dried the air barrier in winter and spring below the condition for the case 4 and case 6 without ventilation, but on the other hand the ventilation increased the moisture content in the fall, and the vapour conditions were similar levels during summer but with more fluctuation for the ventilated case 2.

9.4. Fire regulation

The Danish Building regulation requires that there is no air gap behind the woodrain-screen for apartment buildings. The simulation results indicated that as long as the vapour retarder was tight this gave acceptable conditions for normal insulation thickness. If the insulation thickness was increased special attention should be made, because according to the simulation results the moisture load would increase with the thickness.

For existing walls the vapour retarder is often seen to fail, and here the lack of ventilation can be damaging for the wall structure. Therefore extra attention should be made to ensure the air tightness of walls without ventilation.

9.5. Summary

To conclude on the hypotheses first: Light weight wall structure with normal moisture load does not need ventilation, i.e. the wall can be accepted both for fire and moisture perspective.
The ventilation and the increased insulation thickness have both a negative impact on the moisture load of the materials for a wall with correct functioning vapour retarder. Both with and without ventilation the moisture load was considered acceptable.

Secondly: With heavy moisture load, the ventilation helps the structure to dry out. A wall with a faulty vapour retarder requires ventilation to dry out the moisture coming from the inside. Here increased insulation thickness has a positive effect on the moisture load. However, even a well-ventilated cavity cannot sustain complete absence of a vapour retarder.

It is therefore recommended to keep a ventilated cavity for wall structures, and if this is prohibited, to be extra careful with sealing of the vapour retarder and increase the insulation thickness with care.

10. Discussion and Conclusion

Moisture in buildings result in both degradation of structure and health risk for the users. The objective here was convective moisture transport in ventilated building envelopes. From experience we know that ventilated building envelopes are sustainable, with vent sizes based on rules of thumb. When new designs or materials are introduced, the prediction of moisture load due to convection is limited. The purpose here was a better understanding of the mechanisms for convective moisture transport in ventilated cavities.

10.1. Method for air velocity measurement

It was proposed to use the tracer gas method as an alternative to thermo anemometers in order to measure the directional air velocity in a ventilated cavity, and in order to measure recycling air. By the use of tracer gas, both the velocity and the direction of airflow were measured, and besides the convective moisture transport was determined from the results of tracer gas analysis.

The original idea for using tracer gas was in order to determine recycling or change of air. However, recycling of air was not found present during simultaneous measurements with thermo anemometers. Other tracer gas measurements during nights and for other weather conditions had shown results that might be recycling. This could not be experimentally validated due to the lack of simultaneous measurements of low velocity with changing direction with thermo anemometer and tracer gas method.

From laboratory measurements of low air velocity, the tracer gas showed to be valid and accurate. It was also found to be difficult to measure the low velocity with alternative methods, due to uncertainty on the instruments on the market that were robust for out-door weather exposure. The thermo anemometers used did measure accurately, but these were sensitive and not robust to humid weather.

Changes in mean wind velocity over a short period; seem to be correlated to poor performance of the tracer gas method. Here the tracer gas was unreliable and measured extremely high velocities but these were believed to be an artefact due to directional changes.

The tracer gas method had a long response time, which was found impropriate for short time measurements for analysis of the influence of wind fluctuations on air velocity. The thermal anemometers had however, a short response time, which enabled measurements with the frequency of the wind fluctuations.

The tracer gas method was used together with thermo anemometers for measuring the air velocity. The use of thermo anemometers showed that the average velocity over the cross sectional area could be estimate as 2/3 of the max mean velocity, and further that the mean air velocity measured by thermo anemometers provides multiple measuring points. Alternatively the mean velocity may be measured in a distance of 2/3 from the middle towards the edge, as for measuring duct flow (Sørensen, 1996). However, the field experiments showed that the wind angle affected the symmetry of the velocity field in the cavity, and therefore would disturb the measurement.

10.2. Results from measurements

Air velocity measurements in a ventilated facade cavity, were used for analysis of the correlation between wind pressure and air velocity. The overall impression from these experiments were that wind and buoyancy affected the airflow equally. The wind force was found to be highly fluctuating both in velocity and direction. Measuring with tracer gas method showed a phenomenon of extremely high measured air velocities, which were attributed to an artefact effect of the method.

The air velocity was, for stable periods, measured in the range of –1 to +1 m/s upwards, but could be up to 10 m/s for single measurements for wind velocity between 0.5 m/s and 10 m/s (at height 4.8 m). Jacobsen and Petersen (1998) measured air velocity in the range from 0.2 m/s to 2 m/s for wind velocity between 0.5 m/s and 10 m/s (at height 20 m) using a thermo anemometer on the same test wall, with a different rain screen. Their measurements show a linear correlation between air and wind velocity.

Others have measured lower velocities. Popp and Künzel (1980, referred by Andersen (2000)) report cavity air velocities between 0.05 m/s and 0.4 m/s, both wind force and buoyancy force increase the airflow. Jung (1985, referred by Andersen (2000)) has measured air velocities (brick wall) of 0.01m/s to 0.3 m/s for wind velocity of 0.5 m/s to 8 m/s. All agree that the air velocity is positively correlated to the wind velocity. Nicolajsen (1983) however, measured air velocity 0.02-0.2 m/s for wind velocity 0-8m/s with no correlation between air velocity and wind velocity.

Fluctuation in the wind velocity did not seem to influence on the mean air velocity, as good accordance between thermal anemometers with low response time and tracer gas method with high response time were in accordance.

The difference in wind velocity at two different heights did not show the expected ratio. The theory considers measurements in the undisturbed flow field, which does not exist when buildings and trees are present in the surroundings.

Measurements of the wind pressure coefficients were too few, and also the measured pressure differences were small compared to the uncertainty of the pressure transducers. The dispersions of wind pressure coefficients between measured values with approximately the same wind angle showed this.

The wind pressure coefficients from Knoll (2000) estimated that sideward wind has more influence on the airflow than direct wind. Furthermore it is interesting to note that wind can be affecting the airflow downward on the leeward side. These phenomena were however, not observed experimentally.

10.3. Simulation model

In the model developed the liquid transport was not included. Further the wind pressure was estimated from hourly mean wind data. This was both due to missing weather data on the turbulence and frequency of wind, but also due to a missing mathematical model.

Material data is missing for some materials and very detailed information is available for others. The data are most often from laboratory conditions with constant gradient where only one parameter is changed at a time. An example of this is how to model the moisture hysteresis. Discussions on how to model the scanning curve between absorption and desorption is e.g. described in (Time, 1998).

The developed simulation model showed good accordance with *MATCH* (Pedersen, 1990) simulations and measurements (Nicolajsen and Hansen, 2001). Simulation results however, have their limits. Due to theoretical limitation, the available data, and the assumptions of unimportant effects, some phenomena were excluded from the model. In the analysis of results, both the physical phenomena and the model should be considered, when conclusions are made on the basis of the simulated results. I.e. a new phenomenon should carefully be analysed with respect to the scope of the model. The typical power of simulations is to compare different variations of a model, and less of giving exact results.

10.4. Simulation results

It was found that the ventilation would wet a structure for long periods, and dry it for other periods. The convection removes moisture coming from the inside, and can to a limited extend compensate for an imperfect vapour retarder. The simulation showed that increasing insulation thickness increased the time of critical moisture load. However, the period of critical moisture load did not exceed a critical length of 8-10 weeks, when there was a vapour retarder.

The results from simulations with parameter variation showed that the wall would be robust towards moisture without air cavity, provided that the inside lining was vapour tight and airtight. Walls with perfect inside lining were exposed to a higher moisture load with ventilation than without, so ventilation will in fact increase the moisture load. In this conclusion, was the rain screen pressure equalisation effect not included.

The pressure equalisation rain screen has the positive effect of avoid driving rain to be pressed into the structure by the wind. At the same time the cavity behind the rain screen serves as ventilated cavity. The presented simulation results conclude, that ventilation rises the time of critical moisture load, but in this model the driving rain has not been included. The pressure equalisation effect of the rain screen should however, be included for recommendation of keeping a ventilated cavity behind the rain screen. A topic not being discussed is the benefit of pressure equalisation rain screen. An effect of an air layer behind the rain screen is that driving rain not penetrates to the air barrier. When the air barrier stays dry, water will not be pressed into the structure from wind pressure. The wind pressure on each side of the rain screen is equal, and the pressure load is absorbed in the wall behind the rain screen where no rainwater is present.

Increasing the ventilation for a perfectly sealed wall will increase the time of critical moisture load for highly insulated walls. The cooling effect of ventilation with outdoor air together with heat loss by radiation may course the temperature to be lower than the dew point temperature of the outdoor air, which therefore will condensate when it passes the envelope. Here more ventilation increases the potential for condensation. However, the simulations also show that the ventilation decreases the time with critical moisture conditions, when the moisture load is high due to e.g. lack of vapour retarder. This means that a wall might be robust with imperfect inside lining, if the outside is ventilated with outdoor air.

The ventilation of light weight wall is not provided but recommended. The wall with a both vapour tight and air tight lining does not require ventilation to stay dry, in this case it was shown that the ventilation actually wetted the wall. However, for the non perfect wall the ventilated cavity helps drying the wall and lower the moisture load. So wood facades, without air cavity behind the rain screen, is possibly durable. However, choosing this provides special care with the workman ship of making the vapour barrier both air tight and moisture tight.

Nicolajsen and Hansen (2001) concludes on their experiments together with (Andersen et al. 2001) that the insulation thickness has a insignificant influence on the moisture load, and that the moisture load is unaffected by the ventilation.

The wind pressure coefficients used in this thesis were more detailed than what is normally available data. Comparison with more general values from 8 main wind direction did not affect the simulation results highly. If the fluctuation in the wind direction is included in future simulations, an effect may be seen. Rousseau (1999-a) finds that the effect of simulated wind actually reduced the drying rate for a ventilated wall.

On the basis of simulation results it was suggested that ventilation of building envelopes are continued in residential houses, where it is legal; but it will be of benefit to reconsider the required vent size, when new designs or materials are used. As an alternative to the design of ventilation on the outside of the insulation, the insulation could partly be placed on the cold outside surface, similar to the suggestion by Larsson (2001) of placing part of the insulation on the outer surface of the roof surface for attics. The temperature of the cavity will raise, and more important radiation heat loss will not make the surfaces colder than the dew point temperature of the air. A disadvantage will be a higher installation cost.

10.5. Recommendations for wall design

Parameter study simulation leads to recommendation of:

- The use of vapour retarder.
- Make the inside lining air tight.
- Place some of the insulation on the rain screen.
- Moderate ventilation rate with outdoor air.

10.6. Recommendations for further work

A comprehensive validation of the tracer gas method with thermo anemometers, for measuring convective moisture transport and air velocity for wind oscillations for different seasons, wind velocities, and wind direction; and hereby investigate the presence of recycling air. Further including temperature measurements for determination of the buoyancy force. Use the tracer gas method on different types of rain screen sidings, both open and closed.

Do measurements on walls and other constructions with different orientation, in order to investigate whether north and south walls are more ventilated than east and west wall for dominated west wind.

Statistical analysis of oscillations in air velocity and wind velocity, and formulate a mathematical model of the wind fluctuation. Including fluctuation of wind in simulations also provides fluctuation data in the reference year. Using wavelet theory(Entheridge, 1999) could be a possibility for simulating the fluctuations in the wind.

Wavelet theory is based on a statistical analysis of fast and slow oscillations in e.g. wind velocity. Where the oscillations in the wind can be described with relatively few parameters using a wavelet formula.

Include further parameter variation for simulation with the developed model. The indoor humidity and the vapour diffusion resistance of the vapour retarder could be investigated. Simulations with variation of the vapour tightness of the vapour retarder, by the use of e.g. the Hygro-Diode (Korsgaard, 1985)

Further the model could be improved by:

- Including the liquid transport.
- Modelling the oscillations in wind data.
- Make a toolbox of a more comprehensive critical moisture load criteria, which includes relative humidity, temperature and time for a variety of common fungus species.
- Including sun radiation.
- For the wind load, to include temperature and relative humidity in the estimate of the density of the air.

References

ASHRAE. 1985. ASHRAE Handbook of Fundamentals, American Society of Heating, Refrigerating and Air-Conditioning Engineers, Inc., GA, USA.

ASHRAE. 1989. ASHRAE Handbook of Fundamentals, American Society of Heating, Refrigerating and Air-Conditioning Engineers, Inc., GA, USA.

ASHRAE. 1997. ASHRAE Handbook of Fundamentals, American Society of Heating, Refrigerating and Air-Conditioning Engineers, Inc., GA, USA.

Ahlgren, Lennart. 1972. Moisture fixation in porous building materials. Division of Building Technology. Lund Inst. of Techn. Report 36, Sweden.

Andersen,N.E.; Christensen, G.; and Nielsen, F. 1993. Bygningers fugtisolering. SBI-anvisning 178. Statens Byggeforskningsinstitut. Dyva Bogtryk, Glostrup. Denmark.

Andersen, Karl Terpager. 1989. Kondensforhold i uisolerede stalde. (In Danish) Statens Byggeforskningsinstitut. Danmark

Andersen, Karl Terpager. 2000. Ventilerede hulrum i vægkonstruktioner. –En teoretisk analyse. By og Byg Dokumentation 001. Danish Building and Urban Research, Denmark.

Andersen, Tove; Peder Fynholm, Morten Hjorslev Hansen and Asta Nicolajsen. 2001. Fugtsikre træfacader. –Fugtindhold i højisolerede træfacader. Udkast 4 (In Danish). Danish Building and Urban Research, Denmark.

Bird, R Byron; Stewart, Warren E.; and Lightfoot, Edwin N. 1960. Transport Phenomena. John Wiley and Sons, Inc. USA.

Bottoma, Marcel. 1993. Wind climate and urban geometry. Eindhoven: Technische Universiteit Eindhoven. The Nederlands. ISBN 90-386-0132-8.

Burch, D.M and Thomas, W.C. 1992. An Analysis of Moisture Accumulation in a Wood-Frame Wall Subjected to Winter Climate. Thermal Performance of the Exterior Envelpes of Buildings V. ASHRAE/DOE/BTECC. Florida

Burch, D.M and TenWolde, A. 1993. Computer analysis of moisture accumulation in the walls of Manufactured housing. ASHRAE Transactions. Volume 99 Issue pt 2. Page 977-990. Published by ASHRAE.

Burnett, E. and Straube,J. 1995. Vent, Ventilation Drying, and Pressure Moderation. Research Report. Canada Mortgage and Housing Corporation (CMHC). December 1995.

By- og Boligministeriet. 1995. Tillæg 1 til Bygningsreglement 1995 (in Danish). Bygge- og Boligstyrelsen. Danmark.

Condren, S.J. Vapor Retarders in Roofing Systems: When Are They Necessary?, Moisture Migration in Buildings, ASTM STP 770, M. Lieff and H.R. Trechsel, Eds., American Society for Testing and Materials, 1982, pp. 5-27.

DMI, 2000. www.dmi.dk. Danmarks Meteologiske Institut. København. Danmark.

Duer, Carsten. 2001. Personal contact. Velux International A/S. Denmark.

Duffie, J.A. and Beckman, W.A. 1991. Solar engineering of thermal processes. 2nd ed. New York, Wiley.

Dyrbye, Cläes and Hansen, Svend Ole. 1989. Vindlast på bærende konstruktioner. SBI-anvisning 158 (in Danish). Statens Byggeforsknings Institut. Dyva Bogtryk. Glostrup. Denmark.

Dyrbøll, Susanne. 1998. Heat transfer in Rowckwool modelling and method of measurement. Ph.D thesis. Technical University of Denmark, Department of Buildings and Energy. Denmark.

Etheridge, D.W. 1999. Unsteady Wind Effects in Natural Ventilation Design. CIBSE National Conference 1999. AIVC 12,527.

Etheridge, D.W. 2000. Unsteady flow effects due to fluctuating wind pressures in natural ventilation design –mean flow rates. Building and environment. Vol 35, pp. 111-333.

Gudum, Charlotte 1998. Målinger på en krybekælder i Lundegården (in Danish). Sagsrapport SR-9820. Institut for bygninger og energi. Danmarks Tekniske Universitet. Denmark.

Gudum, Charlotte and Nielsen, Toke R. 1999. Koblet fugt- og varmetransport (Coupled moisture and heat transfer).Course thesis 04415 Modellering af miljørelaterede problemstillinger. IMM at the Technical University of Denmark.

Gudum, Charlotte 2000-a. Even tracer gas dosing in a horizontal plane in a vertical ventilated slot. (Jævn dosering af sporgas i vandret plan på ventileret lodret spalte (in Danish)). SR-0019. Department of Building and Energy, DTU, Denmark.

Gudum, C. 2000-b. Measurement of air velocity in a ventilated slot on vertical facade using tracer gas technique –Calibration of measurement technique. (Måling af lufthastighed i ventileret spalte på lodret facade ved brug af sporgas –Kalibrering af målemetode(in Danish)). SR-0020. Department of Building and Energy, DTU, Denmark.

Hadvig, Sven. 1986. Termisk stråling for ingeniører (in Danish). Polyteknisk forlag. Denmark.

Hagentoft, C-E. and Harderup, E. 1996. Moisture Conditions in a North Facing Wall with Cellulose Loose Fill Insulation: Constructions wtih and without Vapor Retarder and Air Leakage. Journal of Thermal Insulation and Building Environments. Volume 19 – January 1996.

Hagentoft, C.E. 2001. Thermal System Analysis using the Building Physics Toolbox in Simulink. February 23. CIB W40 Heat and Moisture Transfer in Buildings. Meeting 8-11 April 2001. Wellington, New Zealand.

Hagentoft, C.E. 2001-b. Introduction to Building Physics. Chalmers University of Technology. Sweden.

Haghighat, Fariborz; Brohus, Henrik; and Rao, Jiwu. 2000a. Modelling air infiltration due to wind fluctuations –a review. Building and Environment 35 (2000) 377-385.

Hansen, H.E.; Kjærulf-Jensen, P. and Stampe, Ole B. 1992. Varme- og Klimateknik, Grundbog 1.udg, 2 oplag. Danvak. Teknisk Forlag A/S. København. Denmark.

Hansen, Kurt Kielsgaard. 1986. Sorption Isotherm, A Catalogue. Technical Report 162/86. BKM, Technical University of Denmark.

Hukka, A. and Viitanen, H.A. 1999. A mathematical model of mould growth on wooden material. Wood Science and Technology 33 (1999) 475-485.

(EN)ISO 10456:1999 (E). Building materials and products –Procedures for determining declared and design thermal values. European committee for standardization.

Janssens, Arnold and Hens, Hugo. 1996. Condensation and Airtightness: Tolerance of Roof Design. Building Physics in the Nordic Countries. Espoo, Finland.

Janssens, Arnold. 1998. Reliable Control of Interstitial condensation in lightweight Roof Systems. –Calculation and Assessment Methods. Faculteit Toegepaste Wetenschappen Arenbergkasteel. Katholieke Universiteit Leuven. Belgium.

Jacobsen, T. Dalsgaard and Petersen, R.E. Lyng. 1998. Fugt, varme og konvektion i bygningsdele (in Danish). Master thesis at IBE, Technical University of Denmark.

Jakobsen, Arne and Pedersen, Stig Andur. 1996. Engineering Science and the Reality. Technical University of Denmark- Institute for Technology and Science. Denmark.

Jayamaha, S.E.; Wijeysundera, N.E.; and Chou, S.K. 1996. Measurement of Heat Transfer Coefficient for Walls. Building and Environment, Vol 31. No 5, pp. 399-407.

Jensen, M. 1959. Aerodynamik i den naturlige vind. Teknisk forlag, København.

Jensen, J.M. and Lund, H. 1995. Design Reference Year, DRY – Et nyt dansk referenceår. Laboratoriet for Varmeisolering. Meddelelse Nr. 281. Technical University of Denmark.

Jordan, D.A; Hajj, M.R.; Tieleman, H.W. 1997. Wavelet analysis ot hte relation between atmospheric wind and pressure fluctuations on a low-rise building, J. Wind Eng. Ind. Aerodyn. 69-71(1997) 647-655.

Jung, E. 1985. Dauerstandsverhalten von Verblendziegelmauerwerk unter Witterungsbeanspurchung und Auswirkungen von Kerndämm Massnahmen. Messergebnisse aus Labor und Bauwerksuntersuchungen. Baustoffindustrie, 28(5), 185-188.

Kays, W.M. and Crawford, M.E. 1980. Convective Heat and Mass Transfer. McGraw-Hill, New York.

Kays, W.M. and Crawford, M.E. 1993. Convective Heat and Mass Transfer –Third Edition. International edition. McGraw-Hill Book Co. Singapore.

Knoll, B; Phaff J.C; and de Gids W.F. 1996. Pressure Coefficient Simulation Program. Air Infiltration Review, Volume 17, No3, June 1996. World Wide Web Edition.

Knoll, Bas. 2000. Personal contact, TNO Building and Construction Research, Delft, The Netherlands.

Korsgaard, Vagn. 1985. Hygro diode membrane: A new vapor barrier. Thermal performance of the External Envelopes of Buildings III. Atlanta. ASHRAE.

Kragh, Helge and Pedersen, Stig Andur. 1991. Naturvidenskabens teori. En indføring I naturvidenskabernes og teknologiens filosofiske problemer. Nyt Nordisk Forlag. København 1991.

Kargh, Mikkel Kristian. 1998. Microclimativ conditions at the External Surface of Building Envelopes. Ph.D.-Thesis. Department of Buildings and Energy. Technical University of Denmark.

Kronvall, Johnny. 1980. Air Flows in Building Components. Report TVBH-1002. Division of Building Technology, Lund Institute of Technology, Sweden.

Kurnitski, J. 2000. Humidity Control in Outdoor-Air-Ventilated Crawl Spaces in Cold Climate by Means of Ventilation, Ground Covers and Dehumidification. Helsinki University of Technology. Department of Mechanical Engineering. Laboratory of Heating, Ventilating and Air Conditioning. Espoo 2000.

Kurnitski, J. 2001. Ground moisture evaporation in crawl spaces. Building and Environment Vol. 36 pp. 359-373.

Lampinen, M.J. 1996. Aineensiirto-oppi (Mass transfer, in Finnish). Helsinki University of Technology, Laboratory of Applied Thermodynamics, Report 94, Otaniemi.
[This reference has be referred by Kurnitski, 2000]

Larsson, Lars-Eric. 1996. Kallvindsutrymmen –Beräkningsmodell för fukteknisk analys och praktisk tillämpning (in Swedish). Chalmers University of Technology. Department of Building Physics. P-96:1-2. Sweden.

Larsson, Lars-Eric. 2001. Moisture Content in a Wooden Sheathing Above an Attic with High-Insulated Ceiling Construction. CIB W40 Heat and Moisture Transfer in Buildings. Meeting 8-11 April 2001. pp 282-289. Wellington, New Zealand.

Li, Yuguo and Delsante, Angelo. 2001. Natural ventilation induced by combined wind and thermal forces. Building and Environment. Vol 36 pp 59-71.

Lund, Hans. 2001. Personal contact. BYG.DTU. Department of Civil Engineering. Technical University of Denmark.

MATLAB, 2001. http://www.mathworks.com/products/simulink/

Melikov, 2001. Personal contact.

Mossing, Peter. 2001. E-mail. The Danish Building and Urban Research. Denmark.

Nevander,L.E. and Elmarsson 1994. Fukt handbok –Praktik och teori. Svensk Byggtjänst. Sweden.

Nicolajsen, Asta. 1989. Ventileret ydervæg. Vindens indflydelse på varmetabet. Byggeriets Udviklingsrapport. BUR rapport. 1989. København

Nicolajsen, Asta and Hansen, Morten Hjortslev. 2001. Personal contact. The Danish Building and Urban Research. Denmark.

Nielsen, Anker. 1980. Fugt II. Lecture note, 2. edition. Varmeisolering II. Laboratoriet for varmeisolering, DTU.

Nielsen, Toke Rammer; Peuhkuri, Ruut; Weitzmann, Peter & Gudum, Charlotte. 2002: "Modelling building physics in Simulink." Department of Civil Engineering, Technical University of Denmark. Report SR-02-03.

Noyé, P. 2000. Modelling of window energy performance in buildings. Master thesis at Institut for Bygninger og Energi, DTU.

Ojanen ,T. and Kumaran, K. 1996. Effect of Exfiltration on the Hygrothermal Behaviour of a Residential Wall Assembly. Journal of Thermal Insulation and Building Environments. Volume 19 – January 1996.

Orme, Malcolm; Liddament, Martin; and Wilson, Andrew. 1994. An Analysis and Data Summary of the AIVC's Numerical Database. Technical Note AIVC 44. AIVC –University of Warwick Science Park. Great Britain.

Pedersen, Carsten Rode. 1988. Instationære diffusionsberegninger. Laboratoriet for Varmeisolering. Danmarks Tekniske Højskole. Rapport 88-6. April 1988.

Pedersen, Carsten Rode. 1990. Combined Heat and Moisture Transfer in Building Constructions. Thermal Insulation Laboratory. Technical University of Denmark. Report no. 214, September 1990.

Peuhkuri, Ruut. 2000-a. Isoleringsmaterialers fugttekniske egenskaber i klimaskærmen (in Danish). Master Thesis. Department of Building and Energy. Technical University of Denmark.

Peuhkuri, Ruut. 2000-b. Ph.D. project in progress. Department of Civil Engineering. DTU. Denmark

Peuhkuri, Ruut. 2001. Personal Contact. Department of Civil Engineering. DTU. Denmark.

Peuhkuri, Ruut. 2002. Simulink model of coupled heat and moisture transport in material layers." Department of Civil Engineering, Technical University of Denmark. Report SR-02-02 2002.

Popp, W. and Künzel, H. 1980. Untersuchungen über die Belüftung des Luftraumes hinter vorgesetzten Fassadenbekleidungen aus kleinformatigen elementen. Stuttgart: Fraunhofer-Institut für Bauphysik.

Rasmussen, Bent. 1992. Tagdækning (in Danish). Anvisning nr. 18. Tagpapbranchens Oplysningsråd (TOR). Danmark.

Rode, Carsten. 1996. MATCHMAN. v. 1.4. Manual for MATCH. Denmark.

Rode, Carsten. 1998. Fugttransport –Klimaskærmens varme- og fugttekniske forhold. Lecture note. Notat U-022. ISSN 1396-4046. Department of Building and Energy. Technical University of Denmark.

Rousseau, Jacques. 1999-a. Drying of Walls with Ventilated Stucco Cladding: A Parametric Analysis. Technical Series 99-117, Canadian Housing Information Center (CHIC).

Rousseau, Jacques. 1999-b. Rain Penetration control: Applying Current Knowledge. Canada Mortgage and Housing Corporation (CMHC). Canada.

Salonvaara, Mikael H.; Ojanen, Tuomo T.; Kokko, Erikki; and Karagiozis, Achilles N. 1998. Drying Capabilities of Wood Frame Walls with Wood Siding. Thermal Performance of the Exterior Envelopes of Buildings VII, pp 165-177.

Samuelson, Ingemar. 1996. Moisture Balance in Unheated Roof Space –the Importance of Ventilation and Choice of Insulation Materials. Building Physics in the Nordic Countries. Espoo, Finland.

Sedlbauer, Klaus. 2001. Vorhersage von Schimmelpilzbildung auf und in Bauteilen. Fakultät von Bauingenieur- und Vermessungswesen. Universität Stuttgart. Deutchland.

Simiu, Emil and Scanlan, Pobert H. 1996. Wind Effects on Structures –Fundamentals and Applications to Design. Third Edition. John Wiley & Sons, Inc. USA. ISBN 0-471-12157-6

Simonson, Carey J. and Ojanen, Tuomo. 2000. Moisture performance of building envelopes with no plastic vapour retarder in cold climates. Proceedings of Healthy Buildings 2000, Vol. 3. pp 477-482.

Sparrow, E.M.; Ramsey, J.W.; and Mass, E.A. 1979. Effect of finite width on heat transfer and fluid flow about an inclined rectangular plate. ASME Journal of Heat Transfer 101, 199-204.

Swami, M.V. and Chandra, S. 1994. Correlation for Pressure Distribution on Buildings and Calculation of Natural-ventilation Airflow. Ashrae Transactions No. 3127.

Sørensen, Henning Hørup. 1996. Ventilation ståbi (in Danish). Teknisk forlag. Danmark.

Time, Berit. 1998. Hygroscopic Moisture Transport in Wood. PhD thesis 1998:20. Department of Building and Construction Engineering. Norwegian University of Science and Technology.

TenWolde, A, and Rose, W.B. 1996. Moisture Control Strategies for the Building Envelope. Journal of Thermal Insulation and Building Environments. Volume 19 – January 1996.

Uvsløkk, Sivert. 1996. The Importance of Wind Barriers for Insulated Timbre Frame Constructions. Journal of Thermal Insulation and Building Environments. Volume 20 – July 1996.

Vesterløkke, M; Pedersen, C.R.; and Christensen, G. 1992. Moisture Conditions of Non-Ventilated, Wood-Based, Membrane-Roof Components. Thermal Performance of the Exterior Envelopes of Buildings V. Proceedings of the ASHRAE/DOE/BTECC Conference, December 7-10 1992, Clearwater Beach, Florida.

Viitanen, Hannu A. 1997. Modelling the Time Factor in the Development of Mould Fungi –the Effect of Critical Humidity and Temperature Conditions on Pine and Spruce Sapwood. Holzforschung 51 (1997) 6-14.

Walker, I.S. and Forest, T.W. 1995. Field Measurements of Ventilation Rates in Attics. Building and Environment. Vol 30. No.3, pp. 333-347.

Økland, Øyvind. 1998. Convection in highly-insulated building structures. Norwegian University of Science and Technology, Department of Building and Construction Engineering.

Åberg, Olle. 1997. Cics –Kryprumsgrunder. Ventilation, temperatur, fukt og mögel. Beregningsprogram för PC. Hjälpmedel for fuktdimentionering. Byggteknik Olle Åberg AB. 1997-01-01.